RIBONUCLEASE ACTIVITY:

BASIS AND CONTROL

by

Bryan Douglas Smith

A dissertation submitted in partial fulfillment

of the requirements for the degree of

Doctor of Philosophy

(Biochemistry)

at the

UNIVERSITY OF WISCONSIN–MADISON

2006

A dissertation entitled

Ribonuclease Activity:
Basis and Control

submitted to the Graduate School of the
University of Wisconsin-Madison
in partial fulfillment of the requirements for the
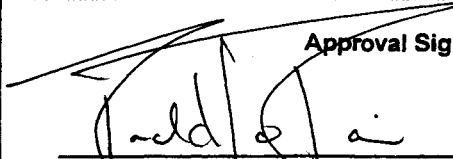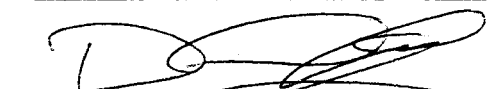degree of Doctor of Philosophy

by

Bryan Douglas Smith

Date of Final Oral Examination: April 21, 2006

Month & Year Degree to be awarded: **December**   **May** 2006 **August**

****

Approval Signatures of Dissertation Committee

Signature, Dean of Graduate School

RIBONUCLEASE ACTIVITY:

BASIS AND CONTROL

Bryan Douglas Smith

Under the supervision of Professor Ronald T. Raines

At the University of Wisconsin–Madison

Bovine pancreatic ribonuclease (RNase A) has been used as a model enzyme in studies of nearly all aspects of protein structure and function. Recently, certain homologs of RNase A have been found to have interesting biological activities, such as toxicity to cancer cells or the promotion of angiogenesis. These findings have once again made members of the RNase A superfamily attractive targets for basic biochemical research, as well as for biotechnological and biomedical applications. This dissertation describes advances in our understanding of RNase A and a homolog, angiogenin.

Chapter Two describes the use of a novel genetic selection system to sift through large libraries of mutants to identify all residues in RNase A and angiogenin that contribute to ribonucleolytic activity. The implications of this work on the structure/function and evolution of ribonucleases, as well as on enzymes in general are discussed.

Historically, the catalytic activity of RNase A *versus* the concentration of salt has been described as a bell-shaped curve, with the enzyme having optimal activity near 100 mM NaCl. This curve is due to inhibition of RNase A at lower salt concentrations by a contaminant in common biological buffers. Chapter Three describes the isolation and

identification of this contaminant as one of the most potent small-molecule inhibitors of any ribonuclease.

Chapter Four describes the creation of surfaces coated with the potent ribonuclease inhibitor identified in Chapter Three. These surfaces could be used to prevent RNA degradation caused by incidental ribonuclease contamination in biochemical and biotechnological experiments.

Angiogenin is involved in the formation of new blood vessels, and as such, is a potential target for preventing tumor growth. Chapter Five describes the use of a genetic selection system to isolate peptide inhibitors of angiogenin, including one that is among the best small-molecule inhibitors of angiogenin identified to date.

Together, these chapters provide new insights into the basis and control of ribonucleases, with advances in the basic knowledge and potential applications of these versatile enzymes.

Acknowledgments

The work completed during the time I have spent in graduate school would not have been possible without the help of many people. First, I would like to thank my wife, Rebecca, for her love, friendship, and immeasurable support. We have shared many unforgettable experiences over the last six years, including moving to a new city, buying our first house, and starting a family. Our daughter, Ava, serves as a constant source of inspiration to us and as a reminder of what matters the most. I thank the rest of my family, especially my parents Doug and Karyl Smith, for fostering my love of science and nature, and for their constant love and support.

I am grateful to my advisor, Ron Raines, for the opportunity to work with him on exciting research projects. Professor Raines is an incredibly talented, intelligent, creative, and hard-working scientist, and a great writer. I thank him for putting up with my never-ending skeptical questions and bad jokes.

My coworkers in the Raines laboratory have provided much assistance and advice on my research projects, and have been the source of great friendships. Brian Miller was an extraordinary mentor. His advice was especially important for the work described in Chapter Two. Matthew "Popo" Soellner served as a collaborator for the work in Chapters Three and Four. Luke Lavis and Josh Higgin were collaborators for the work in Appendix 1. I am grateful for many contributive discussions from Eugene Lee, Steve Fuchs, Tom Rutkoski, Jeet Kalia, and Jeremy Johnson. I thank Cindy Chao, Parit Plainkum, Kenneth Woycechowsky, Kimberly Dickson, Robert Hondal, Chiwook Park, Sunil Chandran, and Kris Staniszewski for their assistance and advice. My coworkers

have helped make this experience rewarding and incredibly fun. I will forever miss the time I spent with them in graduate school in Madison.

I am grateful to many others outside of the Raines laboratory, including Professors W. W. Cleland, Hazel Holden, Brian Fox, and David Lynn for their advice on my research projects. I appreciate Darrell McCaslin's assistance in the Biophysics Instrumentation Facility, as well as his advice and excellent sense of humor. I thank George Hanson, who mentored me during an internship at Invitrogen.

I am grateful to Liana Lamont, Erik Puffer, Jason McCoy, and Michael Hobbs for their friendship and for many discussions about science in general.

Finally, I am grateful to the NIH Biotechnology Training Program, the Wisconsin Alumni Research Foundation, and Professor Raines for funding during my graduate training.

Table of Contents

List of Figures

List of Tables

List of Abbreviations

ε	extinction coefficient
6-FAM	6-carboxyfluorescein
6-TAMRA	6-carboxytetramethylrhodamine
ASA	accessible surface area
ATP	adenosine 5'-triphosphate
B	cytosine, guanine, or thymine
Bamfolate	N^{δ}-bromoacetyl-N^{α}-pteroyl-L-ornithine
BES	N,N-bis(2-hydroxyethyl)-2-aminoethanesulfonic acid
cDNA	complementary deoxyribonucleic acid
CFIS	chain-folding initiation site
CHES	2-(cyclohexylamino)ethanesulfonic acid
D	adenine, guanine, or thymine
ddH_2O	distilled deionized water
DMF	dimethylformamide
DMSO	dimethylsulfoxide
DNA	deoxyribonucleic acid
DTNB	5,5'-dithiobis(2-nitrobenzoic acid)
DTT	dithiothreitol
E	enzyme
EDTA	ethylenediaminetetraacetic acid
EP-PCR	error-prone polymerase chain reaction

F	fluorescence
FBS	fetal bovine serum
FD	folate-deficient
FFRPMI	folate-free Roswell Park Medical Institute medium
FPLC	fast performance liquid chromatography
FRET	fluorescence resonance energy transfer
GSH	reduced glutathione
GSSG	oxidized glutathione
h	hour
H	adenine, cytosine, or thymine
HCl	hydrochloric acid
HPLC	high-performance liquid chromatography
hRI	human ribonuclease inhibitor
I	inhibitor
indels	insertions–deletions
IPTG	isopropyl-1-thio-β-D-galactopyranoside
K	guanine or thymine
k_{cat}	first-order enzymatic rate constant
K_d	equilibrium dissociation constant
kDa	kilodalton
K_i	inhibitor dissociation constant
K_m	Michaelis constant

LB	Luria–Bertani broth
MALDI	matrix assisted laser desorption ionization
MES	2-(N-morpholino)-ethanesulfonic acid
min	minute
mRNA	messenger ribonucleic acid
MW	molecular weight
MWCO	molecular weight cutoff
N	adenine, cytosine, guanine, or thymine
NaCl	sodium chloride
OD	optical density
OVS	oligo(vinylsulfonic acid)
pA	adenosine 5'-phosphate
PBS	phosphate-buffered saline
PCR	polymerase chain reaction
PDB	protein data bank
PIPES	1,4-piperazinebis(ethanesulfonic acid)
pK_a	log of the acid dissociation constant
poly(C)	poly(cytidylic acid)
PVOS	poly(vinylsulfuric acid)
PVP	poly(vinylphosphonic acid)
PVS	poly(vinylsulfonic acid)
rDNA	recombinant DNA

RI	ribonuclease inhibitor
RNA	ribonucleic acid
RNase A	unglycosylated bovine pancreatic ribonuclease
rRNA	ribosomal ribonucleic acid
s	second
SDS–PAGE	sodium dodecyl sulfate–polyacrylamide gel electrophoresis
t	time
TB	terrific broth
Tris	2-amino-2-(hydroxymethyl)-1,3-propanediol
UpA	uridylyl-(3'→5')-adenosine
V	adenine, cytosine, or guanine

Chapter One

Introduction

1.1 Overview

Enzymes can enhance the rates of chemical reactions by more than 10^{19}-fold (Miller and Wolfenden, 2002). Despite the diversity of their biological reactions, enzymes generally achieve k_{cat} values of 10^2–10^3 s^{-1} (Wolfenden and Snider, 2001; Miller and Wolfenden, 2002) while exhibiting high specificity in turning a specific substrate into a specific product (Koshland, 1958). These remarkable properties are ultimately achieved by the formation of functional polypeptide chains from just 20 different amino acids. The linear arrangement of amino acids in a protein encodes its three-dimensional structure (Sela *et al.*, 1957; Anfinsen, 1973). Therefore, the information needed to understand the ability of a protein to fold into a stable structure and catalyze a specific reaction is contained within its amino-acid sequence. Deciphering this information has been the major goal of enzymology.

On a basic level, determining how enzymes catalyze reactions is fundamental to understanding how life works. Life could not exist without enzymes. Organisms harness energy from their environments and replicate genetic information through enzyme-catalyzed reactions. Knowledge of enzyme structure/function also has practical applications. Since many diseases are caused by enzyme dysfunction (DiLella *et al.*, 1987; Walz and Sattler, 2006) or by pathogens and viruses armed with foreign enzymes (Furman *et al.*, 1986), molecules that can alter enzyme activities can serve as potential cures. In addition, the design of enzymes with desired functions is of great interest for many biotechnological applications including therapeutics, biocatalysis, and

bioremediation (Walsh, 2001; Spreitzer and Salvucci, 2002; Woycechowsky and Hilvert, 2004).

1.2 Determining the Basis for Catalysis: Enzyme Modification

Not all residues in an enzyme are necessary for its structure/function. Sequence alignments of homologous proteins sharing the same three-dimensional fold and catalytic activity show that only certain residues are conserved through evolution (Perutz *et al.*, 1965; Chothia and Lesk, 1986). These residues are likely more important than other residues with low sequence conservation. In addition, enzymes are usually larger than their substrates, therefore, only a small percentage of residues in the enzyme directly participate in substrate binding and catalysis (Koshland *et al.*, 1958). The identification of the most important enzymic residues is critical towards an understanding of how enzymes function.

One of the main approaches for studying enzymes is to modify specific residues and determine the effects on structure/function. Rational methods for modifying enzymes involve examining sequence alignments and/or x-ray crystal structures of enzymes to identify potentially important residues. These residues can be specifically altered via site-directed mutagenesis (Hutchison *et al.*, 1978; Kunkel, 1985), semisynthesis (Muir *et al.*, 1998), or total synthesis (Dawson *et al.*, 1994). Site-directed mutagenesis limits amino-acid substitutions to the proteinogenic amino acids, whereas semisynthesis and total synthesis, though much more challenging, allow the use of non-natural amino acids or analogs to probe structure/function in finer detail. "Irrational" approaches of enzyme

modification include chemical modification or, more recently, random mutagenesis. In these studies, after some effect on protein structure/function is observed, then the relevant modification is identified. One main advantage of these techniques over rational approaches like site-directed mutagenesis is that they are unbiased. The most critical residues in the enzyme are revealed by the experiment. The importance of many of these amino acid residues may not be obvious through observations of a crystal structure or sequence alignment.

Prior to the 1980s, the only way to modify enzymes was via chemical modification (Peracchi, 2001). Various reagents can undergo sufficiently specific chemical reactions with certain amino-acid side chains. By pinpointing which modifications cause inactivation of the enzyme, the residues that are important for function can be identified. For example, alkylation of bovine pancreatic ribonuclease (RNase A) with iodoacetate leads to two inactive species in which either His-12 or His-119 are carboxymethylated (Crestfield *et al.*, 1963). Later crystallography and site-directed mutagenesis work confirmed that the two histidine residues are in the active site of RNase A and directly participate in catalysis (Kartha *et al.*, 1967; Thompson and Raines, 1994; Raines, 1998).

Chemical modification has several drawbacks. First, several residues such as Phe, Ala, Val, Leu, Ile, and Gly are unreactive. Nonetheless, those residues likely to be involved directly in catalysis are, by nature, reactive and can be modified with various reagents. Second, most essential residues in a protein are buried (Bowie *et al.*, 1990) and are not accessible by chemical modification reagents in the native conformation of the enzyme. Certain buried residues can be modified by chemically denaturing the enzyme

prior to the addition of the modification reagent, though this is not always practical. Finally, since chemical modification almost always yields a larger residue—which could disrupt enzyme structure through steric effects—false positives can occur (Knowles, 1987). Indeed, chemical modification of enzymes has been compared to "an effort to understand the workings of a motor car by studying the effect of firing a shell through the engine compartment" (Knowles, 1987).

In the last thirty years, with the advent of efficient heterologous protein production systems, such as the pET system (Studier *et al.*, 1990), and site-directed mutagenesis (Hutchison *et al.*, 1978), the contribution of specific residues to structure/function could be determined with new precision. A specific residue can be substituted with any of the 19 other proteinogenic amino acids, and the altered protein can be produced in large quantities for study. The residue of interest can often be replaced with an isosteric residue or a smaller residue, and is thus less likely to be disruptive to protein structure than is chemical modification of that residue.

One main disadvantage of site-directed mutagenesis is that it is a biased approach. Generally, a residue is selected for mutagenesis based upon its sequence conservation or upon insights gained from a crystal structure of the enzyme. Residues that are distant from the enzymic active site or residues that are not conserved in sequence alignments are often ignored, leaving hidden the identity of critical aspects of structure/function.

The explosion of the ability to sequence DNA rapidly has enabled the use of new techniques that, in essence, combine the random approach of chemical modification studies with the precision and side-chain diversity of site-directed mutagenesis. Large

libraries of mutants can be created via random mutagenesis. Each codon in a gene can be mutated individually or in combination through the use of error-prone DNA polymerases, randomized oligonucleotides, or DNA shuffling (Bowie *et al.*, 1990; Cadwell and Joyce, 1992; Stemmer, 1994; Axe *et al.*, 1998). A screening or selection system can be used to identify enzymes with altered catalytic activity, conformational stability, or both. Finally, the corresponding DNA sequence can be determined. In this way, the essential residues in an enzyme can be identified quickly without any *a priori* knowledge.

Chapter Two describes the application of error-prone PCR and genetic selection to identify essential residues in RNase A and a homolog, human angiogenin. RNase A was one of the most-studied enzymes in the 20th century, yet several "new" residues that are essential for its structure/function have been identified, showing the power of a random approach. Extending earlier work, the results show that most essential residues in a protein are buried, including many residues that are not well conserved and far from the enzymic active site (Bowie *et al.*, 1990; Rennell *et al.*, 1991; Markiewicz *et al.*, 1994; Suckow *et al.*, 1996; Axe *et al.*, 1998; Guo *et al.*, 2004). Thus, many essential residues in RNase A and angiogenin were unlikely to be identified as being important by traditional enzyme modification methods. Furthermore, systematic mutation of angiogenin revealed that the set of essential residues between the two homologs has largely stayed the same over more than 180 million years of evolution, yet many important changes have occurred.

1.3 Ribonuclease A

RNase A (EC 3.1.27.5) is thought to function in digestion of the large quantities of RNA produced by microorganisms in the ruminant gut (Barnard, 1969). Its high natural abundance in the bovine pancreas and its extraordinary conformational stability enabled its isolation and use as an early model for the study of protein structure and function (Raines, 1998). Other factors also contributed to its early widespread use in enzymology. The mature enzyme is small (124 amino acids) and quite amenable to protein chemistry techniques (Blackburn and Moore, 1982). The substrate of RNase A, ribonucleic acid, is ubiquitous, and its cleavage is readily monitored by various assays (Richards and Wyckoff, 1971). Early work with RNase A was also substantially advanced when, in the 1950s, the Armour meat-packing company provided more than *one kilogram* of crystalline ribonuclease to researchers throughout the country (Richards and Wyckoff, 1971). In the last 50 years, landmark work has been performed with RNase A on nearly all aspects of protein structure and function, including protein folding and stability, disulfide bond formation, molecular evolution, and catalysis (Blackburn and Moore, 1982; Beintema, 1987; Raines, 1998; Schultz *et al.*, 1998; Wedemeyer *et al.*, 2000; Chatani and Hayashi, 2001).

RNase A is an extremely efficient catalyst, limited by diffusion of its substrate (Park and Raines, 2001). RNase A is also a proficient catalyst. The uncatalyzed rate of hydrolysis of an RNA dinucleotide, UpA, at pH 6.0 and 25 °C is 5×10^{-9} s^{-1} (corresponding to $t_{1/2} = 4$ y) (Thompson *et al.*, 1995). Under the same conditions and via a

similar mechanism, RNase A degrades UpA with $k_{cat} = 1.5 \times 10^3 \, s^{-1}$, amounting to a rate enhancement of 3×10^{11} (Thompson et al., 1995).

RNase A catalyzes the cleavage of the P–O$^{5'}$ bond 3' to pyrimidine nucleotides in RNA (Figure 1.1). The reaction forms a 2',3'-cyclic phosphodiester in one product and a new 5'-hydroxyl on the other product. The enzyme reaction occurs via a general acid–base mechanism (Findlay et al., 1961; Herschlag, 1994; Sowa et al., 1997). His-12 abstracts a proton from the 2'-hydroxyl of ribose, allowing attack on the phosphoryl group. His-119 acts by protonating the leaving 5''-oxygen (Thompson and Raines, 1994). Lys-41 stabilizes the excess negative charge that develops on a nonbridging phosphoryl oxygen during catalysis, donating a hydrogen bond to the transition state (Messmore et al., 1995). Although an alternative mechanism has been proposed (Anslyn and Breslow, 1989; Breslow and Xu, 1993), a general acid–base mechanism involving a slightly associative transition state is more likely to be correct (Figure 1.2) (Herschlag, 1994; Thompson and Raines, 1994; Sowa et al., 1997).

RNase A can also hydrolyze the 2',3'-cyclic phosphodiester product to form a 3' phosphomonoester (Figure 1.1) (Findlay et al., 1962; Thompson et al., 1994). His-12 and His-119 serve opposite roles during this reaction, with His-119 abstracting a proton from H_2O, allowing attack on the cyclic phosphate. Concurrent with this reaction, His-12 acts by protonating the 2'-oxygen to facilitate its displacement. The hydrolysis reaction is slower than transphosphorylation, and the two reactions almost never occur sequentially on the enzyme. This leads to an accumulation of the 2',3'-cyclic phosphodiester when the RNA substrate is not limiting (Thompson et al., 1994).

Like most known ribonucleases, RNase A can make multiple contacts with an RNA substrate (Figure 1.3). RNase A is cationic at physiological pH (pI = 9.3) (Ui, 1971). Several positively-charged residues are located in the enzymic active site and adjacent subsites, and are suited to bind the sequential negatively-charged phosphoryl groups in the RNA backbone through Coulombic interactions (Fontecilla-Camps *et al.*, 1994). There are also subsites on the enzyme for the adjacent nucleobase and ribose moieties. The base subsites impart substrate specificity. The B_1 base subsite binds pyrimidines, whereas B_2 and B_3 bind all nucleobases, but favor adenine and purines, respectively (Tarragona-Fiol *et al.*, 1993; Fontecilla-Camps *et al.*, 1994; delCardayré and Raines, 1995).

The RNase A structure resembles a kidney, with the active site and subsites situated in the cleft (Figure 1.3). Its secondary structure consists of four antiparallel β-strands and three α-helices. Four disulfide bonds stabilize the enzyme. RNase A was the fourth protein for which an x-ray crystal structure was determined (Kartha *et al.*, 1967). Now, more than 100 three-dimensional structures of RNase A and its variants are available in the protein data bank (http://www.rcsb.org), including structures solved at various temperatures and pH values, structures in complex with many different ligands, and structures of domain-swapped multimeric forms of the enzyme.

Recently, there has been a resurgence of interest in RNase A. Certain homologs of RNase A have intriguing biological properties, such as toxicity to cancer cells (Ardelt *et al.*, 1991; Matousek and D'Alessio, 1991), promotion of angiogenesis (Strydom *et al.*, 1985), antiviral activity (Domachowske *et al.*, 1998), or microbicidal activity (Hooper *et*

al., 2003). These findings have led to more intense study of structure/function

relationships of enzymes in the RNase A superfamily (Schein, 1997; Beintema and

Kleineidam, 1998; Raines, 1998) and have made ribonucleases attractive targets in cancer

research (Schein, 1997; Leland and Raines, 2001). Indeed, RNase A itself can be

engineered to kill cancer cells (Leland *et al.*, 1998) or promote the growth of new blood

vessels (Raines *et al.*, 1995). The groundbreaking work on RNase A over the last seven

decades has aided immensely in understanding and exploiting these new findings.

1.4 Angiogenin

Angiogenin was originally isolated as a human tumor derived protein with the ability

to promote angiogenesis, the growth of new blood vessels (Fett *et al.*, 1985). Improperly

regulated angiogenesis is involved in many diseases, most notably tumor growth

(Gimbrone *et al.*, 1972). Therefore, identifying potential inhibitors of angiogenic factors

could lead to new cancer therapies (Folkman and Shing, 1992).

When the amino-acid sequence of angiogenin was determined, surprisingly, it had

35% identity to that of RNase A (Figure 1.4) (Strydom *et al.*, 1985). Angiogenin and

RNase A diverged after a gene duplication event that took place between 180 and 310

million years ago (Cho and Zhang, 2006). Despite their divergence, RNase A and

angiogenin share similar three-dimensional structures (Figure 1.4). Initially, there were

doubts that angiogenin retained ribonucleolytic activity, as it did not appear to degrade

commonly used RNA substrates (Strydom *et al.*, 1985; Shapiro *et al.*, 1986). It was

shown, however, that angiogenin could degrade rRNA to a limited extent (Shapiro *et al.*,

1986; St Clair *et al.*, 1987). Using more sensitive assays, angiogenin was also found to have ribonucleolytic activity ~10^5-fold lower than that of RNase A for commonly used ribonuclease substrates (Leland *et al.*, 2002). Since the ribonucleolytic activity of angiogenin is required for angiogenesis, speculation abounds that the enzyme acts with high activity on an as yet unidentified specific RNA sequence or secondary structural element (Shapiro *et al.*, 1986; Strydom, 1998; Leland *et al.*, 2002).

The two essential histidine residues and lysine residue in the active site of RNase A are conserved in angiogenin (His-13, Lys-40, and His-114) (Figure 1.4). Phosphoryl-group and nucleobase-binding subsites are also found in angiogenin, though there are key differences. The B_1 subsite is occluded by Gln-117, and it appears that angiogenin must undergo a structural change to cleave RNA substrates (Shapiro, 1998). The B_2 subsite of angiogenin is entirely different, as angiogenin lacks the Cys-65–Cys-72 disulfide bond and loop found in RNase A (Harper and Vallee, 1989; Shapiro, 1998). Instead, the loop in angiogenin is involved in its role in angiogenesis. Replacing the equivalent surface loop in RNase A with the loop found in angiogenin engenders an RNase A variant with angiogenic activity (Raines *et al.*, 1995).

The ribonucleolytic activity of angiogenin is essential for its promotion of angiogenesis (Shapiro *et al.*, 1989; Shapiro and Vallee, 1989), though it is still not known how RNA degradation elicits this biological response. Angiogenin has also been found to act as a transcription factor for rRNA (Xu *et al.*, 2003), as well as an antibacterial and antifungal protein involved in host defense (Hooper *et al.*, 2003). Very recently, it has been discovered that mutations that knock out angiogenin activity are linked in some

populations to amyotrophic lateral sclerosis, a neurodegenerative disorder (Greenway *et al.*, 2006). Precisely how angiogenin elicits these diverse biological phenomena is not known.

1.5 Control of Enzymatic Activity

Enzymes provide enormous rate enhancements for chemical reactions. Yet, unregulated enzyme activity can be harmful to organisms. Consequently, enzymes are exquisitely controlled *in vivo*. As a first level of control, organisms regulate the rate of synthesis and degradation of enzymes. The extant pool of enzymes can be regulated by covalent modification, small-molecule activators or inhibitors, or by modulator proteins. In addition, enzymes have generally evolved to have K_M values near the physiological level of substrate, thus the velocity of the enzymatic reaction can change quickly in response to substrate concentration.

Exogenous small molecules can be used to study enzymes *in vivo*. The temporal and spatial control of enzymes through "chemical genetics" can often reveal important information about enzyme function that gene knockouts cannot (Spring, 2005). Enzyme activators and inhibitors also have significant applications. Many diseases are caused by enzyme dysfunction, such as phenylketonuria (DiLella *et al.*, 1987) and chronic myeloid leukemia (Walz and Sattler, 2006). Compounds that can correct faulty enzyme activities can serve as potential therapeutics. In addition, viruses and pathogens encode a plethora of foreign enzymes, such as HIV reverse transcriptase (Furman *et al.*, 1986) or the

bacterial ribosome (Tenson and Mankin, 2006), which are excellent targets for small-molecule therapeutics.

In vitro, enzyme inhibitors can aid in the understanding of the chemical mechanisms of enzyme catalysis (Cleland, 1977). In addition, inhibitors of enzymes such as nucleases and proteases can be useful (sometimes essential) reagents in biochemical and biotechnological experiments.

1.6 Control of Ribonuclease Activity

The control of ribonuclease activity is especially important. RNA is an essential biopolymer for all known life. Unregulated ribonucleases can cause cell death by degrading essential cellular RNA (Saxena *et al.*, 1991; Leland *et al.*, 1998). Organisms have evolved mechanisms to protect RNA. For example, mammalian cells contain a potent inhibitor of RNase A and many of its homologs (Lee *et al.*, 1989; Haigis *et al.*, 2003; Dickson *et al.*, 2005). Although RNase A and its homologs are secreted enzymes, the mammalian inhibitor is a cytosolic protein and prevents RNA degradation by any ribonucleases that inadvertently reach the cytosol (Haigis *et al.*, 2003). Still, not all ribonuclease activity is disadvantageous, as RNA degradation is essential for the biological function of ribonucleases. Angiogenin, for example, uses its ribonucleolytic activity to promote angiogenesis (Shapiro and Vallee, 1989), an important process during development and wound healing (Folkman and Shing, 1992). How RNA degradation is linked to various biological processes is not known. Exogenous control of ribonuclease activity *in vivo* may aid in the understanding of how ribonucleases elicit diverse

biological responses. In addition, inhibitors of ribonucleases such as angiogenin could serve as cancer therapeutics (Kao *et al.*, 2002).

In vitro, the preservation of intact nucleic acids is of central importance in molecular biology. Ribonucleases are generally considered the most problematic nucleases due to their high natural abundance, extraordinary conformational stability, resistance to proteolysis, and lack of requirement for divalent cations or other cofactors (Raines, 1998; Russo *et al.*, 2001). Human skin is an abundant source of multiple nucleases that are readily transferred to surfaces and solutions on contact (Holley *et al.*, 1961). In addition, ribonucleases are called for in many procedures requiring degradation of RNA, but ribonuclease activity can be problematic in ensuing steps of the same experiment (Sweeney *et al.*, 2000). Effective small-molecule ribonuclease inhibitors could be of significant utility in these situations.

Several ribonuclease inhibitors are commercially available. Each, however, suffers from an undesirable attribute, such as low potency, instability, or high cost. For example, the ribonuclease inhibitor protein (RI) binds ribonucleases with femtomolar affinity (Lee *et al.*, 1989)), but is expensive, difficult to produce, and is readily inactivated by oxidation (Kim *et al.*, 1999). In addition, RI only inhibits RNase A and some of its homologs (Raines, 1998). Diethylpyrocarbonate (DEPC) inactivates nucleases, but is toxic and requires time-consuming procedures. Because DEPC will modify proteins and nucleic acids non-specifically (Miles, 1977), as well as react with buffers, it is only useful for the prior treatment of water to be used in experiments.

Chapters Three, Four, and Five describe the identification of potent inhibitors of ribonucleases and their potential applications. Chapter Three describes the isolation and identification of a common buffer contaminant as one of the most potent small-molecule inhibitors of any ribonuclease. Chapter Four describes the creation of surfaces coated with this potent ribonuclease inhibitor. These surfaces could be used to prevent RNA degradation caused by incidental ribonuclease contamination in biochemical and biotechnological experiments. Chapter Five describes the use of a genetic selection system to isolate peptide inhibitors of angiogenin, including one that is among the best small-molecule inhibitors of angiogenin that have been identified. These inhibitors or future derivatives could have the potential to modulate angiogenesis.

1.7 Conclusions

Identifying the enzymic features that are responsible for catalysis and discovering new ways to control enzymatic activity are of utmost importance in basic biochemical research and for biotechnological and medical applications. This dissertation provides new insights into the basis and control of RNase A and angiogenin, with advances in the basic knowledge and potential applications of these versatile enzymes.

Figure 1.1   Mechanism for the reaction catalyzed by RNase A. *A*,

Transphosphorylation. *B*, Hydrolysis. In both reactions, "A" is His-119

and "B" is His-12.
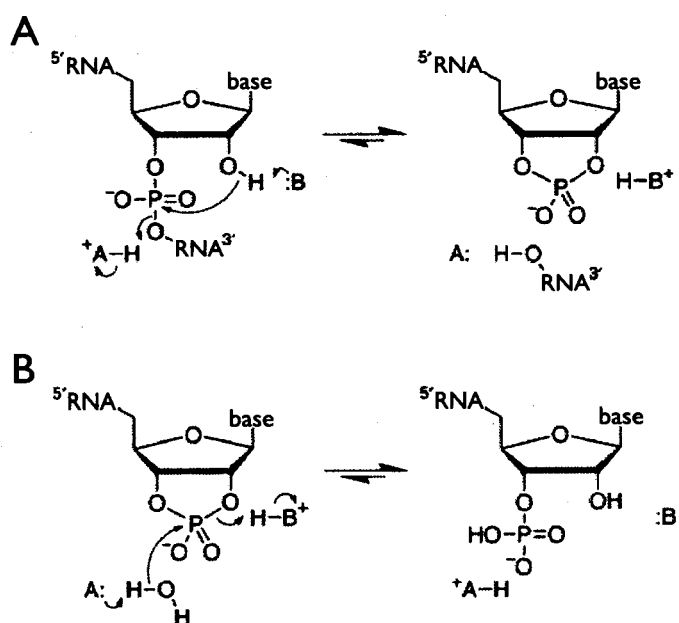
Figure 1.2 Putative structure of the transition state during catalysis by RNase A.
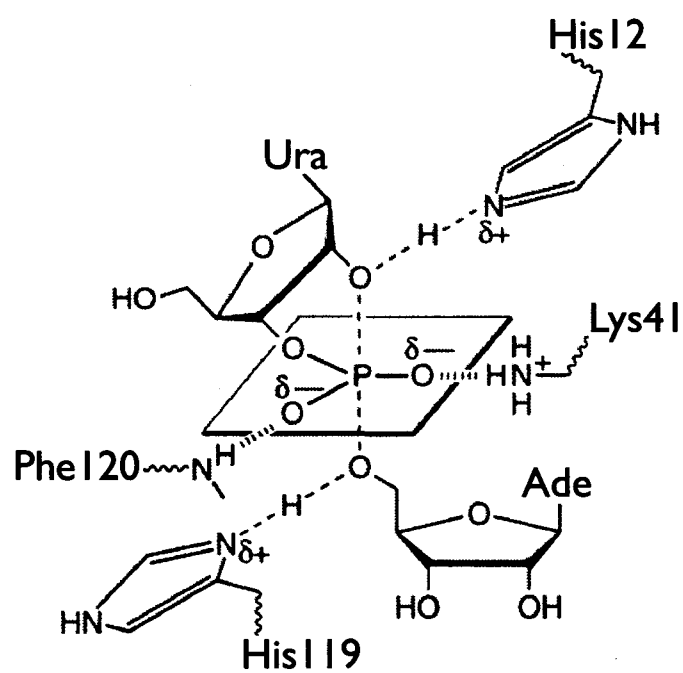
Figure 1.3   Structure of the crystalline ribonuclease A•d(ATAAG) complex (PDB

entry 1RCN (Fontecilla-Camps *et al.*, 1994)). Three phosphoryl-group

binding subsites are indicated. The G residue and a fourth phosphoryl-

group binding subsite (Arg-85 (Fisher *et al.*, 1998)) are not shown.

Residues that comprise each subsite are colored as follows: P_0 subsite

(yellow), P_1 subsite (orange), and P_2 subsite (red). The image of the

structure was prepared with Molscript (Avatar Software AB, Stockholm,

Sweden).
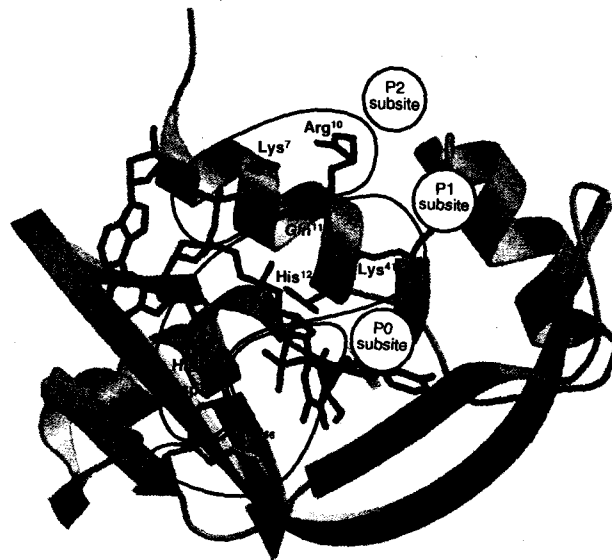
Figure 1.4 Three-dimensional structures and sequence alignment of RNase A and

angiogenin (PDB entries 7RSA (Wlodawer *et al.*, 1988) and 1B1I

(Leonidas *et al.*, 1999)). *A*, Structures are shown in cartoon representation.

Images were generated with Molscript (Avatar Software AB, Stockholm,

Sweden). *B*, Residues conserved between RNase A and angiogenin (ANG)

are boxed. Residues that are found in ≥90% of an alignment of a diverse

set of 266 ribonucleases (not shown) are colored green. Cysteine residues

are colored yellow. Helices, sheets, and turns are indicated by h, s, and t.

The sequence alignment was generated with the ClustalW algorithm.

A

RNase A (PDB: 7RSA)   Angiogenin (PDB: 1B1I)

B

```
         1          10         20         30         40
         --hhhhhhhhhhhh--tt-------tthhhhhhhhttttttsss-ss
RNase A  -KETAAAK F ER Q H M D SSTSAASSSN Y C NQM M KS R N L T KDR C K P
ANG      QDNSRYTH F LT Q H Y D AKPQGRDD-R Y C ESI M RR R G L T SP- C K D
         --thhhhhhhhhhh--tt-----h hhhhhhhhhhttt-tt  ---
         1          10         20         30         40
```

```
         43         50         60         70         80
         sssss---hhhhhhhhh-sss--tt----sss-ss-ssssssss
RNase A  V N TF V H ESLADVQ A V C SQ K N VACKNGQT N CYQ S Y S TMSI T D C R
ANG      I N TF I H GNKRSIK A I C EN K N GNP--HRE N LRI S K S SFQV T T C K
         sssss---hhhhhhhhhttt-sss    stttssss--ssssssss
         42         50         60         70         80
```

```
         86    90        100        110        120  124
         s-ttt-tt-sssssssss-sssssstttttss-ss-ss-
RNase A  ET G S S KY P N C A YKT T QANKHI I VACE GNPYV P VH F D A S V----
ANG      LH G G S PW P P C Q Y RA T AGFRNVV VACE NG--L P VH L D Q S IFRRP
         ss------------ssssssssss-ssssstt  ss-ss-hhhh---
         83         90        100        110        120  123
```

☐ Conserved Residue Between RNase A and Angiogenin
    Conserved Residues Among a Set of 266 Ribonucleases
C Cysteine Residue   hst helix, sheet, turn

Chapter Two

Genetic Selection for Critical Residues in Ribonucleases

Prepared for submission to the *Journal of Molecular Biology* as:

Smith, B. D. and Raines, R. T. (2006) Genetic selection for critical residues in

ribonucleases.

2.1 Abstract

We have identified a large set of critical residues in two mammalian ribonuclease homologs, bovine pancreatic ribonuclease (RNase A) and human angiogenin. By using error-prone PCR to randomly generate single-base substitutions and a novel genetic selection system to isolate inactive ribonuclease variants, we have discovered mutations that decrease ribonucleolytic activity to <1% of that of the wild-type enzymes. Twenty-three of the 124 residues in RNase A are intolerant to substitution with at least one amino acid. Only six residues appear to be wholly intolerant to substitution. Twenty-nine of the 123 residues in angiogenin are intolerant to substitution with at least one amino acid. Again, only six residues are intolerant to substitution of any kind. Interestingly, the two homologous enzymes share most, but not all residues required for their structure/function. The six residues in RNase A and angiogenin that are the least tolerable to substitution (and, therefore, the most important) are the two histidine residues involved in catalysis and four cysteine residues that form two disulfide bonds. Many hydrophobic core residues are essential, yet they generally tolerate several conservative substitutions. With only few exceptions, the critical residues in RNase A and angiogenin are buried in the interior of the proteins. The importance of a particular residue as determined using this genetic selection system correlates with its sequence conservation, though many non-conserved residues are critical for protein structure/function. Despite the large volume of research on RNase A, many critical residues that are identified herein have not been subjected to study, demonstrating the power of using a genetic approach to reveal residues that are critical for protein structure/function.

2.2 Introduction

Nearly 50 years ago, Anfinsen and coworkers employed bovine pancreatic ribonuclease (RNase A; EC 3.1.27.5) to reveal that the primary structure of a protein is sufficient to encode its tertiary structure (Sela *et al.*, 1957; Anfinsen, 1973). Sequence alignments of homologous proteins sharing the same three-dimensional fold provide evidence that only a subset of residues are critical for the formation of that structure (Perutz *et al.*, 1965; Chothia and Lesk, 1986). Systematic mutation studies – in which every residue in a protein is mutated individually or in combination – confirm this finding, as well as extend it by showing the general tolerance of enzymes to amino acid changes, the correlation between sequence conservation and the importance of particular residues, and the intolerance of buried residues to non-conservative substitutions (Bowie and Sauer, 1989; Loeb *et al.*, 1989; Bowie *et al.*, 1990; Rennell *et al.*, 1991; Poteete *et al.*, 1992; Markiewicz *et al.*, 1994; Axe *et al.*, 1996; Suckow *et al.*, 1996; Axe *et al.*, 1998; Guo *et al.*, 2004; Campbell-Valois *et al.*, 2005).

In the decades since Anfinsen's discovery, RNase A has been used as a model to study nearly all aspects of protein structure and function, including protein folding and stability, disulfide bond formation, and molecular evolution (Blackburn and Moore, 1982; Beintema, 1987; Raines, 1998; Wedemeyer *et al.*, 2000; Chatani and Hayashi, 2001). Recent work has shown that certain homologs of RNase A have intriguing biological properties, such as toxicity to cancer cells (Ardelt *et al.*, 1991; Matousek and D'Alessio, 1991). Angiogenin has 35% identity to RNase A (Strydom *et al.*, 1985), and

uses its ribonucleolytic activity to promote angiogenesis, the growth of new blood vessels (Shapiro *et al.*, 1989; Shapiro and Vallee, 1989). Angiogenin has also been found to act as a transcription factor for rRNA (Xu *et al.*, 2003) as well as an antibacterial and antifungal protein involved in host defense (Hooper *et al.*, 2003). Recently, mutations in angiogenin have been linked to amyotrophic lateral sclerosis, a neurodegenerative disorder (Greenway *et al.*, 2006). These findings have led to an increasing interest in structure–function relationships of enzymes in the RNase A superfamily (Schein, 1997; Beintema and Kleineidam, 1998; Raines, 1998) and have made ribonucleases attractive targets and tools in disease research (Schein, 1997; Leland and Raines, 2001).

The extensive array of sequence data and structural information from ribonuclease homologs allows for further study of the interplay between sequence conservation and the structure/function of homologous proteins. Herein, systematic mutation of RNase A and a homolog, human angiogenin, reveals that these proteins largely share the same critical residues, but also have unique features. In general, the essential residues in each enzyme are well conserved and buried in the protein structure, though there are several exceptions. Although RNase A has been the object of extensive research (Blackburn and Moore, 1982; Raines, 1998; Chatani and Hayashi, 2001), we have identified many "new" critical residues.

To enable this work, we have developed a genetic selection system for the rapid identification of residues that are critical for the structure/function of ribonucleases. The selection system is based upon the ability of ribonucleases to cleave cellular RNA and cause cell death. Since enzymes in the RNase A superfamily have multiple disulfide

bonds, they are incapable of properly folding in the reducing environment in the cytosol of wild-type *E. coli*. We find, however, that ribonucleases are toxic to a mutant *E. coli* strain (Bessette *et al.*, 1999) that has a more oxidizing cytosol. By generating libraries of singly-mutated ribonuclease genes via error-prone PCR and selecting for inactive mutants, we identify those enzymic residues that are essential.

2.3 Experimental Procedures

Materials. *Taq* polymerase was from Promega (Cat. #M166B; Madison, WI). Mutazyme® DNA polymerase was from Stratagene (La Jolla, CA). *Escherichia coli* Origami™ B(DE3) cells and DH5α cells were from Novagen (Madison, WI). All other commercial chemicals and biochemicals were of reagent grade or better, and were used without further purification.

Plasmids. Genes encoding RNase A and human angiogenin were inserted into pSH12 (Park and Raines, 2000), which is a pGEX-4T3 based plasmid, at its *Nde*I and *Sal*I restriction enzyme sites. The resulting plasmids were named pGEX-RNase A and pGEX-Ang. Both plasmids code for a methionine residue at the start of the gene, designated Met(−1).

Random Mutation Libraries. Due to the inherent codon bias of the techniques used for generating random mutations during the PCR, libraries were produced in two complementary ways, using Mn^{2+} with *Taq* DNA polymerase (A/T→B/D mutation bias) and Mutazyme® DNA polymerase (C/G→D/H mutation bias).

Error-prone PCR with Taq DNA Polymerase. Error-prone PCR was performed by the methods described previously (Matsumura and Ellington, 2002), with the following modifications. Error-prone PCR reaction mixtures (50 μL) contained 1× Cloned *Pfu* Buffer (which was 20 mM Tris–HCl buffer at pH 8.8, containing $MgSO_4$ (2 mM), KCl (10 mM), $(NH_4)_2SO_4$ (10 mM), Triton® X-100 (0.1% w/v), and nuclease-free BSA (0.1 mg/mL); Stratagene, La Jolla, CA), dNTPs (200 μM), forward and reverse primers (200 nM each), template DNA (20 fmol), *Taq* DNA Polymerase (5 U), and varying amounts of 1× Mutagenic PCR buffer (which contained dTTP (0.8 mM), dCTP (0.8 mM), $MgCl_2$ (4.8 mM), and $MnCl_2$ (0.5 mM)). The amount of Mutagenic PCR buffer added to the reaction mixture affected the rate of mutation. (For example, adding 12.5 μL of 1× Mutagenic PCR buffer to a 50-μL PCR mixture was found to generate approximately one mutation per 500 bp of DNA, for a mutation rate of 0.2%.) After the PCR was performed (25 cycles at 95 °C for 30 s, 54 °C for 60 s, and 72 °C for 60 s), *Taq* DNA polymerase was eliminated by adding proteinase K (50 μg/mL), EDTA (5 mM), and SDS (0.5% w/v) at pH 8.5, and incubating for 15 min at 65 °C. The PCR product was then purified with the Wizard SV Gel and PCR Clean-Up kit (Promega; Madison, WI).

Error-prone PCR with Mutazyme. Mutazyme DNA Polymerase was used to perform error-prone PCR according to the protocol of the manufacturer (Stratagene; La Jolla, CA). Briefly, 50 μL PCR mixtures contained 1× Mutazyme Reaction Buffer, dNTPs (800 μM), forward and reverse primers (200 nM each), target DNA (10 or 100 ng), and Mutazyme DNA Polymerase (2.5 U). After the PCR was performed (30 cycles; 95 °C for 30 s, 54 °C for 30 s, 72 °C for 60 s), *Dpn*I (10 U; Promega, Madison, WI) was added to

digest template DNA, and the samples were incubated at 37 °C for 1–2 h. DNA

Polymerase was eliminated by adding proteinase K (50 µg/mL), EDTA (5 mM), and SDS

(0.5% w/v) at pH 8.5, and incubating for 15 min at 65 °C. The PCR product was then

purified with the Wizard SV Gel and PCR Clean-Up kit (Promega; Madison, WI).

Ligation of Mutagenized PCR Product. Purified mutagenized PCR products were

digested with *Nde*I and *Sal*I (20 U each) at 37 °C for 2 h. Plasmid pGEX-RNase A (20

µg) was digested with *Nde*I and *Sal*I (30 U each). (Unlike an empty expression vector,

any uncut pGEX-RNase A will be toxic to Origami™ cells at later steps, and hence will

not generate any colonies.) The restriction enzymes were inactivated by heating at 65 °C

for 15 min. Digests were purified with the Wizard SV Gel and PCR Clean-Up kit

(Promega; Madison, WI), and eluted with ddH$_2$O (25 µL). Additionally, cut pGEX-

RNase A was purified using S-500 Sephacryl HR (Pharmacia, Piscataway, NJ) to remove

the RNase A gene. S-500 Sephacryl (800 µL) was added to a microspin column. The

column was subjected to centrifugation at 2000g for 1 min. The tip of the column was

dried to remove any excess buffer, and the column was then placed into a new microfuge

tube. Cut plasmid DNA (20 µL) was added, and the column was subjected to

centrifugation again at 2000g for 1 min. The eluate was then run over another S-500

Sephacryl microspin tube as above to ensure that all of the excised fragment had been

separated from the plasmid. The linear plasmid (4 µg) and mutated PCR product (10 µL)

were added to a ligation reaction mixture (30 µL) containing 1× ligase buffer, DNA

ligase (6 U; Promega, Madison, WI), and additional ATP (1 mM). The ligation reaction

mixtures were placed at 14 °C overnight. Sodium acetate (0.3 M) and 3 volumes of ice-

cold ethanol were added to the reaction mixture, and the tube was placed at –20 °C for 1 h to precipitate the DNA. The ligated DNA was subjected to centrifugation at 10,000g for 10 min. The ethanol was removed by aspiration, and 250 μL of an ice-cold aqueous solution of ethanol (70% v/v) was added. The sample was subjected to centrifugation again. The ethanol was removed by aspiration, and the pellet was allowed to dry. The dry pellet was dissolved in ddH$_2$O (10 μL) and desalted over an AutoSeq G50 column (GE Healthcare, Piscataway, NJ). Ligated DNA was transformed by electroporation into competent *E. coli* DH5α cells to analyze the quality and randomness of the mutagenic PCR libraries. Cells were electroporated (1.80 kV, 200 Ω, and 25 μF) with 1 μL of the desalted and purified ligated DNA. SOC (1.0 mL) was added immediately, and the cells were allowed to recover at 37 °C for 1 h before being plated on LB agar containing ampicillin (100 μg/mL). Ligated DNA was transformed into competent *E. coli* Origami™ cells for selection experiments. Origami™ cells were electroporated as above, but allowed to recover for 1.5 h before being plated on LB agar containing ampicillin (100 μg/mL), kanamycin (15 μg/mL), and tetracycline (12.5 μg/mL). Plates were placed at 37 °C for 2 d.

Library Analysis. Colonies were grown in deep-well 96-well plates and DNA was isolated with the Wizard SV 96 Plasmid DNA Purification System (Promega, Madison, WI). Plasmid DNA was eluted in ddH$_2$O (100 μL). DNA sequencing was performed in 96-well plates. A DNA sequencing reaction mixture (5 μL) contained Big Dye 3.1 (0.5 μL), Big Buffer (0.75 μL), ddH$_2$O (0.75 μL), primer (0.5 μL from a 10 μM stock), and plasmid DNA (2.5 μL). Reaction mixtures were subjected to thermocycling (36

cycles; 96 °C for 20 s, 48 °C for 30 s, and 58 °C for 5 min). The sequencing reaction

mixtures were purified with the CleanSEQ Dye-terminator Removal kit (Agencourt

Bioscience, Beverly, MA). DNA sequences were obtained in the forward and reverse

directions. As an alternative to the expensive and time-consuming step of isolating

plasmid DNA, crude lysate was directly sequenced using a recently published heat-lysis

technique (Ganguly *et al.*, 2005) with the following modifications. Briefly, 1 mL cultures

grown in LB for 24 h were centrifuged at 1,500*g* for 15 min. The supernatant was

decanted, and cells were resuspended in ddH$_2$O (500 µL). The cells were spun again, then

washed again with ddH$_2$O (500 µL). After another centrifugation step, the supernatant

was carefully decanted, as the pellets were loose. Cells were suspended in ddH$_2$O (125

µL) and transferred to a 96-well PCR plate. The plate was sealed, and cells were placed

in boiling water for 5 min. The resulting crude lysate was centrifuged at 1,000*g* for 10

min. Sequencing reactions were performed as above, substituting 2.5 µL of crude lysate

for purified plasmid DNA. Sequence data were analyzed with the Staden software

package (http://Staden.sourceforge.net) and its Mutation Scanner module was used to

detect mutations automatically. Each sequence was then scanned manually for indels or

any other artifacts that would lead to a false positive (*e.g.*, a cloning artifact, star activity,

etc.).

  x-factor. Due to the mutational bias of error-prone PCR, the protein and nucleotide *x*-

factors were calculated for A/T→G/C, A/T→T/A, and C/G→T/A mutations (which are

saturated in our libraries).

Accessible Surface Area Calculations. The accessible surface area per amino acid residue was calculated for pdb entries 7RSA (Wlodawer *et al.*, 1988) and 1B1I (Leonidas *et al.*, 1999) using the module AREAIMOL in the program CCP4 (Collaborative Computational Project Number 4, 1994).

Assays of Thermal Stability. Circular dichroism spectroscopy was used to assess the thermal stability of angiogenin. A solution of angiogenin (20 μM) was heated from 25–80 °C in 3 °C increments, and the change in molar ellipticity at 215 nm was monitored after a 5-min equilibration at each temperature. Spectra were fitted to a two-state model for denaturation to determine the value of T_m.

2.4 Results and Discussion

Genetic Selection System for Ribonuclease A

Genetic selection can be used to identify positives from libraries as large as 10^{10}, allowing discoveries to be made that are not possible via manual screening (Woycechowsky and Hilvert, 2004). To identify non-functional variants in RNase A and angiogenin, it was necessary to develop a genetic selection system for these ribonucleases. A genetic selection system using *E. coli* would be ideal, given its high transformation efficiency (Dower *et al.*, 1988). RNase A and its homologs, however, are not toxic when produced in typical strains of *E. coli*. These enzymes contain three or four disulfide bonds, and cannot fold in the reducing environment of the *E. coli* cytosol (Figure 2.1) (Wedemeyer *et al.*, 2000). Recently, several strains of *E. coli* have been engineered to allow for disulfide bond formation in the cytosol (Derman *et al.*, 1993;

Prinz *et al.*, 1997; Bessette *et al.*, 1999). The *E. coli* Origami™ strain (Novagen,

Madison, WI) has mutations in both the thioredoxin reductase and glutathione reductase

genes that combine to enable disulfide bond formation in the cytosol. Consequently,

plasmid-encoded RNase A homologs are highly toxic to Origami™ cells, thus providing

a suitable genetic selection system to identify inactive enzyme variants (Figure 2.1).

Electrocompetent Origami™ cells used in this study had a transformation efficiency of

1.4×10^9, allowing for the examination of large mutant libraries. As ribonucleases are not

toxic to typical laboratory strains of *E. coli*, rDNA experiments can be performed with

DH5α cells before selecting for inactive ribonuclease variants with Origami™ cells.

RNase A and angiogenin are quite toxic to Origami™ cells (Figure 2.2). Leaky

expression of RNase A or angiogenin from a P_{tac} promoter is sufficient to kill cells. To

identify the threshold activity necessary to allow for cell growth, Origami™ cells were

transformed with plasmids encoding previously studied active-site variants of the

enzymes that display a range of ribonucleolytic activities. As an aside, the catalytic

activity of a ribonuclease is typically measured *in vitro* on well-defined substrates with

specific RNA sequences (Messmore *et al.*, 1995; Kelemen *et al.*, 1999). In contrast, a cell

contains a myriad of RNA sequences and structures that will be digested at different rates

(Axe *et al.*, 1999). Thus, even though decreases in the catalytic activity of ribonuclease

variants have been quantified for specific substrates, these values are only

approximations in Origami™ cells.

The catalytic activity of K41R RNase A is ~140-fold lower than wild-type RNase A

(Messmore *et al.*, 1995), yet this variant is toxic to Origami™ cells. An H12A active site

mutation in RNase A that causes a $>10^4$-fold decrease in ribonucleolytic activity (Thompson and Raines, 1994) allows for cell growth (Figure 2.2). Thus, the threshold activity for growth in our selection system is between ~0.01% and ~0.7% of wild-type activity. This threshold activity is an important value, as the number of "essential" residues in a protein varies depending on the stringency of selection (Axe et al., 1998). Weaker selection leads to more positives, but reveals little about which residues are the most important to protein structure/function, whereas more stringent selection leads to a smaller set of essential residues, but reveals no information about residues that possibly have a substantial, yet non-selectable impact on protein structure/function. The activity threshold of our selection system is similar to the system described previously for the bacterial ribonuclease, barnase, in which inactive variants had at least a ~10^3-fold decrease in activity (Axe et al., 1998), a stringency greater than for most other systematic mutation studies.

Angiogenin has a ribonucleolytic activity that has been measured to be more than five orders-of-magnitude lower than that of RNase A (Leland et al., 2002). Given the results above, it might be expected that angiogenin would not be toxic to Origami™ cells. Yet, angiogenin is toxic to Origami™ cells even without induction. The in vitro catalytic activity of angiogenin has generally been measured with small well-defined RNA substrates (Shapiro et al., 1986; Leland et al., 2002). Angiogenin may be a much more effective catalyst of the cleavage of specific RNAs, certain RNA secondary structures or RNA•protein complexes in cells. Indeed, it has been hypothesized that angiogenin might have a specific substrate in vivo (Shapiro et al., 1986; St Clair et al., 1987; Leland et al.,

2002). This substrate could be conserved between *E. coli* and humans, such as rRNA (St Clair *et al.*, 1987; St Clair *et al.*, 1988).

Because angiogenin is toxic to Origami™ cells, the activity threshold that would allow for growth was determined. A K40R substitution in the active site of angiogenin that decreases catalytic activity by ~50-fold (Shapiro *et al.*, 1989) allows for cell growth. Yet, when transcription of the gene is induced with 100 µM IPTG, the over-production of K40R angiogenin is cytotoxic. H13A angiogenin, which has $\geq 10^4$ lower ribonucleolytic activity (Shapiro and Vallee, 1989), allows for cell growth even when induced by 100 µM IPTG (Figure 2.2).

To compare angiogenin and RNase A more directly, all selection experiments described herein were performed in the absence of IPTG for RNase A and the presence of 100 µM IPTG for angiogenin. Nevertheless, the threshold activity for this selection system could be tuned to almost any desirable level by altering the concentration of the inducer or by changing the promoter in the plasmid encoding for the enzymes.

Close inspection of Figure 2.2 shows that a small number of colonies grow from transformations of plasmids that normally should cause cell death. These colonies appear at a rate of $\sim 10^{-6}$. DNA sequence analysis of the angiogenin or RNase A gene from these rare colonies was performed to determine the basis for their growth. They are due to mutations in the gene encoding for RNase A or angiogenin in the plasmids (including insertions–deletions (indels)) or due to recombination of the plasmid (data not shown). Prior to transformation, plasmids were prepared in wild-type *E. coli*. It is likely that these

low-level mutations are due to the background rate of errors produced by the *E. coli* replication machinery (Fujii *et al.*, 1999).

Creation of Single-base Substitution Libraries

Error-prone PCR was used to generate libraries of mutant RNase A and angiogenin genes. Mutations occurred throughout each gene—no mutational hot spots were detected (Figure 2.3). The gaps in Figure 2.3 are spots in which no mutations were detected, however, these would be likely filled in if more sequences were obtained. Indeed, mutations in these apparent gaps were obtained during selection (*vide infra*). The percentage of indels generated by error-prone PCR was low (Table 2.1), as these mutations would inevitably lead to false positives during a selection for the absence of ribonucleolytic activity. To overcome the inherent mutational bias of specific error-prone PCR techniques (Rowe *et al.*, 2003; Neylon, 2004; Vanhercke *et al.*, 2005), two libraries of mutants were prepared for each gene. First, *Taq* polymerase and Mn^{2+} were used to generate mutations (Cadwell and Joyce, 1992; Matsumura and Ellington, 2002). This technique dramatically favors A/T→G/C and C/G→T/A transitions as well as A/T→T/A transversions (Matsumura and Ellington, 2002; Vanhercke *et al.*, 2005). PCR products were double-digested and readily ligated into a pGEX-based plasmid to generate libraries that contain $\sim 10^6$ variants ($\sim$1,000-fold larger than needed for 1X coverage of the genes; Table 2.1). The mutational bias and randomness of the prepared mutant libraries were analyzed in *E. coli* DH5α cells (*nb*: RNase A and angiogenin are not toxic to this strain of *E. coli*). In agreement with previous results, using *Taq* polymerase in the presence of

Mn^{2+} leads to a large excess of A/T→G/C mutations, but C/G→T/A and A/T→T/A mutations are also well represented. A/T→C/G, C/G→A/T, and C/G→G/C mutations are nearly absent from the libraries (Table 2.2). This mutational bias would lead to fewer potential amino acid changes than are possible under ideal conditions in which all possible single-base substitutions are represented equally.

To partially resolve this problem, error-prone PCR libraries were also prepared with *Mutazyme* polymerase (Stratagene, La Jolla, CA), which is biased towards C/G→D/H mutations (Cline and Hogrefe, 2000). Using both *Taq* and *Mutazyme* polymerases to create more diverse libraries has been described recently (Rowe *et al.*, 2003; Neylon, 2004; Vanhercke *et al.*, 2005). We find that *Mutazyme* polymerase is biased slightly towards C/G→D/H mutations (and less biased than indicated by the manufacturer (Cline and Hogrefe, 2000)). Moreover, *Mutazyme* polymerase is biased specifically towards C/G→T/A mutations. A/T→G/C and A/T→T/A mutations are also well represented (Table 2.2). Thus, for both *Taq* and *Mutazyme* polymerases, the three most common mutations, on average, are A/T→G/C, A/T→T/A, and C/G→T/A, but their proportions are altered. A/T→C/G, C/G→A/T, and C/G→G/C mutations are underrepresented in the libraries, but are more abundant in the *Mutazyme* libraries than the *Taq* libraries. Thus, it is difficult to obtain all possible single-base substitutions at each residue of RNase A and angiogenin.

Single-base substitutions allow one codon to be altered to nine other codons. Due to the redundancy of the genetic code, amino acid residues can be replaced with, on average, 6.1 other residues. Because the mutational bias of error-prone PCR favors some

types of mutations over others, this number is reduced further. For example, Lys-41 in RNase A is encoded by an AAG codon. A rare A→C mutation to make a CAG or ACG codon (encoding glutamine or threonine, respectively) would likely inactivate the enzyme, but these mutations are not obtained with the selection system (*vide infra*). Nevertheless, we still select for three inactivating substitutions (to methionine, glutamate, and asparagine) at position 41 (a fourth mutation, to arginine, has been shown previously to decrease catalytic activity by only 140-fold (Messmore *et al.*, 1995), which is not sufficient to allow for cell growth). Even with mutational bias, much diversity can be obtained at each position.

Libraries were set up to attain about one mutation per gene. Under our conditions, the *Taq* libraries had a mutation rate of ~0.24% (1 mutation per ~400 bp), whereas the *Mutazyme* libraries had a mutation rate of ~0.14% (1 mutation per ~700 bp) (Table 2.1). Because this is an average mutation rate, some sequences contained zero, two, or more mutations (Table 2.1). Clones with zero mutations are toxic in our selection system, and do not affect results. Clones with multiple missense mutations were excluded from the analysis, as it is unclear which mutation or combination thereof is important. Approximately 30% of all mutations are silent. Many sequences with two or more mutations contain only one coding mutation. No clones were isolated with only a silent mutation via genetic selection, indicating that rare codons likely do not affect this system.

Error-prone PCR offers certain advantages over other methods for systematic mutagenesis. Other methods can be arduous, such as using primer-based methods to mutate each residue (Axe *et al.*, 1998; Campbell-Valois *et al.*, 2005) or using amber-

suppression strains with a library of clones containing amber codons (Rennell *et al.*, 1991; Markiewicz *et al.*, 1994; Suckow *et al.*, 1996). In contrast, error-prone PCR is a facile technique that can be used to generate a library of mutations. Still, one evident drawback of error-prone PCR is its inherent mutational bias, a problem that can be rectified somewhat by using *Taq* and *Mutazyme* polymerases to generate libraries (Vanhercke *et al.*, 2005). As more error-prone PCR technologies are developed, this problem could be resolved completely. Other drawbacks for the use of error-prone PCR in experiments in which the absence of function is necessary for growth, as herein, are that clones containing more than one missense mutation must be excluded from analysis and that false positives due to indels or other artifacts represent a significant amount of total positives. In experiments in which function is required for growth, these false positives do not interfere with selection experiments and multiple mutations can be desirable (Guo *et al.*, 2004). Another drawback with error-prone PCR is that it is difficult to know with certainty that a specific mutation is found in a library. For example, an F8I RNase A variant should be present in our libraries, as it requires a common A/T→T/A mutation in the gene coding for RNase A. An F8S substitution inactivates RNase A and allows for growth in Origami™ cells (*vide infra*), but an F8I substitution in RNase A was not isolated and thus it can only be assumed that it is not sufficiently deleterious to enzyme structure/function. Despite these drawbacks, error-prone PCR can be used to identify quickly and globally those residues that are essential for protein structure/function, as long as a suitable screening or selection system is used. Reagents for error-prone PCR are inexpensive and the protocols are neither time-consuming nor

difficult. Libraries can be created in a few days, after which the only limiting factors on experiments are the number of colonies that can be cultured at a time, and the throughput of DNA sequencing and analysis.

Selection for Inactivating Mutations

Error-prone PCR libraries were transformed into Origami™ cells. Colonies were picked after 2 d of growth at 37 °C (Origami™ cells grow slower than wild-type *E. coli*). It is possible that allowing colonies to grow for longer could reveal ribonuclease variants with enough catalytic activity to slow cell growth, but not enough to kill cells. Thus, a standard growth time is important. Another important factor is the growth temperature. The results presented herein are for colonies that grew at 37 °C, although experiments were also performed at lower temperatures. Fewer colonies are obtained at lower temperatures (data not shown), presumably because a substitution would then have to reduce the conformational stability of the enzyme more drastically to allow for colony growth.

Colonies were picked and grown in 96 x 1-mL cultures for 24 h at 37 °C. Plasmid DNA was isolated using 96-well miniprep kits and the RNase A or angiogenin gene was sequenced in both directions. As an alternative method that avoids time-consuming and expensive minipreps, a recently described heat lysis technique allowed for the direct sequencing of crude lysates of overnight cultures (Ganguly *et al.*, 2005). Sequencing data were aligned and mutations were detected with the Staden software package

(http://staden.sourceforge.net) (Staden *et al.*, 2000). Each sequence was then scanned manually for indels or other artifacts.

RNase A and Angiogenin – A Global View of Inactivating Mutations

The structure/function of RNase A is quite tolerant of single amino acid substitutions. Mutations at only 23 of the 124 residues of RNase A inactivate the enzyme (Figures 2.4 and 2.5; Table 2.3). Moreover, only six residues in the enzyme appear to be wholly intolerant of mutation. The chance of randomly replacing an amino acid residue in RNase A and inactivating the enzyme is 12.7%. This value, which has recently been dubbed the "*x*-factor" (Guo *et al.*, 2004), includes the generation of stop codons. Due to the degeneracy of the genetic code, the probability of inactivating RNase A with a single nucleobase substitution (the nucleotide *x*-factor) is 9.4%. The structure/function of angiogenin is slightly more sensitive to mutations. The *x*-factor for angiogenin is 16.2% (11.5% on the nucleotide level). This greater sensitivity is due, at least in part to angiogenin having lower ribonucleolytic activity than RNase A. In Origami™ cells, inducing the expression of the angiogenin gene with IPTG likely brings absolute ribonucleolytic activity close to (but likely not equal to) that achieved with just the leaky expression of RNase A (Figure 2.2). Mutations at just 29 of the 123 residues of angiogenin inactivate the enzyme. Moreover, 23 of those 29 residues are tolerant of some substitutions.

The low probability for protein inactivation is similar to a study that revealed that ~5% of single amino acid replacements inactivated barnase (Axe *et al.*, 1998) and to a

study that showed that ~16% of amino acid changes inactivated T4 lysozyme (Rennell *et al.*, 1991). It has been noted that the *x*-factor may vary with protein size or surface-to-volume ratio (Guo *et al.*, 2004). RNase A and angiogenin are small ~14 kDa enzymes (124 and 123 residues, respectively) that are similar in size to barnase (110 residues) and T4 lysozyme (164 residues). The *x*-factor of each enzyme in this group does indeed correlate with protein size. However, it is likely that the major contributing factor is the activity threshold used in the selection. Barnase mutations were identified only if they reduced enzymatic activity by at least ~10^3 fold (Axe *et al.*, 1998). The selection system described herein requires greater than a ~140-fold reduction in the ribonucleolytic activity of RNase A to allow for growth and greater than a ~50-fold reduction in the ribonucleolytic activity of angiogenin (Figure 2.2). T4 lysozyme activity had to be decreased by ~30-fold to be scored as defective (Rennell *et al.*, 1991). The 33-kDa human 3-methyladenine DNA glycosylase has an *x*-factor of 34 ± 6%, and under the conditions of the assay, mutations that decreased wild-type activity by less than ~20-fold were identified (Guo *et al.*, 2004). Thus, the protein *x*-factor largely depends on the definition of "enzyme inactivation". The activity threshold is often set arbitrarily, due to constraints of the selection or screening method used to identify positives. Systematic mutation studies have revealed the percentage of residues that are essential at various levels of enzyme inactivation. Extrapolation of these values to what would occur *in vivo* is, however, difficult (Guo *et al.*, 2004).

In all selection systems, residues are identified as essential only if they are critical for the function that is being selected for or against. Given that a protein can have many

functions, protein-interaction partners, targeting sequences, *etc.*, the essential residues identified for a specific function constitute a subset of total residues in a protein that are necessary for all its functions. In our assay, mutations were identified only if they severely decrease the ribonucleolytic activity of RNase A or angiogenin. *In vivo*, both enzymes would also have essential residues that are involved in protein–protein interactions, such as with the ribonuclease inhibitor protein (Dickson *et al.*, 2005) or the angiogenin receptor (Hu *et al.*, 1997), and other biologically-relevant functions, such as angiogenesis for angiogenin (Acharya *et al.*, 1994). In addition, it is possible that many substitutions that decrease enzymatic activity but do not reach the activity threshold of our selection system would be under selective pressure *in vivo*. Then again, there could be many compensatory changes *in vivo* that could render these residues non-essential. Thus, we have identified the residues that are most critical for ribonucleolytic activity, but the total number of residues critical for all functions of each enzyme is likely to be higher. A recent analysis of the chimpanzee and human genomes found that, on average, ≥77% of amino acid changes are deleterious enough to be eliminated by purifying selection (Chimpanzee Sequencing and Analysis Consortium, 2005). (The number of synonymous (or silent) mutations compared to nonsynonymous (or amino acid altering) mutations for human angiogenin *versus* chimpanzee angiogenin falls within this range, though there are too few changes for this specific case to be reliable.) In general, if 77% of amino acid changes are deleterious enough to be removed by natural selection and systematic mutagenesis experiments reveal that ~34% of mutations are deleterious enough to decrease activity to ~5–10% wild-type activity (Guo *et al.*, 2004), then there

exists a gap that could arise from at least three possibilities. First, the level of inactivation for an enzyme that is selected against in a population of organisms is, on average, less than ~20-fold. Second, there are a significant number of residues that are critical for protein–protein interactions and other biological functions that are not accounted for when genetic selection experiments are performed to study a particular protein function under a specific set of conditions. Third, the few proteins that have been a part of systematic mutagenesis studies are not representative of most other proteins. A combination of these possibilities may be likely, and this issue awaits further study.

RNase A – Essential Residues

To simplify analysis, the set of inactivating mutations was divided into four basic groups, similar to those found for a high-throughput mutagenesis study on barnase (Axe *et al.*, 1998). Group I contains mutations that alter residues directly involved in catalysis. Group II consists of substitutions of buried residues. Group III comprises mutations in which proline is the only residue found at a specific position. Group IV contains substitutions of essential half-cystines. Barnase lacks disulfide bonds, thus this group is new to our study. There is crosstalk among the groups, for example, many buried residues (Group II) affect catalysis by interacting with a residue directly involved in catalysis (Group I).

His-12 and His-119. There are three Group I replacements in RNase A. The two extensively studied active-site histidine residues (His-12 and His-119) are essential (Crestfield *et al.*, 1963; Raines, 1998). His-12 is thought to abstract the proton from the

2'-hydroxyl group on the ribose ring, allowing attack on the phosphoryl group during catalysis. His-119 adds a proton to the 5'' oxyanion during RNA cleavage. Both of these residues have been well studied, and mutations at either residue have been shown to reduce enzymatic activity drastically (Thompson and Raines, 1994). Isolating mutations at these positions confirms that error-prone PCR and the Origami™ selection system described herein can be used to identify inactive ribonuclease variants.

Lys-41. Several substitutions at residue 41 inactivate RNase A. Lys-41 has been shown previously to be critical for ribonucleolytic activity, as it donates a hydrogen bond to the pentavalent transition state (Messmore *et al.*, 1995). The K41A RNase A variant has a k_{cat}/K_M that is ~10^4-fold lower than the wild-type enzyme (Thompson *et al.*, 1995). Yet, Lys-41 can be replaced by arginine with only a ~10^2-fold decrease in catalytic activity (Messmore *et al.*, 1995). Gratifyingly, a K41R RNase A variant was not isolated, but K41M, K41N, and K41E substitutions were – all of which would be expected to cause decreases in catalytic activity sufficient to be identified as inactive in our selection system. Two other possible mutations at position 41 were not isolated due to the mutational bias of error-prone PCR. Both the K41Q and K41T substitutions would likely inactivate RNase A, however, these substitutions are encoded by CAG and ACG codons, which would require rare A→C mutations in the AAG codon encoding lysine.

Group II Residues (Buried Residues)

The various clusters in the hydrophobic core of RNase A have been well described (Lenstra *et al.*, 1977; Beintema, 1987; Beintema *et al.*, 1988; Kolbanovskaya *et al.*, 1992;

Kolbanovskaya *et al.*, 1993; Chatani and Hayashi, 2001; Chatani *et al.*, 2002), though the residues that contribute the most to RNase A structure/function are largely unknown. With the Origami™ selection system, the most important subset of these previously described residues has been identified, including residues whose importance is not obvious from the analysis of sequence alignments or crystal structures. We isolate mutations in the hydrophobic core of RNase A that inactivate the enzyme at positions 8, 44, 46, 54, 57, 73, 75, 97, 106, 108, 109, and 120. Many of the residues are in regions of the protein that have been shown previously to be important for folding and protein stability (Matheson and Scheraga, 1978; Matheson and Scheraga, 1979; Montelione and Scheraga, 1989). Hydrophobic core residues typically tolerate substitution with other similar hydrophobic residues, but do not tolerate replacement with polar and/or charged amino acids (Bowie and Sauer, 1989; Bowie *et al.*, 1990; Rennell *et al.*, 1991; Markiewicz *et al.*, 1994; Axe *et al.*, 1996; Axe *et al.*, 1998; Balaji *et al.*, 2003). Most substitutions in the hydrophobic core that were identified via genetic selection had a hydrophobic amino acid residue replaced with a polar or charged residue. In several cases, large residues were replaced with much smaller residues. Polar residues whose hydrogen-bonding potential has been saturated are allowed in the hydrophobic core (Bowie *et al.*, 1990). We find several examples of mutations to these residues that disrupt the structure/function of RNase A.

Phe-8. The side chain of Phe-8 forms a cation–π interaction with essential catalytic residue His-12 (Shoemaker *et al.*, 1990). It is also involved in the main cluster of the hydrophobic core of the protein (Kolbanovskaya *et al.*, 1993). Both F8S and F8V

substitutions inactivate RNase A sufficiently to allow for growth in our selection system. Previous work on RNase S (a form of RNase A in which the S-peptide (residues 1-20) and S-protein (residues 21-124) are associated non-covalently) showed that when Phe-8 is replaced with an alanine residue in the S-peptide, essential residue Phe-120 rotates to fill in the nascent cavity (Ratnaparkhi and Varadarajan, 2000). Replacing Phe-8 with serine or valine could cause similar effects. On a similar note, the F8W variant of RNase A, created for the purposes of studying local and global unfolding in the enzyme, was found to lack ribonucleolytic activity (Navon *et al.*, 2001).

Asn-44. The side chain of Asn-44 accepts hydrogen bonds from two critical residues involved in catalysis—His-12 and Lys-41. In addition, the main-chain oxygen and nitrogen of Asn-44 form hydrogen bonds with the main-chain nitrogen and oxygen of the essential residue Cys-84, as these residues are located in an antiparallel β-sheet. Asn-44 is buried in RNase A and conserved universally, but has not been reported to be essential for catalysis (barring the likely erroneous results on 63-residue RNase A analogs (Gutte, 1978)). Only the A44Y variant of RNase A was isolated. Since Asn-44 is completely buried, it is possible that substitution with tyrosine at this position is particularly disruptive due to its large size.

Phe-46. Phe-46 is a critical residue in the hydrophobic core of RNase A, linking two separate clusters of hydrophobic residues (Chatani *et al.*, 2002). Phe-46 is also a chain-folding initiation site (CFIS) residue, important for the rapid folding of the enzyme (Chatani *et al.*, 2002; Kadonosono *et al.*, 2003). Replacing Phe-46 with glutamate or lysine in RNase A has been shown to decrease greatly the conformational stability of the

protein, whereas replacement of Phe-46 with valine has less of an effect (Chatani *et al.*, 2002; Kadonosono *et al.*, 2003). A F46Y substitution in RNase A retains nearly full enzymatic activity, but has a T_m value that is 9 °C less than that of the wild-type protein (Markert *et al.*, 2001). F46S and F46C substitutions were isolated with the selection system. Clones that encode for isoleucine, leucine, and tyrosine at position 46 should be present in our library, but are not isolated, suggesting that these mutations are less disruptive (Table 2.3).

Val-54 and Val-57. Substitutions of Val-54 and Val-57 with anionic residues inactivated RNase A. These residues have not been previously studied, though several have noted that they comprise part of the hydrophobic core of RNase A (Kolbanovskaya *et al.*, 1992; Kolbanovskaya *et al.*, 1993; Chatani *et al.*, 2002). In addition, the region of RNase A encompassing residues 54 and 57 has been shown to be important for its folding (Montelione and Scheraga, 1989). Val-54, Val-57, and essential residue Cys-58 form a (*i, i + 3, i + 4*) triplet in the crystal structure of RNase A (Lenstra *et al.*, 1977).

Tyr-73 and Ile-108. The side-chain of Tyr-73 is largely buried, but does extend to the surface of RNase A. Interestingly, Tyr-73 is not well conserved. Among the subset of ribonucleases that contain the Cys-65–Cys-72 disulfide bond, position 73 is always histidine, tyrosine, or phenylalanine (in that order of abundance). Two groups of ribonucleases that lack the Cys-65–Cys-72 disulfide bond are angiogenins and frog ribonucleases. Angiogenins contain arginine at the equivalent position, whereas frog ribonucleases have leucine. It has been shown previously that residues 73 and 108 are part of an evolutionary coupled replacement (Beintema *et al.*, 1988). Pancreatic

ribonucleases with His-73 usually contain Ile-108, whereas pancreatic ribonucleases with Tyr-73 have Val-108, although there are exceptions. The main chains of residue 73 and 108 form two hydrogen bonds to each other in an antiparallel β-sheet in the crystal structure of RNase A. Val-108 is also an essential residue in RNase A, showing the importance of this pair of residues to the structure/function of RNase A. We find that mutations at Val-108 to glutamate or glycine inactivate RNase A. Previous work revealed that Val-108 is a critical residue involved in the hydrophobic core of RNase A and that it serves as CFIS residue (Torrent *et al.*, 1999; Torrent *et al.*, 2001). A V108G mutation in RNase A significantly destabilizes the enzyme (Coll *et al.*, 1999; Torrent *et al.*, 1999; Torrent *et al.*, 2001).

Ser-75 and Ile-106. The side-chain hydroxyl of Ser-75 forms a hydrogen bond with the main-chain nitrogen of essential residue Ile-106 in the hydrophobic core of RNase A. In addition, the main-chain nitrogen of Ser-75 forms a hydrogen bond with the main-chain oxygen of Ile-106. It has been shown previously that Ile-106 is important in RNase A, as a substitution to alanine lowers the T_m value of the enzyme by 14 °C (Coll *et al.*, 1999). Ser-75 has not been studied previously. Several have noted the possibility that Ser-75 is important for the conformational stability of RNase A (Beintema, 1987; Beintema *et al.*, 1988), but we have provided the first evidence showing that this residue is indeed critical, and that substitutions at this residue can cause deleterious effects.

Tyr-97. The side chain of Tyr-97 donates a hydrogen bond to the main-chain oxygen of active-site residue Lys-41. A previous study found that the replacement of Tyr-97 with alanine or glycine lowers the value of k_{cat}/K_M ~500-fold, and possibly more significantly,

lowers the value of T_m by 34 °C (Eberhardt *et al.*, 1996). Replacement of Tyr-97 with phenylalanine lowers the value of T_m by 10 °C, but only lowers k_{cat}/K_M by 3-fold (Eberhardt *et al.*, 1996). Y97N and Y97C variants of RNase A were isolated with our selection system. It seems unlikely that either of these smaller side-chains would be able to form a hydrogen bond with Lys-41 or fill the empty volume created by the replacement of a buried residue. A Y97F substitution is likely present in our library, but was not isolated via selection, probably due to its lesser effects on catalysis and thermal stability (Table 2.3). Because a Y97F substitution is just slightly deleterious (Eberhardt *et al.*, 1996), the formation of a hydrogen bond from Tyr-97 to Lys-41 is likely not the most essential function for residue 97. We also find indirect evidence for this assertion – when the cysteine residues of the Cys-40–Cys-95 disulfide bond are replaced with serine residues, the Tyr-97–Lys-41 hydrogen bond is lost (Shimotakahara *et al.*, 1997; Chatani and Hayashi, 2001). Yet, we do not select for any mutations at residue 40 or 95, even though substitutions at these positions would also decrease the conformational stability of the enzyme significantly (*vide infra*).

Ala-109. An A109D substitution in RNase A inactivates the enzyme sufficiently to allow for growth in Origami™ cells. Ala-109 is in van der Waals contact with catalytic residue His-119 and could be involved in imparting substrate specificity in the B_2 subsite of RNase A (Holloway *et al.*, 2005) (B.D. Smith, J. E. Lee and R.T. Raines, unpublished results). The side chain of Ala-109 is within 4 Å of the adenosine nucleobase in the B_2 subsite of an RNase A•d(ApTpApApG) complex (Fontecilla-Camps *et al.*, 1994). Ala-109 has been of some interest in previous work with cytotoxic ribonucleases, as residue

109 forms key contacts with the ribonuclease inhibitor protein (RI). An A109R RNase A variant was designed to cause disruption of the RI•RNase A complex (Leland *et al.*, 1998). Although its catalytic activity was not measured, the enzyme was not cytotoxic as was expected (a condition that requires ribonucleolytic activity). Thus, it seems likely that the lack of cytotoxicity was due to inactivation of the enzyme. An A109R mutation in human pancreatic ribonuclease decreases catalytic activity by ~100-fold (R.J. Johnson and R.T. Raines, unpublished results). Ala-109 is also a part of a CFIS, and an A109G variant of RNase A has slightly lower thermal stability (Coll *et al.*, 1999). Finally, Ala-109 is well conserved among diverse ribonucleases, though frog ribonuclease have a threonine or lysine residue in this position (and have different base specificities in the B_2 subsite) (Leu *et al.*, 2003).

Phe-120. The main-chain nitrogen of Phe-120 forms a hydrogen bond with a nonbridging oxygen of the pentavalent transition state. Previous work showed that replacement of Phe-120 with glutamate or alanine decreased catalytic activity by <50-fold for both enzymes, and lowered the T_m values of the proteins by 15 °C and 12 °C, respectively (Tanimizu *et al.*, 1998). An F120S variant was isolated via genetic selection. Substitution of Phe-120 with the smaller serine residue would likely cause detrimental effects to the conformational stability and catalytic activity of RNase A. The enzyme likely tolerates other changes to this residue (*i.e.*, genes encoding for isoleucine, leucine, and tyrosine at position 120 should be present in the library, but were not isolated via selection; Table 2.3). Residue 120 is semi-conserved in the RNase A superfamily. Angiogenin and many other ribonucleases contain leucine in the equivalent position.

Pronghorn and giraffe ribonuclease have tyrosine in this position (Beintema, 1987). As for RNase A, the only substitution that was isolated for angiogenin at this position was to serine (*vide infra*), thus large non-polar residues are favored at position 120.

Hydrophobic nuclei. Several hydrophobic nuclei ($\gamma 1$, $\gamma 2$, and $\gamma 3$) and microclusters in RNase A have been identified (Kolbanovskaya *et al.*, 1992). In gratifying agreement, the residues that we identified as being essential in our genetic selection system coincide with the most important hydrophobic nuclei. Essential residues Phe-8, His-12, Val-54, Val-57, Cys-58, Tyr-73, Ile-106, Val-108, Cys-110, and Phe-120 constitute a subset of residues located in the well-conserved hydrophobic nucleus $\gamma 1$. The second hydrophobic nucleus, $\gamma 2$, is smaller and not well conserved. The only residues that were identified as being essential in this nucleus are Cys-65 and Cys-72, which form a disulfide bond that is important for the conformational stability of RNase A. The third hydrophobic nucleus, $\gamma 3$, is similar to $\gamma 1$ in that its residues are well conserved, its residues make a high number of contacts (on average), and the temperature factors of its side-chain hydrocarbon atoms are low (on average) (Kolbanovskaya *et al.*, 1992). Mutations were isolated at a subset of the residues involved in this cluster – Cys-26, Asn-44, Phe-46, Cys-84, and Tyr-97. Thus, our results not only agree well with previous work on the hydrophobic core of RNase A, but also build upon the work, as we have identified which residues are likely to be the most important in each hydrophobic nucleus.

Group III Residues (Proline Substitutions)

Proline substitutions are well known to be deleterious to protein structure (Rennell *et al.*, 1991; Markiewicz *et al.*, 1994; Axe *et al.*, 1998). There are only two examples of Group III mutations in RNase A—residues 60 and 82. Residue 60 lies between an α-helix and a β-sheet. The main-chain nitrogen of residue 60 forms a hydrogen bond to the main-chain oxygen of critical residue Val-57. Residue 82 lies in the middle of a β-sheet. In addition, the backbone of residue 82 forms two hydrogen bonds to the main-chain atoms of essential residue Phe-46. Proline can be substituted only at specific places in the enzyme, as we employ single-nucleotide substitutions. A greater number of Group III mutations would be obtained if proline were substituted for each residue in the enzyme.

Group IV Residues (Essential Half-cystines)

Four cysteines that contribute to the two most important disulfide bonds in the enzyme (Cys-26–Cys-84 and Cys-58–Cys-110) (Klink *et al.*, 2000; Wedemeyer *et al.*, 2000) appear to be wholly intolerant of substitution. *In vitro*, C26A/C84A RNase A ($T_m = 27\ °C$) and C58A/C110A RNase A ($T_m = 24\ °C$) have T_m values that are ~35 °C lower than that of the wild-type enzyme (Klink *et al.*, 2000). It is not surprising that substitutions at these residues were identified in this study, as genetic selection experiments were performed at a temperature, 37 °C, at which both these enzymes would be substantially unfolded.

RNase A has two other disulfide bonds (Cys-65–Cys-72 and Cys-40–Cys-95). Previous studies have shown that substitutions at these cysteine residues with alanine

residues reduce the T_m values of these proteins to ~40 °C, and lower catalytic activity by 40-fold (Klink *et al.*, 2000). Other work has shown that RNase A variants lacking either disulfide bond are stable at room temperature and remain catalytically active (Laity *et al.*, 1993). In our genetic selection system, we isolated substitutions at the cysteine residues in the Cys-65–Cys-72 disulfide bond, but not the Cys-40–Cys-95 disulfide bond. This result is surprising, because the Cys-40–Cys-95 bond is absolutely conserved in the RNase A superfamily, whereas the Cys-65–Cys-72 bond is not (Table 2.3). Given that an RNase A variant lacking the Cys-40–Cys-95 disulfide bond has a T_m value greater than 37 °C, is catalytically active, and only has local disorder around the disulfide bond (Laity *et al.*, 1993; Pearson *et al.*, 1998), it is not surprising that substitutions were not isolated at either residue 40 or residue 95 (Figure 2.4). An RNase A variant lacking the Cys-65–Cys-72 disulfide bond also has a T_m value greater than 37 °C and is catalytically active (Laity *et al.*, 1993), thus it seems to be surprising that mutations at these residues were isolated with our selection system. The Cys-65–Cys-72 disulfide is, however, particularly important in the oxidative folding pathway of RNase A (Shin *et al.*, 2003), which could account for its decreased tolerance to mutation. Still, the Cys-65–Cys-72 disulfide bond is somewhat tolerable to changes, as only two substitutions per residue were identified with our selection system. Mutations that should be present in our libraries (such as Cys-65 to serine or arginine or Cys-72 to tyrosine or arginine) are not isolated (Table 2.3).

Implications

Recently, several homologs of RNase A have been found to be cytotoxic to cancer cells. The frog ribonuclease, Onconase™, is in clinical trials for the treatment of malignant mesothelioma (Mikulski *et al.*, 2002). It has also been discovered that RNase A variants can be toxic to cancer cells, if they have been engineered to evade RI (Leland *et al.*, 1998; Leland and Raines, 2001). There is now an increasing interest in developing cytotoxic mammalian and human ribonucleases (Rutkoski *et al.*, 2005), which could have fewer side effects or problems with immunogenicity. Changes to the essential residues identified herein clearly should be avoided, as ribonucleolytic activity is necessary for cytotoxicity. Indeed, RNase A variants at Ala-109 have been generated to evade RI, but have been found to not be cytotoxic (Leland *et al.*, 1998).

Angiogenin – Essential Residues

The set of substitutions that inactivate angiogenin largely intersect with the set for RNase A. The following discussion focuses on the differences found in angiogenin. The catalytic activity of angiogenin is lower than that of RNase A. Although the gene coding for angiogenin was expressed at a higher level in our selection system to compensate for this difference (Figure 2.2), it is possible that the absolute level of ribonucleolytic activity obtained with angiogenin remains lower than that obtained by just the leaky expression of RNase A. Some of the differences between angiogenin and RNase A are likely due to this phenomenon. To our knowledge, the thermal stability of angiogenin had not been measured previously. Via circular dichroism spectroscopy, we find that the T_m value of

angiogenin in PBS is 63.6 ± 0.6 °C. The T_m value for RNase A in PBS is 64 ± 2 °C

(Rutkoski et al., 2005). Thus, it is likely that few of the excess substitutions that

inactivate angiogenin would result from changes in thermal stability. Nevertheless, some

of the differences between angiogenin and RNase A cannot be explained by either of

these effects.

Group I Residues (Catalytic Residues)

All three residues involved in catalysis in RNase A are essential for the

ribonucleolytic activity of angiogenin.

Group II Residues (Buried Residues)

The hydrophobic cores of angiogenin and RNase A are similar, though angiogenin

appears to rely more on residues in the γ-1 and γ-3 hydrophobic nuclei, and less on

residues in the γ-2 nucleus for conformational stability (*vide supra*). This reliance could

arise because angiogenin lacks the loop containing the Cys-65–Cys-72 disulfide bond and

other important hydrophobic residues in the γ-2 nucleus, and instead contains a loop

necessary for its promotion of angiogenesis (Raines et al., 1995). Substitutions in the γ-1

nucleus that can inactivate angiogenin occur at residues 9, 13, 44, 46, 53, 56, 57, 72, 78,

103, 112, and 115. Substitutions at residues Thr-44, Ile-46, Val-78, and Pro-112

(corresponding to Thr-45, Val-47, Ile-81, and Pro-117 in RNase A) inactivate

angiogenin, but not RNase A.

Thr-44. Substitutions of Thr-44 in angiogenin have been shown to decrease catalytic activity by up to 50-fold and affect substrate specificity (Curran *et al.*, 1993). This threonine residue is buried in both angiogenin and RNase A. The equivalent residue in RNase A, Thr-45, imparts substrate specificity as it forms hydrogen bonds to the nucleobase in the B_1 subsite of the enzyme (delCardayré and Raines, 1994). Thr-45 could also be involved in ground-state destabilization during catalysis (Kelemen *et al.*, 2000). No substitutions were isolated at residue 45 in RNase A via genetic selection, but T44K and T44P substitutions in angiogenin were isolated.

Ile-46 and Val-78. Ile-46 and Val-78 are within 5 Å of each other. Val-78 is in van der Waals contact with essential residue Phe-45. Ile-46 interacts with critical hydrophobic core residue Ile-53. In addition, the main-chain nitrogen of Ile-46 forms a hydrogen bond with the main-chain oxygen of active-site residue His-13. Intriguingly, a substitution of Ile-46 in angiogenin has been linked to amyotrophic lateral sclerosis (Greenway *et al.*, 2006), confirming the importance of this residue to the function of angiogenin *in vivo*.

Pro-112. Replacement of Pro-117 with alanine in RNase A destabilizes the enzyme (Juminaga *et al.*, 1998), though substitutions at this position in RNase A are not deleterious enough to be isolated with our genetic selection system. Yet, replacement of the equivalent proline in angiogenin, Pro-112, with histidine, serine, or arginine allows for growth in Origami™ cells. We did not isolate a P112L substitution with our selection system, indicating that this substitution is not sufficiently deleterious (Table 2.4). Still, once again, it is difficult to be certain that P112L RNase A is present in our libraries, even though its generation would require a common C/G→T/A mutation.

Mutations at residues Arg-70, Val-105, and Ala-106 (corresponding to Tyr-73, Val-108, and Ala-109 in RNase A) do not inactivate angiogenin, though they do inactivate RNase A. Tyr-73 is only found in ribonucleases with the Cys-65–Cys-72 disulfide bond. Furthermore, residues 73 and 108 in RNase A form two hydrogen bonds between their main-chain atoms and are part of an evolutionary coupled replacement (*vide supra*). It is interesting that we did not isolate mutations at either of these positions in angiogenin. Ala-109 in RNase A could be part of the B_2 nucleobase-binding subsite (*vide supra*). Angiogenin lacks some of the residues involved in the B_2 subsite in RNase A due to the loop replacement discussed above. Thus, Ala-106 in angiogenin may be less important, as this subsite already differs substantially in the two enzymes (Russo *et al.*, 1996).

Substitutions in the γ-3 nucleus that inactivate angiogenin occur at residues 26, 30, 33, 40, 43, 45, 47, 79, 81, and 94. Substitutions at residues Met-30, Arg-33, and His-47 (corresponding to Met-30, Arg-33, and His-48 in RNase A) inactivate angiogenin, but not RNase A.

Met-30. Met-30 is conserved in almost all ribonucleases in the RNase A superfamily. An M30L substitution in angiogenin is fully active, though its effect on thermal stability of the enzyme is unknown (Shapiro *et al.*, 1988). Replacing Met-23 (corresponding to Met-30 in angiogenin and RNase A) with leucine in the frog ribonuclease, Onconase™, causes decreased thermal stability and increased sensitivity to proteolysis (Notomista *et al.*, 2000). We isolated an M30K substitution in angiogenin. Since Met-30 is in the hydrophobic core of angiogenin, a substitution to lysine would be expected to be quite

disruptive. Mutations to several other hydrophobic residues at position 30 are not isolated via selection (Table 2.4).

Arg-33. Substitution of Arg-33 in angiogenin with alanine has been shown to decrease catalytic activity by 7-fold (Shapiro and Vallee, 1992). Arg-33 interacts with essential residue Phe-45, which may account for this decrease in activity. Arg-33 also shields Met-30 and Cys-26 from solvent (Lenstra *et al.*, 1977).

His-47. His-47 is located at the bottom of a hinge in the enzyme. Studies on the equivalent residue in RNase A, His-48, have found that this residue is involved in a conformational change of the enzyme during catalysis (Blackburn and Moore, 1982; Beintema, 1987; Hammes, 2002).

Group III Residues (Proline Substitutions)

There are three examples in which proline is the only substitution that inactivates angiogenin at a particular residue. These occur at residues 10, 12, and 95. Residues 10 and 12 are in the first α-helix in angiogenin and lie between essential residues Phe-9 and His-13. Disruption of this helix with a proline residue could disrupt the important cation–π interaction between residues Phe-9 and His-13. Arg-95 lies in a β-sheet. Mutation of Arg-95 to proline may disrupt the orientation of neighboring essential residue Tyr-94.

Group IV Residues (Essential Half-cystines)

Unlike RNase A, angiogenin has only three disulfide bonds. As discussed above, angiogenin lacks the Cys-65–Cys-72 disulfide bond, as the region containing this

disulfide bond has been replaced by a loop that binds to the putative angiogenin receptor. All three of the disulfide bonds in angiogenin are essential, though, the Cys-39–Cys-92 disulfide bond tolerates some amino-acid changes (Table 2.4). This result indicates that the Cys-26–Cys-81 and Cys-57–Cys-107 disulfide bonds are the two most important in angiogenin, as is the case for RNase A. Since angiogenin lacks the Cys-65–Cys-72 disulfide that is found in most other ribonucleases, it is interesting that the thermal stability of angiogenin is equivalent to that of RNase A (*vide supra*). As discussed above, angiogenin appears to rely more on hydrophobic residues away from this surface loop and towards the γ-3 hydrophobic nucleus for its conformational stability. Other ribonucleases, such as Onconase™, lack the Cys-65–Cys-72 disulfide bond, but clearly have compensated for this loss, as Onconase™ has a T_m value of ~90 °C (Notomista *et al.*, 2000). Frog ribonucleases contain the three disulfide bonds of angiogenin, but also have a fourth disulfide bond (distinct from that found in RNase A) that is important for thermal stability (Leland *et al.*, 2000).

Implications

Recently, several mutations in angiogenin have been linked to the neurodegenerative disorder, amyotrophic lateral sclerosis (Greenway *et al.*, 2006). We have identified several substitutions of these residues with our genetic selection system (*e.g.*, at residues 12, 39, 40, and 46). Accordingly, our results confirm that substitutions at these residues likely decrease the ribonucleolytic activity of angiogenin and prevent its proper function *in vivo*. In addition, given the importance of angiogenin in many biological processes

(Folkman and Shing, 1992; Hooper *et al.*, 2003; Greenway *et al.*, 2006), our results provide an excellent basis for future study of mutations that result in angiogenin dysfunction.

Surface Accessibility vs. Essentiality

The surface accessibility of residues for RNase A and angiogenin was calculated for the PDB entries 7RSA (Wlodawer *et al.*, 1988) and 1B1I (Leonidas *et al.*, 1999), respectively. Most essential residues in RNase A and angiogenin are buried (Figure 2.6; Tables 2.3 and 2.4). Among the essential residues that are not completely buried are Lys-41 and His-119 (RNase A numbering), which are involved directly in catalysis. The side-chain of essential residue Tyr-73 in RNase A extends to the surface, though most of it is buried. Phe-120 is partially surface exposed in RNase A, as the main-chain nitrogen of residue 120 makes a hydrogen bond with the pentavalent phosphoryl group that forms during catalysis. In angiogenin, Arg-33 is surface exposed and serves to shield Cys-26 and Met-30 from solvent. The Cys-57–Cys-107 disulfide bond in angiogenin is somewhat exposed (more so than the equivalent disulfide bond in RNase A). Whether this disulfide bond is more susceptible to reduction in angiogenin is unknown.

The ASA of a specific residue is not alone sufficient to establish its importance. A few residues that are completely buried and several residues that are substantially buried in angiogenin and RNase A are not essential, and tolerate non-conservative changes.

Sequence Conservation vs. Essentiality

An alignment of 338 ribonuclease amino-acid sequences was downloaded from the

HOVERGEN database (gene family HBG008396) (Duret *et al.*, 1994). Duplicate entries

and fragments were removed, leaving a set of 266 sequences. This alignment was

imported into Microsoft Excel for analysis (data not shown). This set of diverse

sequences includes pancreatic ribonucleases, angiogenins, eosinophil-associated

ribonucleases, and other ribonucleases in the RNase A superfamily from many mammals,

several amphibians, and a chicken. The molecular evolution of pancreatic ribonucleases

has been well studied, and pancreatic ribonuclease amino-acid sequences have been

determined from many species (Beintema, 1987; Beintema *et al.*, 1988; Kolbanovskaya

et al., 1993), thus sequence conservation numbers are biased towards pancreatic

ribonucleases. For example, if all angiogenins have a specific amino acid residue at one

position in the enzyme that differs from other ribonucleases, the sequence conservation of

this residue would look more rare than it actually is. Still, there is an enormous amount of

diversity in this set of sequences (only 18 residues are >90% conserved), and it serves as

a valuable resource for studying sequence conservation and molecular evolution in the

RNase A superfamily. The percentage of this set of sequences that contains the residue

found in RNase A or angiogenin at each position is shown in Figure 2.7, panels A and B.

Essential residues are circled in red.

To alleviate bias problems in the alignment for the purposes of this study, a second

alignment of angiogenin and pancreatic ribonuclease amino-acid sequences from 13

selected species was generated (data not shown). The percentage of this set of sequences

that contains the residue found in RNase A or angiogenin at each position is shown in Figure 2.7, panels C and D. Many residues are 50% conserved (100% conserved among pancreatic ribonucleases and/or 100% conserved among angiogenins). These residues could be important for the biological functions of each enzyme.

Most of the residues that are >95% conserved among the set of 266 ribonucleases are essential for ribonucleolytic activity (Figure 2.7). For RNase A, the exceptions are Met-30, Cys-40, Thr-45, Cys-95, and Val-118. Several of these residues are important for RNase A structure/function, but substitutions to these residues may not be sufficiently deleterious to reach the threshold of our selection system. Intriguingly, the only residue in angiogenin with >95% sequence conservation that we do not identify as being essential is Val-118. Several substitutions at this position should be present in our error-prone PCR libraries, including a non-conservative replacement with aspartate. It is possible that changes to this residue could be found if more clones were sequenced. Still, its omission in both angiogenin and RNase A likely indicates that this is not the case. Val-118 has been replaced with cysteine in RNase A and human pancreatic ribonuclease variants engineered to have five disulfide bonds. The resulting enzymes retain >10% of wild-type catalytic activity and have increased thermal stability (Futami *et al.*, 2000; Klink and Raines, 2000). Val-118 is substantially buried in RNase A and angiogenin (Val-113), thus it seems unlikely that this residue is involved in a protein–protein interaction or other biological function.

Many other well-conserved residues are not critical. Again, these conserved residues could be involved in a function other than ribonucleolytic activity. Clearly, the loop in

angiogenin that binds the angiogenin receptor to effect angiogenesis would fall into this category. Alternatively, mutations that cause decreases in catalytic activity less than the threshold of our selection system could be under stricter selection *in vivo*. This explanation is plausible for residues such as Gln-11, Asn-71, and Asp-121, each of which is highly conserved and known to be important for the productive binding of substrate, substrate specificity, or catalytic activity, respectively (Tarragona-Fiol *et al.*, 1993; Fontecilla-Camps *et al.*, 1994; delCardayré *et al.*, 1995; Schultz *et al.*, 1998).

Interestingly, many residues that are not well conserved were found to be important for ribonucleolytic activity (Figure 2.7; Tables 2.3 and 2.4). Most, but not all, of these are hydrophobic core residues that tolerate changes to other hydrophobic amino acid residues. Examples include residues Val-54, Val-57, Ile-106, and Phe-120 in RNase A (corresponding to Ile-53, Ile-56, Val-103, and Leu-115 in angiogenin). Exceptions include Tyr-73 in RNase A and Arg-33 in angiogenin.

2.5 Conclusions

We have identified the essential residues in RNase A and angiogenin that contribute to ribonucleolytic activity. After more than 180 million years of evolution, the two enzymes still share most of the residues important for their structure/function. Yet, many significant changes have occurred. Although research with RNase A has been extensive, we have identified several "new" residues that are critical for its structure/function. The biological activities of members of the RNase A superfamily, such as the role of angiogenin in the growth of new blood vessels, are now being elucidated. The work

described herein should aid in deciphering the myriad functions of these fascinating enzymes.

Table 2.1	Error-prone PCR library overview: Data from *E. coli* DH5α			
Gene	*Angiogenin*	*RNase A*	*Angiogenin*	*RNase A*
Polymerase	*Taq*	*Taq*	*Mutazyme*	*Mutazyme*
Library Size	9.6×10^5	1.1×10^6	2.6×10^5	1.5×10^5
Base Pairs Sequenced	33210	33480	35793	30132
Mutations	82	81	44	45
Mutation Rate	0.25%	0.24%	0.12%	0.15%
Insertions[a]	0 (0%)	0 (0%)	0 (0%)	1 (2.2%)
Deletions[b]	1 (1.2%)	4 (4.7%)	3 (6.4%)	0 (0%)
Sequences with 0 mut.	36.7%	47.8%	60.8%	63.0%
Sequences with 1 mut.	43.3%	30.0%	34.0%	23.5%
Sequences with 2 mut.	13.3%	13.3%	4.1%	8.6%
Sequences with 3+ mut.	6.7%	8.9%	1.0%	4.9%

[a]The number in parentheses indicates the percentage of total mutations that resulted from insertions.

[b]The number in parentheses indicates the percentage of total mutations that resulted from deletions.

Table 2.2	Error-prone PCR library bias: Data from *E. coli* DH5α			
Gene	*Angiogenin*	*RNase A*	*Angiogenin*	*RNase A*
Polymerase	*Taq*	*Taq*	*Mutazyme*	*Mutazyme*
A/T→C/G	1.2%	2.5%	9.1%	8.9%
A/T→G/C	59.8%	56.8%	15.9%	22.2%
A/T→T/A	26.8%	12.4%	18.2%	13.3%
C/G→A/T	1.2%	6.2%	6.8%	13.3%
C/G→G/C	0.0%	1.2%	15.9%	8.9%
C/G→T/A	11.0%	21.0%	34.1%	33.3%
Ts/Tv[a]	2.4	3.5	1.0	1.2
A/T→B/V	87.8%	71.6%	43.2%	44.4%
C/G→D/H	12.2%	28.4%	56.8%	55.6%

[a]Transitions/Transversions

Table 2.3 Inactivating mutations in RNase A

Group	Residue	Mutations isolated	Mutations not isolated	% Conserved[a]	% Conserved[b]	ASA ($Å^2$)	Notes
I	H12	D,L,Q,R,Y		98.1	100.0	10.8	Abstracts proton from 2'OH during catalysis
I	K41	E,M,N	R	99.3	100.0	37.8	H-bond to transition state
I	H119	L,Q,R,Y		98.9	100.0	82.8	Adds proton to leaving group during catalysis
II	F8	S,V	I,L,Y	98.1	100.0	3.5	Interacts with His-12; hydrophobic core
II	N44	Y	D,I,S	98.1	100.0	3.2	H-bonds to His-12 and Lys-41; hydrophobic core
II	F46	C,S	I,L,Y	99.6	100.0	0.0	Hydrophobic core; CFIS
II	V54	D	A,I	72.2	50.0	0.1	Hydrophobic core
II	V57	E	A,M	63.2	50.0	0.0	Hydrophobic core
II	Y73	D	C,F,H,N	26.7	34.6	32.4	Hydrophobic core
II	S75	I,R	C,G,N	89.5	100.0	1.9	Hydrophobic core
II	Y97	C,N	F,H	99.6	100.0	10.0	H-bond to Lys-41; hydrophobic core
II	I106	N	F,T,V	49.6	80.8	0.0	Hydrophobic core; CFIS
II	V108	E,G	A,M	77.4	92.3	0.0	Hydrophobic core; CFIS
II	A109	D	T,V	88.0	84.6	2.6	Interacts with His-119; hydrophobic core; CFIS
II	F120	S	I,L,Y	45.5	61.5	25.6	H-bond to transition state; hydrophobic core
III	Q60	P	L,R	34.6	50.0	42.4	H-bond to Val-57
III	T82	P	A,I,S	86.1	100.0	0.2	Two H-bonds to Phe-46
IV	C26	R,S,Y		100.0	100.0	0.0	Forms disulfide with Cys-84
IV	C58	F,G,R,S,Y		100.0	100.0	9.5	Forms disulfide with Cys-110
IV	C65	F,Y	R,S	79.3	50.0	8.4	Forms disulfide with Cys-72
IV	C72	S,W	R,Y	80.1	50.0	0.0	Forms disulfide with Cys-65
IV	C84	R,S,Y		98.9	100.0	0.0	Forms disulfide with Cys-26
IV	C110	R,S,Y		99.6	100.0	2.0	Forms disulfide with Cys-58

[a]Percentage of a set of 266 ribonucleases that contain the residue found in RNase A.

[b]Percentage of a set of pancreatic ribonucleases and angiogenins from 13 species that contain the residue found in RNase A.

Table 2.4 Inactivating mutations in angiogenin

Group	Residue	Mutations isolated	Mutations not isolated	% Conserved[a]	% Conserved[b]	ASA ($Å^2$)	Notes
I	H13	D,L,Q,R,Y		98.1	100.0	12.2	Abstracts proton from 2'OH during catalysis
I	K40	E,I,N	R	99.3	100.0	61.3	H-bond to transition state
I	H114	L,N,P,Q,R,Y		98.9	100.0	92.5	Adds proton to leaving group during catalysis
II	F9	C,I,S,V	L,Y	98.1	100.0	3.4	Interacts with His-13; hydrophobic core
II	M30	K	I,L,T,V	97.4	100.0	0.0	Hydrophobic core
II	R33	G,P	C,H	50.4	96.2	60.6	Shields Met-30 and Cys-26 from solvent
II	N43	Y	D,I,S	98.1	100.0	0.0	H-bonds to His-13 and Lys-40; hydrophobic core
II	T44	K,P	A,I,S	98.9	100.0	0.0	Base specificity; hydrophobic core
II	F45	C,S	I,L,Y	99.6	100.0	0.0	Hydrophobic core
II	I46	N	F,T,V	22.6	46.2	0.1	Hydrophobic core
II	H47	Q,R	L,Y	84.2	100.0	10.8	Conformational change in catalysis
II	I53	N	F,T,V	17.7	50.0	3.3	Hydrophobic core
II	I56	N	F,T,V	26.7	50.0	0.0	Hydrophobic core
II	S72	N,R	C,G	89.5	100.0	5.0	Hydrophobic core
II	V78	D	A,I	16.9	42.3	1.5	Hydrophobic core
II	T79	A,N,P	I,S	86.1	100.0	0.0	Hydrophobic core
II	Y94	N	C,F,H	99.6	100.0	2.7	H-bond to Lys-41; hydrophobic core
II	V103	D	A,I	8.7	19.2	0.1	Hydrophobic core
II	P112	H,R,S	L	98.5	100.0	0.2	Hydrophobic core
II	L115	S	M	50.0	38.5	6.9	H-bond to transition state; hydrophobic core
III	L10	P	Q	16.2	50.0	21.7	Lies in α-helix between Phe-9 and His-13
III	Q12	P	L,R	83.8	80.8	30.8	Lies in α-helix between Phe-9 and His-13
III	R95	P	Q	24.8	84.6	95.8	Interacts with Tyr-94
IV	C26	R,S,W,Y		100.0	100.0	0.0	Forms disulfide with Cys-81
IV	C39	F,Y	R,S	99.6	100.0	21.0	Forms disulfide with Cys-92
IV	C57	F,G,R,S,Y		100.0	100.0	27.5	Forms disulfide with Cys-107
IV	C81	G,R,S,W,Y		98.9	100.0	0.0	Forms disulfide with Cys-26
IV	C92	R	S,Y	99.6	100.0	7.1	Forms disulfide with Cys-39
IV	C107	R,S,Y		99.6	100.0	39.2	Forms disulfide with Cys-57

[a]Percentage of a set of 266 ribonucleases that contain the residue found in angiogenin.

[b]Percentage of a set of pancreatic ribonucleases and angiogenins from 13 species that contain the residue found in angiogenin.

Figure 2.1   Model of the ribonuclease genetic selection system. Ribonucleases

aggregate when produced in typical laboratory strains of *E. coli*. The

Origami™ strain of *E. coli* has a more oxidizing environment in the

cytosol, allowing for disulfide bond formation. Ribonucleases that are

capable of folding and catalytically active are toxic to Origami™ cells. *E.*

coli DH5α cells were used to analyze library quality. *E. coli* Origami™

cells were used for genetic selection.

wild-type *E. coli*

Origami™ *E. coli*
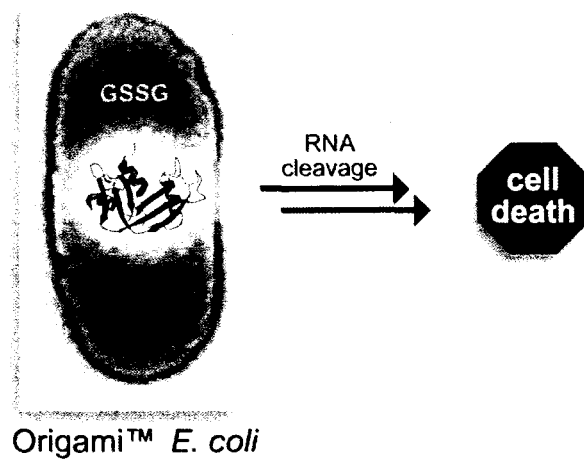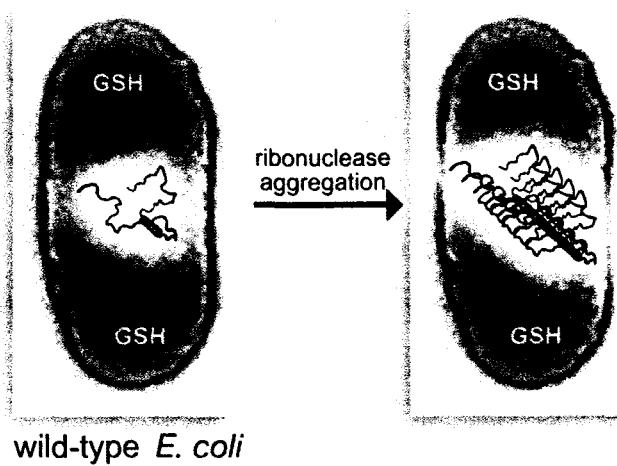
Figure 2.2   Activity threshold of the ribonuclease genetic selection system. The

activity threshold of the Origami™ genetic selection system was probed

with previously studied active-site variants. Clones were transformed into

Origami™ cells and allowed to grow for 2 d in the absence and presence

of IPTG. 1, Angiogenin; 2, K40R angiogenin (~2% of catalytic activity);

3, H13A angiogenin (~0.1% of catalytic activity); 4, RNase A; 5, K41R

RNase A (~0.7% of catalytic activity); 6, H12A RNase A (~0.01% of

catalytic activity).
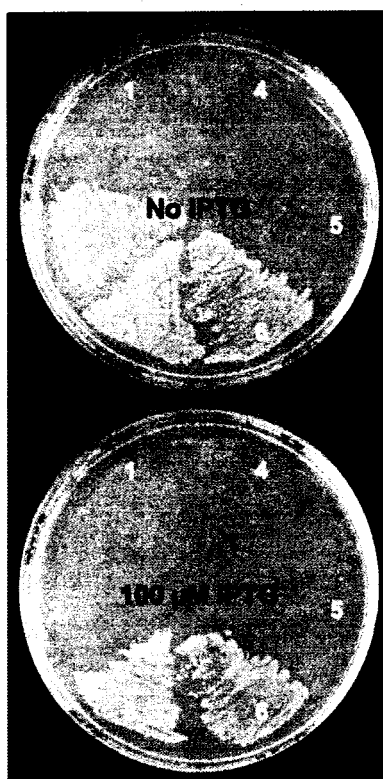
Figure 2.3   Distribution of error-prone PCR mutations. Mutations generated by error-prone PCR techniques occur throughout each gene (*i.e.*, there are no mutational hotspots). Libraries were transformed into *E. coli* DH5α cells and ~96 sequences were obtained in the forward and reverse directions. The position of each mutation is plotted versus the total number of mutations identified. *A*, RNase A cDNA. ■ , *Taq* polymerase + Mn^{2+}; ● , *Mutazyme* polymerase. *B*, Angiogenin (ANG) cDNA. ■ , *Taq* polymerase + Mn^{2+}; ● , *Mutazyme* polymerase.

A

Position of Mutation in RNase A cDNA

B

Position of Mutation in ANG cDNA
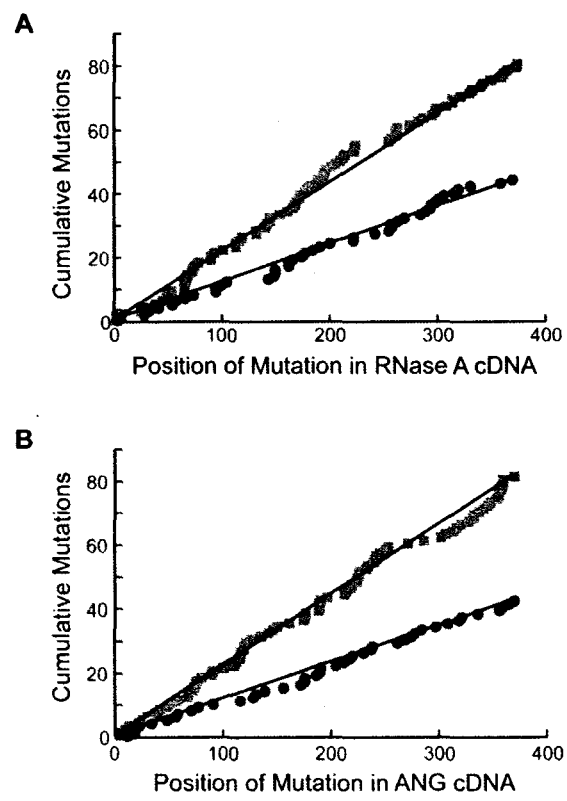
Figure 2.4   Amino-acid sequence alignment of RNase A and angiogenin (ANG). The

sequence alignment was generated with the ClustalW algorithm.

Substitutions that were found to inactivate RNase A are listed above each

section of the alignment. Substitutions that inactivate angiogenin are listed

below each section. Residues that are conserved between RNase A and

angiogenin are boxed. Residues that are found in ≥90% of ribonuclease

sequences are colored green. Cysteine residues are colored yellow.

Helices, sheets, and turns are indicated by h, s, and t.

```
                              D
                              L
                              Q                        R                    E
                   S          R                        S                    M
                   V          Y                        Y                    N
         1         10                  20              30             40
         - - h h h h h h h h h h h - - t t - - - - - - t t h h h h h h h h t t t t s s s - s s
RNase A  - K E T A A A K F E R Q H M D S S T S A A S S S N Y C N Q M M K S R N L T K D R C K P
ANG      Q D N S R Y T H F L T Q H Y D A K P Q G R D D - R Y C E S I M R R R G L T S P - C K D
         - - t h h h h h h h h h h h - - t t - - - - - h   h h h h h h h h h t t t - t t   - - -
         1         10                  20              30             40
                   C P   P D                           R       K       G        Y E
                   I     L                             S       P                F I
                   S     Q                             W                        , N
                   V     R                             Y
                         Y
```

```
                              F
                              G
                              R                                                    R
                   C          S                F            S       I              S
               Y   S          D     E Y   P    Y            W D      R         P    Y
         43        50                60             70              80
         s s s s s - - - h h h h h h h h h - s s s - - t t - - - - s s s - s s - s s s s s s s
RNase A  V N T F V H E S L A D V Q A V C S Q K N V A C K N G Q T N C Y Q S Y S T M S I T D C R
ANG      I N T F I H G N K R S I K A I C E N K N G N P - - H R E N L R I S K S S F Q V T T C K
         s s s s s - - - h h h h h h h h h t t t - s s s       s t t t s s s s - - s s s s s s s s
         42        50                60             70              80
             Y K C N Q            N       N F                      N          D A    G
               P S   R                    G                        R          N R    R
                                          R                                   P    S
                                          S                                        W
                                          Y                                        Y
```

```
                                                            L
                                      R                     Q
                         C            E     S               R
                         N            N   G D Y             Y S
         86      90              100            110             120   124
         s - t t t - t t - s s s s s s s s s s - s s s s s s t t t t s s - s s - s s -
RNase A  E T G S S K Y P N C A Y K T T Q A N K H I I V A C E G N P Y V P V H F D A S V - - - -
ANG      L H G G S P W P P C Q Y R A T A G F R N V V V A C E N G - - L P V H L D Q S I F R R P
         s s - - - - - - - - s s s s s s s s s s - s s s s s t t       s s - s s - h h h h - - -
         83      90              100            110             120   123
                         R   N P              D     R              H   L S
                                                    S              R   N
                                                    Y              S   P
                                                                       Q
                                                                       R
                                                                       Y
```

☐ Conserved Residues Between RNase A and Angiogenin
    Conserved Residues Among a Set of 266 Ribonucleases
C   Cysteine Residue
hst helix, sheet, turn

Figure 2.5   Essential amino acid residues in RNase A and angiogenin. Group I

residues (residues involved in catalysis) are colored green. Polar residues

in Group II (buried residues) are colored blue. Hydrophobic Group II

residues are colored red. Group III residues (proline substitutions) are

colored orange. Group IV residues (cysteine residues) are colored yellow.

The surface is transparent gray, and the backbone is in cartoon

representation. *A*, Front view of RNase A (PDB: 7RSA). *B*, Back view of

RNase A. *C*, Top view of RNase A. *D*, Front view of angiogenin (PDB:

1B1I). *E*, Back view of angiogenin. *F*, Top view of angiogenin. Images

were prepared with PyMol (Delano Scientific, South San Francisco, CA).

A
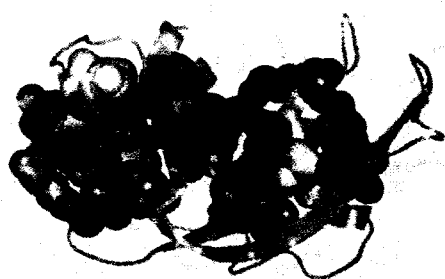
D

B

E
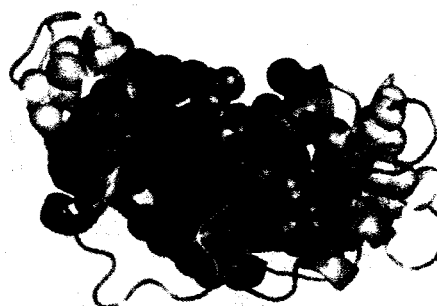
C

F

Figure 2.6   Accessible surface area per amino acid residue for RNase A and

angiogenin. Essential residues are circled in red. *A*, RNase A. *B*,
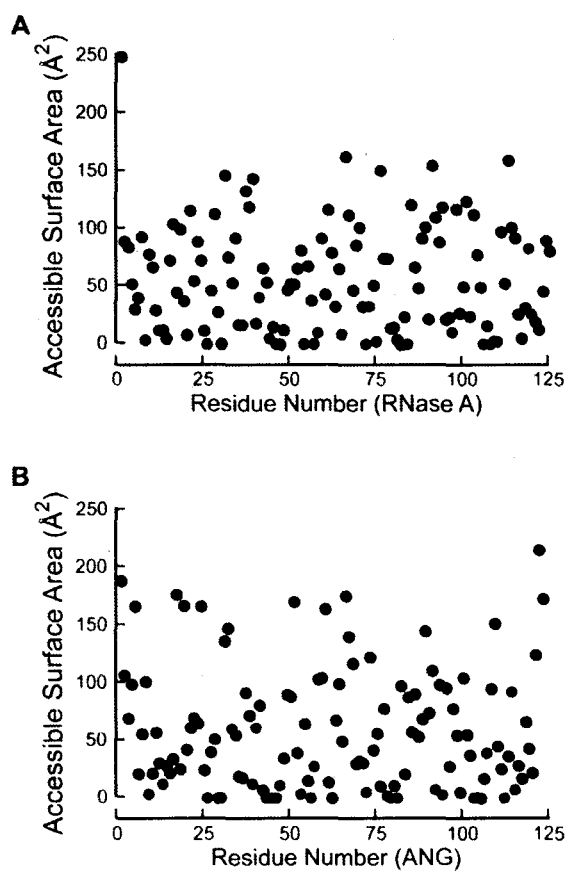
Angiogenin.

A

B

Figure 2.7   Sequence conservation per amino acid residue in RNase A and

angiogenin. Essential residues are circled in red. *A*, Percent identity per

residue of RNase A to a set of 266 ribonuclease amino-acid sequences. *B*,

Percent identity per residue of angiogenin to a set of 266 ribonuclease

amino-acid sequences. *C*, Percent identity per residue of RNase A to a set

of pancreatic ribonuclease and angiogenin amino-acid sequences from 13

species. *D*, Percent identity per residue of angiogenin to a set of pancreatic

ribonuclease and angiogenin amino-acid sequences from 13 species.
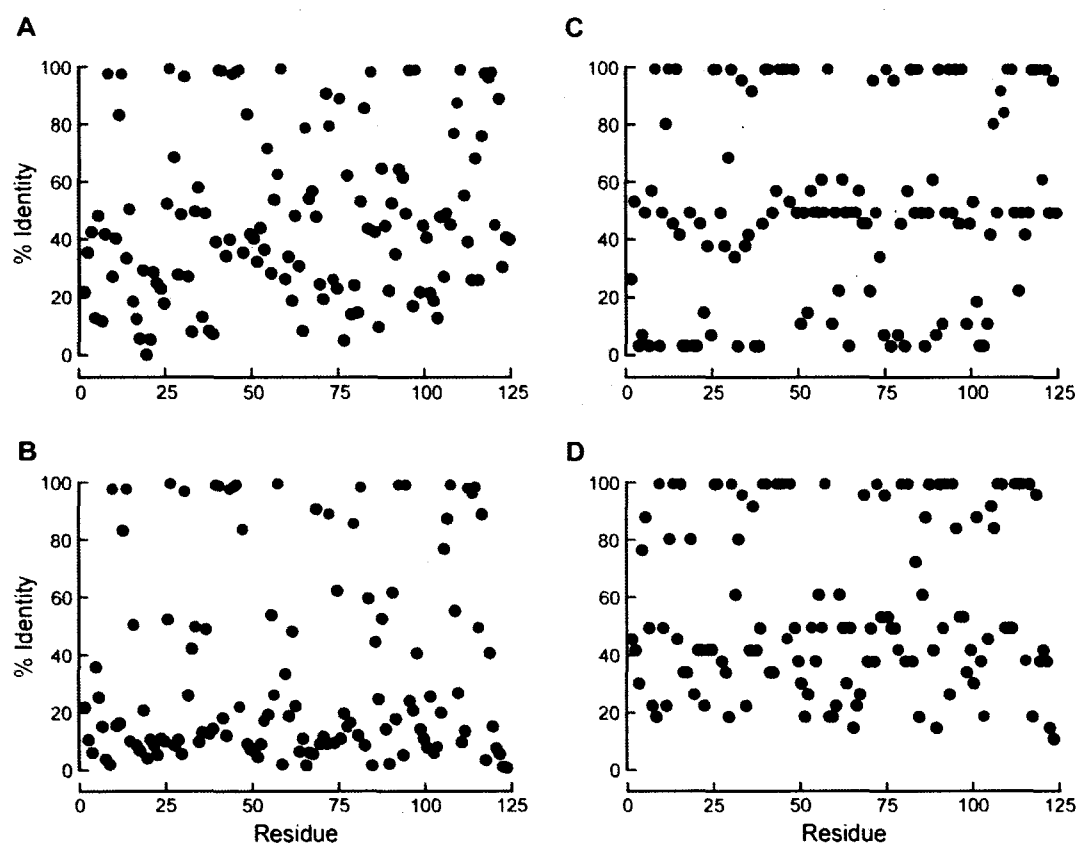
Chapter Three

Potent Inhibition of Ribonuclease A by Oligo(vinylsulfonic acid)

This chapter was published as:

Smith, B. D., Soellner, M. B., and Raines, R. T. (2003) Potent inhibition of

ribonuclease A by oligo(vinylsulfonic acid). *J. Biol. Chem.* **278:** 20934-20938.

3.1 Abstract

Ribonuclease A (RNase A) can make multiple contacts with an RNA substrate. In particular, the enzymic active site and adjacent subsites bind sequential phosphoryl groups in the RNA backbone through Coulombic interactions. Here, oligomers of vinylsulfonic acid (OVS) are shown to be potent inhibitors of RNase A that exploit these interactions. Inhibition is competitive with substrate and has $K_i = 11$ pM in assays at low salt concentration. The effect of salt concentration on inhibition indicates that nearly 8 favorable Coulombic interactions occur in the RNase A•OVS complex. The phosphonic acid and sulfuric acid analogs of OVS are also potent inhibitors, though slightly less effective. OVS is also shown to be a contaminant of 2-(*N*-morpholino)-ethanesulfonic acid (MES) and other buffers that contain sulfonylethyl groups. Oligomers greater than nine units in length can be isolated from commercial MES buffer. Inhibition by contaminating OVS is responsible for the apparent decrease in catalytic activity that has been observed in assays of RNase A at low salt concentration. Thus, OVS is both a useful inhibitor of RNase A and a potential bane to chemists and biochemists who use ethanesulfonic acid buffers.

3.2 Introduction

RNA is the least stable of the biopolymers that effect information transfer in biology (Wolfenden and Snider, 2001). Yet, the lifetime of RNA *in vivo* is most often determined by the rate of its enzymatic degradation (Ross, 1996). *In vitro*, ribonuclease inhibitors are often employed to mitigate damage to RNA from incidental contamination with secretory ribonucleases, such as the human homolog of ribonuclease A (RNase A, EC 3.1.27.5 (Raines, 1998)). The abundance and diversity of natural ribonucleases has led to an ever-increasing interest in inhibitor design and discovery (Russo *et al.*, 2001).

Like most known ribonucleases, RNase A can make multiple contacts with an RNA substrate (Figure 3.1). The enzymic active site and adjacent subsites bind sequential phosphoryl groups in the RNA backbone through Coulombic interactions (Fontecilla-Camps *et al.*, 1994). The most potent RNase A inhibitors take advantage of this extended interface. For example, a pyrophosphate-linked oligonucleotide (pdUppA-3'-p), which occupies three subsites, is the tightest known small-molecule inhibitor of RNase A (Russo *et al.*, 2001). Nature also uses this strategy to inhibit RNase A and its homologs. The 50-kDa ribonuclease inhibitor protein (RI) forms a tight 1:1 complex with RNase A ($K_d \sim 10^{-14}$ M (Lee *et al.*, 1989)), chelating all of its phosphoryl-group binding subsites (Kobe and Deisenhofer, 1996). The utility of pyrophosphate-linked oligonucleotides and RI is limited, both by the difficulty and expense of their production and by their intrinsic instability. For example, pyrophosphate-linked oligonucleotides are susceptible to hydrolysis (Russo and Shapiro, 1999), and RI is readily inactivated by oxidation (Kim *et al.*, 1999).

While studying RNase A catalysis as a function of salt concentration, we found that a contaminant in common biological buffers was a potent inhibitor in solutions of low salt concentrations (Park and Raines, 2000). We estimated that the K_i value for this inhibitor was approximately 0.1 nM, which is 10^2-fold lower than that for any other small-molecule RNase A inhibitor. Herein, we identify this inhibitor as a byproduct of the synthesis of commercial buffers containing sulfonylethyl groups. Next, we find that this inhibitor acts in a competitive manner and is the most potent known small-molecule inhibitor of a ribonuclease. In addition, we identify the number of Coulombic interactions that the inhibitor makes upon binding to RNase A. Finally, we examine RNase A inhibition by analogs of the inhibitor.

3.3 Experimental Procedures

Materials. Poly(cytidylic acid) [poly(C)] was from Midland Certified Reagents (Midland, TX). Poly(C) was purified prior to use by precipitation in aqueous ethanol (70% v/v). The fluorogenic ribonuclease substrate, 6-FAM~dArUdAdA~6-TAMRA (where 6-FAM is a 5' 6-carboxyfluorescein group and 6-TAMRA is a 3' 6-carboxytetramethylrhodamine group), was from Integrated DNA Technologies (Coralville, IA). Oligo(vinylsulfonic acid) (M_r ~2,000) and poly(vinylphosphonic acid) (M_r ~20,000) were from Polysciences (Warrington, PA). Vinylsulfonic acid and poly(vinylsulfuric acid) (M_r ~170,000) were from Aldrich (Milwaukee, WI). All other commercial chemicals and biochemicals were of reagent grade or better, and were used without further purification.

Synthesis of Diethanesulfonic Acid Ether (3). 2-Mercaptoethylether (5.0 g, 36.2

mmol; Caution: Stench!; Aldrich, Milwaukee, WI) was dissolved in glacial acetic acid

(5 mL). The resulting solution was then cooled to 0 °C. While stirring at 0 °C, a mixture

(50 mL:45 mL) of glacial acetic acid and aqueous hydrogen peroxide (30% v/v) was

added to the solution dropwise over 1 h. The reaction mixture was then heated at 60 °C

for 90 min. The solvent was removed under reduced pressure. Addition of toluene

enabled residual acetic acid to form azeotropes of low boiling point. The resulting yellow

oil was used without further purification. **Spectral Data.** ^{1}H NMR (300 MHz, D_2O) δ

2.88 (t, $J = 7.1$ Hz, 4H), 2.17 (t, $J = 7.0$ Hz, 4H) ppm; MS (ESI) m/z 232.9791 (M⁻H

$[C_4H_9O_7S_2]$ = 232.9795).

Instruments. UV absorbance measurements were made with a Cary Model 3

spectrophotometer (Varian, Palo Alto, CA). Fluorescence measurements were made with

a QuantaMaster 1 Photon Counting Fluorometer equipped with sample stirring (Photon

Technology International, South Brunswick, NJ).

Production of RNase A. Plasmid pBXR (delCardayré *et al.*, 1995) directs the

production of RNase A in *E. coli*. That RNase A is significantly more pure than is

RNase A available commercially. RNase A was produced and purified as described

previously (Kim and Raines, 1993) with the following modifications. *E. coli* strain

BL21(DE3) transformed with pBXR was grown to an OD of 1.8 at 600 nm in terrific

broth medium containing ampicillin (0.40 mg/mL). Expression of the RNase A cDNA

was induced by addition of isopropyl-1-thio-β-D-galactopyranoside (IPTG; to 0.5 mM).

Cells were collected 4 h after induction and lysed with a French pressure cell. Inclusion

bodies were recovered by centrifugation and resuspended for 2 h in 20 mM Tris–HCl buffer, pH 8.0, containing guanidine–HCl (7 M), dithiothreitol (DTT; 0.10 M), and EDTA (10 mM). The protein solution was diluted 10-fold with aqueous acetic acid (20 mM), subjected to centrifugation to remove any precipitate, and dialyzed overnight against aqueous acetic acid (20 mM). Any precipitate was removed again by centrifugation. The supernatant was diluted to a protein concentration near 0.5 mg/mL in a refolding solution of 0.10 M Tris–HCl buffer, pH 8.0, containing NaCl (0.10 M), reduced glutathione (1.0 mM), and oxidized glutathione (0.2 mM). RNase A was refolded for 16 h and concentrated by ultrafiltration with a YM10 membrane (10,000 M_r cut-off; Millipore, Bedford, MA). Concentrated RNase A was applied to a Superdex G-75 gel filtration FPLC column (Pharmacia, Piscataway, NJ) in 50 mM sodium acetate buffer, pH 5.0, containing NaCl (0.10 M) and NaN_3 (0.02% w/v). Protein from the major A_{280} peak was collected and applied to a Mono S cation–exchange FPLC column (Pharmacia, Piscataway, NJ). RNase A was eluted from the column with a linear gradient of NaCl (0.2–0.4 M) in 50 mM sodium acetate buffer, pH 5.0. Protein concentration was determined by UV spectroscopy using $\varepsilon = 0.72$ mL mg^{-1} cm^{-1} at 278 nm (Sela *et al.*, 1957).

Inhibition of RNase A Catalysis. Inhibition of ribonucleolytic activity was measured by using either poly(C) or a fluorogenic substrate. The total cytidyl concentration of poly(C) was quantitated using $\varepsilon = 6,200$ $M^{-1}cm^{-1}$ at 268 nm (Yakovlev *et al.*, 1992). The cleavage of poly(C) was monitored by the decrease in ultraviolet hypochromicity. The $\Delta\varepsilon$ value for this reaction, calculated from the difference in molar absorptivity of the

polymeric substrate and the mononucleotide cyclic phosphate product, was 2,380 $M^{-1}cm^{-1}$

at 250 nm (delCardayré and Raines, 1994). Assays were performed at 25 °C in 50 mM

imidazole–HCl buffer, pH 6.0, containing NaCl (0.10 M), poly(C) (10 μM–1.5 mM),

OVS (0–2.8 μM), and enzyme (1.0 nM). Molar values of OVS were calculated by using

its average molecular mass of 2,000 g/mol. It is possible that a polymer of this size could

bind two enzymes. Thus, actual K_i values could be twofold higher. Kinetic parameters

were determined from initial velocity data with the program DELTAGRAPH 4.0

(DeltaPoint, Monterey, CA).

For the fluorescence assay, inhibition of ribonucleolytic activity was assessed at

25 °C in 2.0 mL of 50 mM imidazole–HCl buffer, pH 6.0, containing NaCl (0–0.25 M),

6-FAM~dArUdAdA~6-TAMRA (60 nM), and RNase A (1–5 pM), as described

previously (Kelemen et al., 1999; Park et al., 2001). Fluorescence (F) was measured

using 493 and 515 nm as the excitation and emission wavelengths, respectively. The

value of $\Delta F/\Delta t$ was measured for 3 min after the addition of RNase A. Next, an aliquot of

inhibitor (I) dissolved in the assay buffer was added, and $\Delta F/\Delta t$ was measured in the

presence of the inhibitor for 3 min. The concentration of inhibitor in the assay was

doubled repeatedly in 3-min intervals. Excess RNase A was then added to the mixture to

ensure that less than 10% of the substrate had been cleaved prior to completion of the

inhibition assay. Apparent changes in ribonucleolytic activity due to dilution were

corrected by comparing values to an assay in which aliquots of buffer were added to the

assay. Values of K_i were determined by non-linear least squares regression analysis of

data fitted to Equation 1 (Kelemen et al., 1999; Park et al., 2001),

$$\Delta F/\Delta t = (\Delta F/\Delta t)_0 (K_i/(K_i + [\mathrm{I}]))$$ (Eq. 1)

At 0 M NaCl, the enzyme concentration ($[\mathrm{E}]_{total}$) caused a significant depletion in inhibitor concentration, thus data were fitted to Equation 2, which describes tight-binding inhibition (Henderson, 1972),

$$\Delta F / \Delta t = ((\Delta F / \Delta t)_0 / 2[\mathrm{E}]_{total})\left\{\left[(K_i + [\mathrm{I}] - [\mathrm{E}]_{total})^2 + 4K_i[\mathrm{E}]_{total}\right]^{1/2} - (K_i + [\mathrm{I}] - [\mathrm{E}]_{total})\right\}$$ (Eq. 2)

In Equations 1 and 2, $(\Delta F/\Delta t)_0$ was the ribonucleolytic activity prior to inhibitor addition.

3.4 Results

Purification of Inhibitor from a Commercial Buffer

Previously, we reported that a contaminant in MES buffer inhibits catalysis by RNase A, especially in solutions of low salt concentration (Park and Raines, 2000). We subsequently found that other ethanesulfonic acid buffers (*i.e.*, "Good" buffers (Good *et al.*, 1966)), such as BES, CHES, and PIPES, similarly inhibited RNase A (data not shown). Thus, we speculated that the inhibitor was a byproduct of ethanesulfonic acid buffer synthesis. We have shown that the byproduct responsible for RNase A inhibition would likely be anionic (Park and Raines, 2000) because the RNase A active site and RNA binding sites are cationic (pI = 9.3 (Ui, 1971)). Thus, we chose to purify the inhibitor by anion-exchange chromatography. The low concentration of this inhibitor in

MES buffer (~2 ppm (Park and Raines, 2000)) necessitated purifying the contaminant from a large amount of MES buffer. We first tested the inhibitory activity of a number of different commercial lots of MES buffer. All MES buffers tested exhibited substantial RNase A inhibition at low salt concentrations, but the inhibition per mol of MES did vary by 20-fold in different lots. Thus, we passed 0.50 kg of the most inhibitory MES buffer (Sigma Chemical, St. Louis, MO; 5.0 L of a 0.50 M solution, pH 3.0) through a column containing 50 g of AG® 1-X8 anion-exchange resin (chloride form; Biorad, Hercules, CA). No inhibitory activity was detected in the flow-through, indicating that the inhibitor was anionic and could be purified with anion-exchange chromatography. (*nb*: The flow-through of this column can be recrystallized from water to yield MES buffer that is devoid of inhibitor.) Likewise, no inhibitory activity was observed in a 0.1 M HCl wash of the column. The inhibitor was eluted with a 1–4 M linear gradient of HCl. Inhibitory activity was found in fractions corresponding to 1.7–4 M HCl. These fractions were pooled and evaporated to dryness, yielding 40 mg of material.

Identification of Inhibitor

In ethanesulfonic acid buffer synthesis, a nucleophile attacks 2-bromoethanesulfonic acid in H_2O to yield the buffer product (Figure 3.2). Hydrolysis or β-elimination of 2-bromoethanesulfonic acid could yield 2-hydroxyethanesulfonic acid (**1**) or vinylsulfonic acid (**2**). Nucleophilic attack of 2-hydroxyethanesulfonic acid on 2-bromoethanesulfonic acid or Michael addition to vinylsulfonic acid could generate diethanesulfonic acid ether (**3**). Indeed, all three of these byproducts were identified by

NMR spectroscopy and mass spectrometry in the material purified from MES buffer (data not shown).

Commercial 2-hydroxyethanesulfonic acid (1) and vinylsulfonic acid (2) were tested as inhibitors of RNase A. Neither was a potent inhibitor in solutions of low salt concentration (Figure 3.2). (nb: In contrast, divinylsulfone ($CH_2CHS(O)_2CHCH_2$) is an irreversible inhibitor of RNase A, forming covalent bonds to active-site residues by Michael addition (Ciglic et al., 1998). Mechanism-based inactivation of RNase A by Michael addition has also been described previously (Stowell et al., 1995).) Diethanesulfonic acid ether (3) was synthesized (vide supra), but likewise failed to inhibit RNase A. Thus, the sought-after inhibitor was not byproduct 1, 2, or 3.

Next, we used a Vivaspin concentrator (5,000 MWCO; Vivascience AG, Hannover, Germany) to purify the inhibitor based on its affinity for RNase A. RNase A (10 mg) was mixed in ddH$_2$O (10 mL) with the inhibitor (10 mg) that had been purified by anion-exchange chromatography. The sample was subjected to centrifugation at 6,000 rpm for 15 min, washed with ddH$_2$O (3 × 15 mL), and subjected again to centrifugation. Molecules that bind tightly to RNase A remained in the retentate, whereas impurities were washed into the eluate. MALDI mass spectrometry of the retentate containing RNase A and the inhibitor revealed a heterogeneous mixture of small molecules of molecular mass 900–2,000 g/mol. The inhibitor was then separated from RNase A by adding a solution of ammonium acetate (0.10 M) to the mixture. After repeatedly concentrating and adding ammonium acetate solution to the mixture, unbound inhibitor moved to the eluate, whereas RNase A remained in the retentate. MALDI mass

spectrometry of the free inhibitor revealed the same heterogeneous distribution of molecular mass, with individual peaks separated by 108 g/mol (Figure 3.3). Because the molecular mass of vinylsulfonic acid (2) is 108 g/mol, we reasoned that the inhibitor was likely an oligomer of vinylsulfonic acid (OVS; 4). Like 1–3, OVS is a likely byproduct of ethanesulfonic acid buffer synthesis, with ultraviolet light possibly initiating the radical-mediated polymerization of vinylsulfonic acid (3; Figure 3.2) (Breslow and Hulse, 1954).

Characterization of Inhibition by OVS

Inhibition of RNase A activity was measured in 0.05 M imidazole–HCl buffer, pH 6.0, containing NaCl (0.10 M) and commercial OVS (M_r ~2,000; 0–2.8 μM). OVS inhibition of RNase A was not time-dependent (data not shown). The addition of NaCl diminishes the OVS inhibition of RNase A, indicating that OVS is a reversible inhibitor of the enzyme. OVS inhibits RNase A at concentrations well below that of substrate, thus inhibition by OVS is not due to its sequestering of RNA. Double-reciprocal plots of RNase A catalytic activity versus the concentration of poly(C) at different OVS concentrations reveal that OVS inhibits RNase A in a competitive manner (Figure 3.4). With poly(C) as a substrate, the apparent K_i = (0.40 ± 0.03) μM at 0.10 M NaCl. A replot of $(K_m/V_{max})_{app}$ versus [OVS] reveals a straight line, which is indicative of simple competitive inhibition (Cleland, 1977).

Reproduced with permission of the copyright owner. Further reproduction prohibited without permission.

Salt-Dependence of Inhibition by OVS

The K_i of OVS was measured at four different salt concentrations in 50 mM imidazole–HCl buffer, pH 6.0. Because OVS inhibits RNase A in a competitive manner, we were able to use a sensitive fluorescent assay to assess inhibition by OVS. OVS inhibition of RNase A is highly salt-dependent (Figure 3.5A). At 0 M NaCl, OVS inhibits catalysis by RNase A with an astonishingly low inhibition constant of $K_i = (11 \pm 2)$ pM. At 0 M NaCl, the inhibition curve was fitted to a tight-binding inhibitor equation, yet the curve still exhibits some cooperativity. At 0.10 M NaCl, OVS inhibits RNase A with an inhibition constant of $K_i = (120 \pm 10)$ nM. (*nb*: In theory, the value of *Ki* for a competitive inhibitor should be independent of the substrate used in the assay. Yet, the observed value of *Ki* for OVS is 3-fold higher when poly(C) rather than 6-FAM~dArUdAdA~6-TAMRA is the substrate for RNase A. This effect of polymeric substrates has much precedence and several proposed explanations (Nelson and Hummel, 1961; Sela, 1962; Richards and Wyckoff, 1971).)

According to polyelectrolyte theory, the slope of a plot of $\log(K_i)$ versus $\log([\text{cation}])$ reveals the number of Coulombic interactions between a ligand and a polyanion (Record *et al.*, 1976). OVS makes, on average, 7.8 ionic interactions with RNase A (Figure 3.5B). Poly(vinylsulfuric acid), an OVS analog, exhibits a similar salt-dependence (data not shown).

RNase A Inhibition by OVS Analogs

To assess the importance of the sulfonic acid group for RNase A inhibition, we tested poly(vinylphosphonic acid) (PVP) and poly(vinylsulfuric acid) (PVOS) for inhibition of ribonucleolytic activity in our fluorescent assay. These analogs are also good inhibitors of RNase A, but are slightly less effective than is OVS (Table 3.1). The average molecular masses of PVP and PVOS were 20,000 and 170,000 g/mol, respectively. Nevertheless, by mass spectrometry, the minimum number of OVS units that bound tightly to RNase A was nine. Thus, each chain of commercial OVS (~2,000 g/mol) could tightly bind to two RNase A molecules per chain, whereas each chain of PVP or PVOS could tightly bind to more. Hence, to enable direct comparison of inhibition by OVS, PVP, and PVOS, the data listed in Table 3.1 are in units of mass rather than moles.

3.5 Discussion

Purification and Characterization of Inhibitor

OVS is an extremely low-level contaminant in MES buffer (~2 ppm (Park and Raines, 2000)). Its purification is thus problematic. We were able to isolate <2 mg of OVS from 0.5 kg of MES buffer. This material was difficult to separate from other anionic byproducts of ethanesulfonic acid buffer synthesis (Figure 3.2). OVS has no distinct properties that allow it to be detected during purification. NMR spectroscopy failed to detect OVS in the material purified from MES, as <5% of that material was OVS. Mass spectrometry did, however, enable the identification of OVS in MES buffer as the cause of RNase A inhibition in solutions of low salt concentration (Figure 3.3).

Specifically, oligomers of 9–17 units were responsible for the inhibition. It is likely that oligomers shorter than 9 units in length are also present in MES buffer, but these were not observed after anion-exchange chromatography and affinity purification. Because purification of the inhibitor was monitored by RNase A inhibition assays, oligomers of fewer than 9 units are likely to be less-effective inhibitors of RNase A.

After our identification of OVS in MES buffer, we found a previous report that large polymers (~50,000 g/mol) of poly(vinylsulfonic acid) comprised about 1% of a single lot of MES buffer (Niehaus and Flynn, 1993). This lot of MES buffer inhibited the catalytic activity of 6-phosphogluconate dehydrogenase. Other lots of MES buffer failed to inhibit the enzyme, as only long polymers were inhibitory (Niehaus *et al.*, 1995). We suspect that oligo(vinylsulfonic acid) and, occasionally, poly(vinylsulfonic acid) contaminate commercial MES buffer and other ethanesulfonic acid buffers, and that the amount of these contaminants varies from lot to lot.

Kinetic Analyses

OVS inhibition of RNase A follows a simple competitive model (Figure 3.4). As OVS (~2000 g/mol) has on average only 18 monomer units per molecule, it is on the cusp of consideration as a polyelectrolyte (Record *et al.*, 1976). Nonetheless, a double-log plot of K_i versus [cation] indicates that OVS forms 7.8 Coulombic interactions with RNase A (Figure 3.5B). The inhibition of RNase A by poly(vinylsulfuric acid) (PVOS; ~170,000 g/mol) shows a similar salt-dependence (data not shown). The number of Coulombic interactions between OVS and RNase A is in gratifying agreement with a

previous report that single-stranded DNA forms 7 Coulombic interactions with RNase A (Record *et al.*, 1976). Thus, OVS likely saturates the same phosphoryl-group binding subsites as does a single-stranded nucleic acid (Figure 3.1).

Multivalent Inhibition

Polyanions are known to be effective inhibitors of RNase A (Richards and Wyckoff, 1971). Heparin, tyrosine–glutamate copolymers, and many different polysulfates and polyphosphates have been shown previously to inhibit catalysis by the enzyme (Zöllner and Fellig, 1953; Heymann *et al.*, 1958; Sela, 1962). We were surprised to learn that, 40 years ago, even poly(vinylsulfonic acid) had been tested as an inhibitor of RNase A. Those data suggested that poly(vinylsulfonic acid) was a worse inhibitor of RNase A than other polyanions (Fellig and Wiley, 1959; Littauer and Sela, 1962) or, alternatively, that only long polymers (>9,000 g/mol) were good inhibitors of RNase A (Bach, 1964). We do not know the basis for the disparity with our data.

OVS, like PVP and PVOS, is similar to a nucleic acid backbone in having anionic nonbridging oxygen atoms. In addition, the phosphorous atoms in a nucleic acid and alternating sulfur atoms in OVS are separated by 5 other atoms. There is, however, a major difference between OVS and a nucleic acid. With its 3 nonbridging oxygens per monomer unit, OVS provides many more opportunities to form strong hydrogen bonds than does a nucleic acid. Pyrophosphate-linked ribonuclease inhibitors also display extra nonbridging oxygens, which is likely to enhance their affinity for RNase A (Russo and Shapiro, 1999).

OVS compares favorably with the most potent known small-molecule inhibitor of RNase A, a pyrophosphate-linked oligonucleotide: pdUppA-3'-p (Russo *et al.*, 2001). Under similar buffer conditions with 0.10 M NaCl, each has a K_i near 120 nM. Yet, unlike pdUppA-3'-p, OVS is simple to prepare and extremely stable. Accordingly, OVS could be useful in preventing incidental ribonuclease contamination and RNA degradation in experiments involving RNA. Indeed, poly(vinylsulfuric acid), an OVS analog, has been added to experiments involving isolation of mRNA (Cheng *et al.*, 1974) or cell-free translation (Mach *et al.*, 1968).

Other enzymes are known to be inhibited by poly(vinylsulfonic acid). For example, poly(vinylsulfonic acid) inhibits catalysis by RNA polymerase and reverse transcriptase (Chambon *et al.*, 1967; Althaus *et al.*, 1992). We believe that OVS could be an inhibitor any enzyme that binds strands of RNA or DNA.

Buffer Contamination

The presence of OVS in all lots of MES buffer tested herein and in many other ethanesulfonic acid buffers is troubling. The amount of OVS varies from lot to lot, and thus some lots of buffers could contain high concentrations of OVS. We recommend that all ethanesulfonic acid buffers be purified by anion-exchange chromatography prior to their use in assays of enzymatic activity. Alternatively, an OVS-free buffer should be used instead. Imidazole, bistris, and tris buffer are suitable alternatives, depending on the pH of the assay.

MES buffer has been the buffer of choice in assays of the catalytic activity of RNase A, as the pK_a of MES buffer ($pK_a = 6.15$ (Good *et al.*, 1966)) is near the pH of maximal activity (pH = 6.0 (del Rosario and Hammes, 1969)). Many RNase A assays are performed in the presence of 0.10 M NaCl, at which the K_i of OVS is about 120 nM (Figure 3.5A). We find that the OVS concentration in many lots of MES buffer is near 2 ppm. In 0.10 M MES buffer, the concentration of OVS is near 0.2 μM, which is greater than its K_i value! Historically, RNase A has been reported to have a bell-shaped salt–rate profile, with optimum salt concentration near 0.1 M NaCl (Edelhoch and Coleman, 1956; Irie, 1965; Libonati and Sorrentino, 1992). We believe that this observed bell-shape is an artifact due to contaminating OVS in MES buffer. Indeed, the salt–rate profile of RNase A has been measured recently in bistris buffer, revealing that ribonucleolytic activity increases to the diffusion limit as salt concentration decreases (Park and Raines, 2000; Park and Raines, 2001; Park and Raines, 2003).

3.6 Conclusions

We have found that OVS is a common contaminant of ethanesulfonic acid buffers. Although present in only ppm concentrations, OVS is a potent inhibitor of RNase A, making nearly 8 favorable Coulombic interactions with the enzyme. OVS is inexpensive and extremely stable, unlike other known ribonuclease inhibitors. Accordingly, OVS has the potential to be a useful prophylactic in many chemical, biochemical, and biotechnical experiments involving RNA. Finally, we note that the purity of the buffer used to assay RNase A and other enzymes deserves special consideration.

Acknowledgements. We are grateful to Drs. W. W. Cleland, B. G. Miller, and C. Park for contributive discussions.

Table 3.1   Inhibition of ribonuclease A catalysis by commercial oligo(vinylsulfonic acid) and its phosphonic acid and sulfuric acid analogs

Inhibitor	K_i (µg/mL)^a
oligo(vinylsulfonic acid)	0.24 ± 0.02
poly(vinylphosphonic acid)	0.35 ± 0.02
poly(vinylsulfuric acid)	0.38 ± 0.06

^{a} Values of K_i were obtained in 0.05 M imidazole–HCl buffer (pH 6.0), containing 0.1 M NaCl. Values of K_i are in units of µg/mL to account for the different average molecular mass of each polymer.

Figure 3.1 Structure of the crystalline ribonuclease A•d(ATAAG) complex (PDB

entry 1RCN (Fontecilla-Camps *et al.*, 1994)). Three phosphoryl-group

binding subsites are indicated. The G residue and a fourth phosphoryl-

group binding subsite (Arg[85] (Fisher *et al.*, 1998)) are not shown. Residues

that comprise each subsite are colored as follows: P_0 subsite (yellow), P_1

subsite (orange), and P_2 subsite (red).
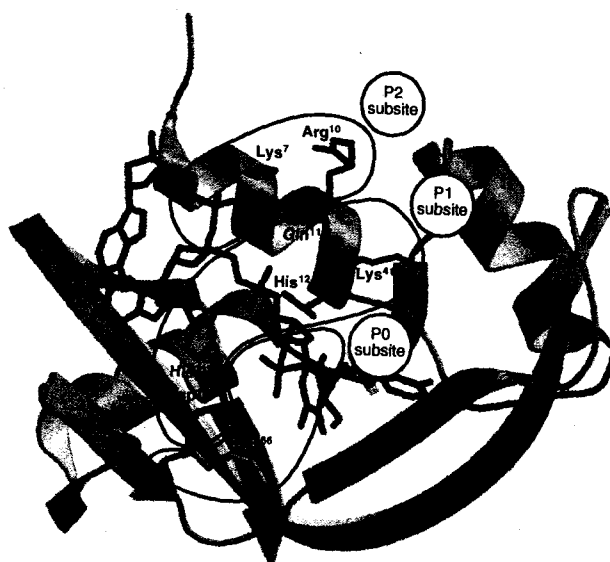
Figure 3.2   Byproducts of MES buffer synthesis. Values of K_i are listed for inhibition

of catalysis of 6-FAM~dArUdAdA~6-TAMRA cleavage by

ribonuclease A in 50 mM imidazole–HCl buffer (pH 6.0). The K_i for OVS

inhibition is calculated based on a molecular mass of 2,000 g/mol.

2-hydroxyethanesulfonic acid (1)
($K_i > 1$ mM)

diethanesulfonic acid ether (3)
($K_i > 0.5$ mM)

base
H_2O

base

MES

base

vinylsulfonic acid (2)
($K_i > 1$ μM)

uv light

OVS (4)
($K_i = 11 \pm 2$ pM)
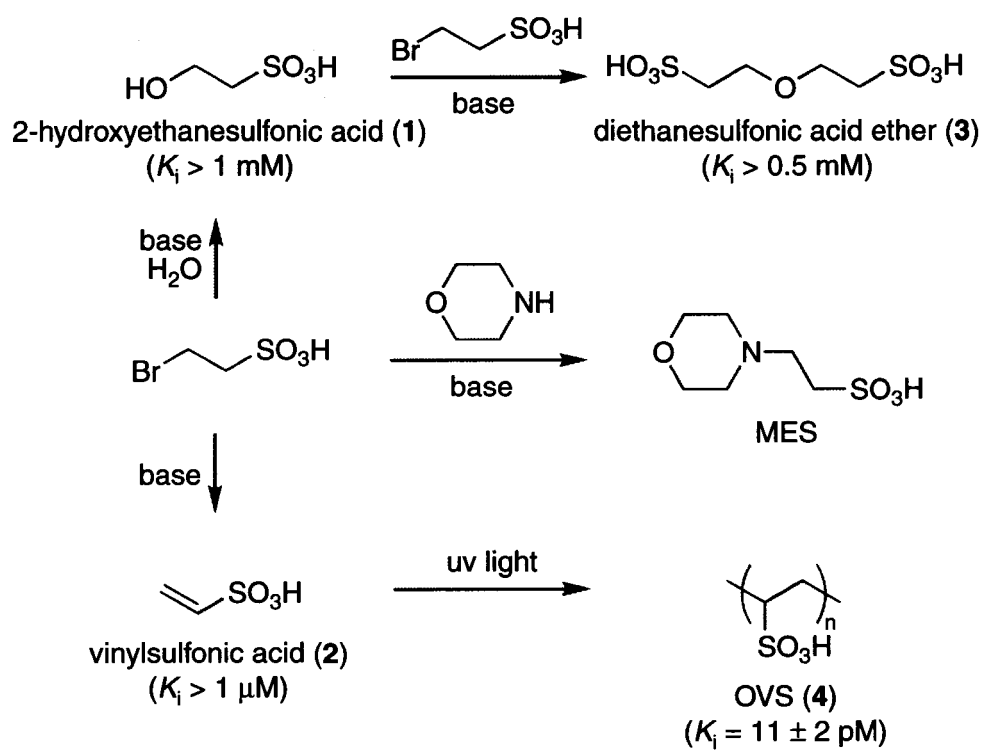
Figure 3.3 Mass spectrum of oligo(vinylsulfonic acid) purified from MES buffer. The

molecular mass of vinylsulfonic acid ($C_2H_4O_3S$) is 108 g/mol.
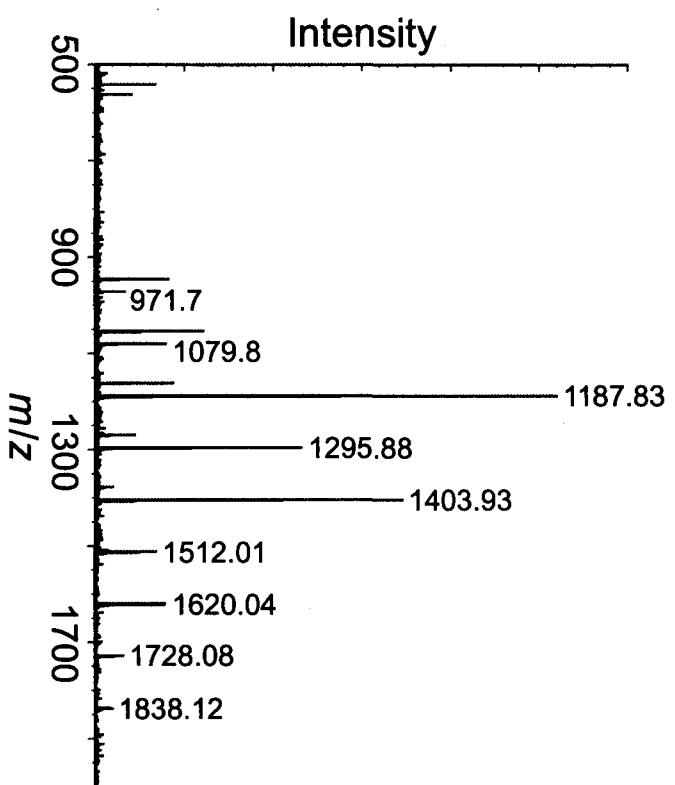
Figure 3.4   Effect of commercial oligo(vinylsulfonic acid) on catalysis of

poly(cytidylic acid) cleavage by ribonuclease A. Lineweaver–Burk plots

are shown for five concentrations of oligo(vinylsulfonic acid): 0.0 (■),

0.35 (●), 0.7 (▲), 1.4 (◆), and 2.8 µM (★). Assays were performed at

25 °C in 50 mM imidazole–HCl buffer (pH 6.0) containing NaCl

(0.10 M). Inset: Slope-replot of the kinetic data.
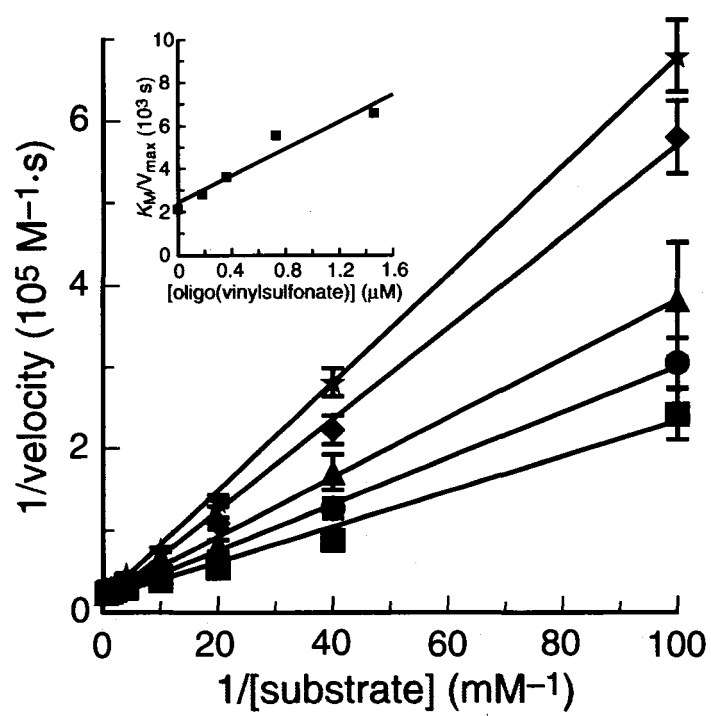
Figure 3.5 Salt-dependence of commercial oligo(vinylsulfonic acid) inhibition of

catalysis of 6-FAM~dArUdAdA~6-TAMRA cleavage by ribonuclease A.

A, Assays were performed at 25 °C in 50 mM imidazole–HCl buffer (pH

6.0) containing NaCl (■, 0; ●, 0.05; ▲, 0.10; ◆, 0.25 M). Rates

determined at 0.05–0.25 M NaCl were fitted to Equation 1; rates

determined at 0 M NaCl were fitted to Equation 2. *B*, Values of K_i were

calculated from the data in panel A. [Cation] refers to the concentration of

Na^+ plus imidazolium ion.
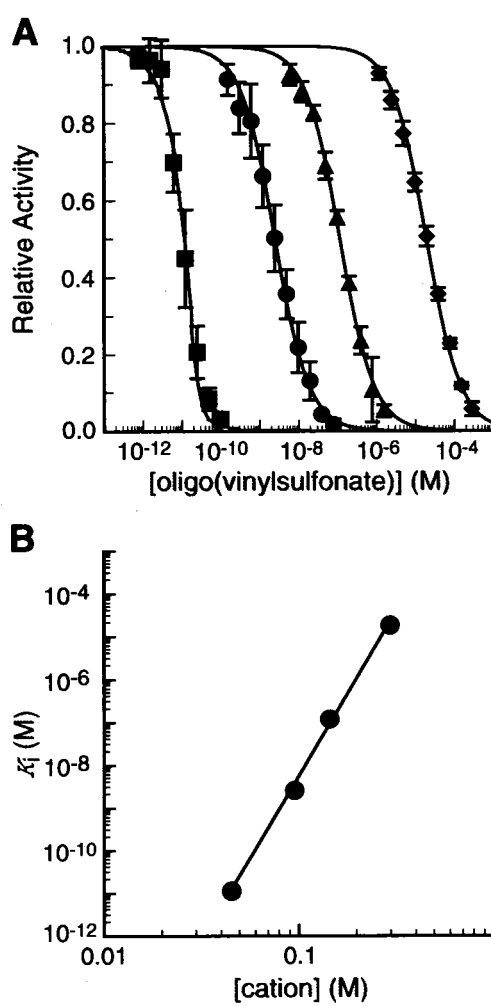
Chapter Four

Synthetic Surfaces for Ribonuclease Adsorption

This chapter was published as:

4.1 Abstract

Intact RNA and DNA are of central importance to biochemical research and biotechnology. The preservation of these nucleic acids requires the absence of nuclease activity. Here, radical-mediated polymerization of vinylsulfonate on resin and glass surfaces is shown to produce a high-density poly(vinylsulfonate) coating that sequesters ribonucleases from aqueous solutions quickly and completely. The adsorptive efficacy of this coating exceeds that of other known coatings by $\geq 10^7$-fold. Surfaces coated with poly(vinylsulfonate) could be used to maintain the integrity of ribonucleic acids in a variety of contexts.

4.2 Introduction

Biochemical research and biotechnology rely on polymeric nucleic acids. Yet during their storage and use, nucleic acids encounter nucleases, both advertently and inadvertently. For example, nucleases are often added with the intent of destroying RNA in a DNA sample, or *vice versa*. Residual amounts of these nucleases can affect downstream steps in protocols (Sweeney *et al.*, 2000; Pasloske, 2001). Alternatively, human skin is an abundant source of nucleases that can be transferred accidentally to surfaces and solutions (Holley *et al.*, 1961). Moreover, reagents (including those labeled "nuclease free") are often contaminated with nucleases (Hengen, 1996).

Ribonucleases are perhaps the most problematic of nucleases because of their high natural abundance, prodigious catalytic activity, notorious conformational stability and resistance to proteolysis, and lack of requisite cofactors (D'Alessio and Riordan, 1997;

Raines, 1998). Although several ribonuclease inhibitors have been described (Raines,

1998; Pasloske, 2001; Russo *et al.*, 2001), each suffers from one or more undesirable

attribute. For example, the ribonuclease inhibitor protein (RI) (Hofsteenge, 1997;

Shapiro, 2001) binds ribonucleases with femtomolar affinity, but is expensive and highly

sensitive to oxidation (Kim *et al.*, 1999). In addition, RI inhibits only ribonuclease A

(RNase A, EC 3.1.27.5) (Cuchillo *et al.*, 1997; Raines, 1998) and some of its homologs.

Although diethylpyrocarbonate (DEPC) inactivates many nucleases, it is toxic and its use

requires time-consuming procedures. Moreover, DEPC-treatment results in the covalent

modification of many proteins, nucleic acids, and small molecules (Miles, 1977).

Recently, we discovered that oligo(vinylsulfonate) is an extremely potent inhibitor of

catalysis by RNase A (as well as a contaminant in common buffers that contain

sulfonylethyl groups) (Smith *et al.*, 2003). Its inhibitory activity is due to its high density

of anionic charges, which are displayed in a manner reminiscent of that in a polymeric

nucleic acid (Figure 4.1A). Previous work had demonstrated that poly(vinylsulfonate)

(PVS) is also a potent inhibitor of deoxyribonucleases (Tunis and Regelson, 1963; Bach,

1964). Still, the utility of PVS as a general nuclease inhibitor has been limited by the

difficulty of separating PVS from nucleic acids, which are likewise polyanionic.

We envisioned that surfaces coated with PVS could be useful in many contexts

(Narang *et al.*, 1995; Rahman *et al.*, 1996; Raines, 1998). The addition of PVS-coated

resin, followed by filtration or centrifugation, could be used to remove nucleases from

solution. Alternatively, PVS-coated glassware or plasticware could adsorb a

contaminating nuclease, thereby providing safe long-term storage for valuable nucleic

acids. To test these hypotheses, we coated two distinct surfaces with PVS. To maximize

the density of the coating, we chose to synthesize PVS directly on the surfaces rather than

couple the polymer to a surface. The results indicate that PVS-coated surfaces provide an

extraordinary means to sequester ribonucleases.

4.3 Experimental Procedures

Materials. Reagents were from Sigma–Aldrich (St. Louis, MO). Anhydrous THF,

DMF, and CH_2Cl_2 were withdrawn from a CYCLETAINER solvent delivery system

from Mallinckrodt–Baker (Phillipsburg, NJ). Other anhydrous solvents were from

Sigma–Aldrich, and were withdrawn from septum-sealed bottles.

Silica gel functionalized with 3-aminopropyltriethoxysilane was from Silicycle

(Québec City, Canada). Glass slides functionalized with 3-aminopropyltriethoxysilane

were from CEL Associates (Pearland, TX).RNase A was produced in *Escherichia coli* as

described previously (delCardayré *et al.*, 1995). The A19C variant of RNase A (Sweeney

et al., 2000) was labeled with fluorescein as described previously (Abel *et al.*, 2002). A

fluorogenic ribonuclease substrate, 6-FAM–dArUdAdA–6-TAMRA (Kelemen *et al.*,

1999), was from Integrated DNA Technologies (Coralville, IA).

Synthesis of Acrylamide-Coated Silica. Silica gel functionalized with

3-aminopropyltriethoxysilane (5.0 g, 7.3 mmol) was suspended in CH_2Cl_2 (50 mL).

Dimethylaminopyridine (0.9 g, 7.3 mmol) was then added. The resulting suspension was

flushed with Ar(g) and cooled to 0 °C. Finally, acrolyl chloride (2.6 g, 29.2 mmol) was

added dropwise, followed by the dropwise addition of Hunig's base

(diisopropylethylamine; 7.55 g, 58.4 mmol). The reaction mixture was allowed to warm to room temperature, and then stirred for 12 h under Ar(g). The resin was isolated by filtration, and washed with CH_2Cl_2 (5 x 100 mL), DMF (5 x 100 mL), H_2O (5 x 100 mL), and Et_2O (5 x 100 mL). The resin was then dried under reduced pressure for 12 h and stored at 4 °C.

Synthesis of PVS-Coated Silica. Silica gel functionalized with acrylamide (1.0 g, 1.35 mmol) was suspended in degassed H_2O (30 mL). The resulting suspension was flushed with Ar(g). Sodium vinylsulfonate (17.5 g, 135 mmol, purified to remove MEHQ and dried to a white paste) was added, followed by 2,2'-azobis(2-methylpropionamideine) dihydrochloride (42 mg, 0.15 mmol). The reaction mixture was heated to 70 °C and allowed to stir for 48 h under Ar(g). The resin was isolated by filtration, and washed with CH_2Cl_2 (5 x 100 mL), DMF (5 x 100 mL), H_2O (5 x 100 mL) and Et_2O (5 x 100 mL). The resin was then dried under reduced pressure for 12 h and stored at 4 °C.

Synthesis of Acrylamide-Coated Glass. A glass slide (75 x 25 mm) functionalized with 3-aminopropyltriethoxysilane was placed in CH_2Cl_2 (50 mL). Dimethylaminopyridine (0.9 g, 7.3 mmol) was then added. The slide was flushed with Ar(g) and cooled to 0 °C. Finally, acrolyl chloride (2.6 g, 29.2 mmol) was added dropwise, followed by the dropwise addition of Hunig's base (7.55 g, 58.4 mmol). The reaction mixture was allowed to warm to room temperature, and then stirred for 12 h under Ar(g). The slide was washed with CH_2Cl_2 (5 x 100 mL), DMF (5 x 100 mL), H_2O

(5 x 100 mL), and Et₂O (5 x 100 mL). The slide was then dried under reduced pressure

for 12 h and stored at 4 °C.

Synthesis of PVS-Coated Glass. An acrylamide-coated glass slide (75 x 25 mm) was

placed in degassed H_2O (30 mL), which was then flushed with Ar(g). Sodium

vinylsulfonate (17.5 g, 135 mmol, purified to remove MEHQ and dried to a white paste)

was added, followed by 2,2'-azobis(2-methylpropionamideine) dihydrochloride (42 mg,

0.15 mmol). The reaction mixture was heated to 70 °C, and then allowed to stir for 48 h

under Ar(g). The slide was washed with CH_2Cl_2 (5 x 100 mL), DMF (5 x 100 mL), H_2O

(5 x 100 mL), and Et₂O (5 x 100 mL). The slide was then dried under reduced pressure

for 12 h and stored at 4 °C.

Quantitative Analysis of the Adsorption of a Ribonuclease by PVS-Coated Silica.

RNase A (1–128 μM) was incubated with PVS-coated silica (0.1 mg) for 2 h at room

temperature in 0.10 mL of 50 mM MES–NaOH buffer, pH 6.0, containing NaCl

(0.10 M). The resin was collected by centrifugation at 5000g for 10 s. The supernatant

was tested for ribonucleolytic activity with a sensitive assay based on a fluorogenic

substrate: 6-FAM–dArUdAdA–6-TAMRA (Kelemen *et al.*, 1999). The concentrations of

free and bound RNase A were determined and subjected to Scatchard analysis. Assays

were performed in triplicate.

The ability of PVS-coated silica to adsorb RNase A was also assessed in Dulbecco's

phosphate-buffered saline (PBS), which is KCl (2.68 mM), KH_2PO_4 (1.47 mM), NaCl

(136.89 mM), and Na_2HPO_4 (8.06 mM).

Time Course for the Adsorption of a Ribonuclease by PVS-Coated Silica. PVS-coated silica (100 mg/mL) was pre-equilibrated with buffer for several days. The resin (0.1 mg, 0.4 nmol of tight-binding sites) was then mixed with 0.10 mL of 50 mM MES–NaOH buffer, pH 6.0, containing NaCl (0.10 M) and RNase A (2 μM, 0.2 nmol). At several time points, the resin was collected by centrifugation at 5000g for 5 s, and an aliquot of the supernatant was assayed for ribonucleolytic activity (Kelemen *et al.*, 1999).

Reuse of PVS-Coated Silica. PVS-coated silica (10 mg) was mixed at room temperature for 2 h with RNase A (1.0 μM) in 1.0 mL of 0.05 M MES–NaOH buffer, pH 6.0, containing NaCl (0.10 M). The resin was collected by centrifugation at 5,000g for 10 s. The supernatant was removed, and an aliquot was assayed for ribonucleolytic activity (Kelemen *et al.*, 1999). The resin was then washed with 1.0 M NaCl (2 x 1.0 mL). The resin was again collected by centrifugation, and the supernatant was assayed for ribonucleolytic activity (Kelemen *et al.*, 1999). The resin was then washed thoroughly with H_2O. A new aliquot of RNase A was then added, and the entire process was repeated five times.

Adsorption of Contaminating Human Ribonucleases by PVS-Coated Silica. 0.05 M MES–NaOH buffer, pH 6.0, containing NaCl (0.10 M) was contaminated with secretory ribonucleases by swiping a human finger on the inside of the tube. The buffer was passed through a 0.2-μm sterile filter to remove any human or microbial cells. One mL of ribonuclease-contaminated buffer was mixed with PVS-coated resin (10 mg), acrylamide-coated resin (10 mg), or no resin for 2 h at room temperature. The resin was collected by centrifugation at 5,000g for 10 s. The supernatant was removed and assayed for

ribonucleolytic activity as follows. Each sample was incubated with 16S and 23S rRNA (4 μg; Roche) overnight at 37 °C. As controls, a sample of non-contaminated buffer and a sample of RNase A (10 pM) were incubated likewise. An aliquot (10 μL) of each sample was then mixed with loading dye and subjected to electrophoresis for 15 min at 100 V through a 1.0% (w/v) agarose gel in TAE buffer (40 mM Tris–acetic acid, 1 mM EDTA) containing ethidium bromide (6 μg/mL).

4.4 Results and Discussion

We synthesized PVS on silica gel and glass slides (Figure 4.1B) that had been modified so as to display amino groups (Lesaicherre et al., 2002). Reaction of the surface amino groups with acryolyl chloride converted the amino groups into acrylamide groups, which have electron-deficient alkenes that undergo facile polymerization. We then performed radical-mediated polymerization of vinylsulfonate ($CH_2=CHSO_3^-$) on the acrylamide-coated surfaces. The resulting surfaces were washed until free PVS was no longer detectable with a sensitive assay for ribonuclease inhibition (Smith et al., 2003).

PVS-coated surfaces sequester a fluorescently-labeled ribonuclease (Figure 4.2). We quantified the ability of PVS-coated silica to remove a ribonuclease from 50 mM MES–NaOH buffer, pH 6.0, containing NaCl (0.10 M). A Scatchard plot of the data is curvilinear (Figure 4.3A), as expected for the binding of a ligand to a lattice of sites (McGhee and von Hippel, 1974). We determined the equilibrium dissociation constants for the tightest binding sites from the limiting slope of the Scatchard plot (Rahman et al., 1996). The PVS-coated silica has 4.1 μmol/g of tight-binding sites for RNase A and $K_d =$

80 nM for these sites. This K_d value is in gratifying agreement with the inhibition constant observed using free PVS (K_i = 120 nM) (Smith *et al.*, 2003). In the presence of PVS-coated silica with excess tight-binding sites, residual ribonucleolytic activity is not detectable (<0.01%).

PVS-coated surfaces sequester a ribonuclease quickly. The enzymatic activity of an added ribonuclease was measured at known times after exposure to PVS-coated silica in which the number of tight-binding sights was only twofold greater than the amount of ribonuclease. Half of the ribonuclease was bound within 1 min; maximum binding occurred within 1 h (Figure 4.3B). In contrast, acrylamide-coated silica did not remove any ribonuclease after 4 h (Figure 4.4).

PVS-coated surfaces far exceed the capacity and affinity for nucleases of other known surfaces. In the most effective prior example, poly[2'-O-(2,4-nitrophenyl)]poly(A) [DNP–poly(A)] was attached to acrylic beads (Rahman *et al.*, 1996). This material has 0.017 μmol/g of binding sites for RNase A (which is 240-fold less than PVS-coated silica) and K_d = 0.41 μM in a solution of low salt concentration (which is 3.7 x 10^4-fold greater (Smith *et al.*, 2003)). Accordingly, the adsorptive efficacy of PVS-coated silica exceeds that of other known surfaces by $\geq 10^7$-fold.

PVS-coated silica is also able to remove RNase A from PBS. This buffer has a pH of 7.4, which allows for only weak Coulombic interactions between the two active-site histidine residues of RNase A and a polyanion (Park *et al.*, 2001). Moreover, PBS contains inorganic phosphate, which like PVS binds to the active site of RNase A (Richards and Wyckoff, 1971). Still, PVS-coated silica was able to sequester RNase A

from PBS (data not shown), though less effectively than from 50 mM MES–NaOH buffer, pH 6.0, containing NaCl (0.10 M).

PVS-coated surfaces can be regenerated and reused many times. PVS-coated silica was incubated with RNase A such that the amount of free RNase A was <0.5%. After the incubation, nearly 100% of the bound RNase A was eluted by washing with 1.0 M NaCl. This incubation/elution cycle was repeated a total of five times with no detectable change in the amount of ribonuclease sequestered or released (Figure 4.5).

Finally, PVS-coated surfaces bind the most prevalent human ribonuclease, RNase 1. Under conditions similar to those used for RNase A, a solution of human RNase 1 is >99.5% bound by PVS-coated silica (data not shown). In addition, migration rates during electrophoresis in an agarose gel indicate that PVS-coated silica diminishes RNA degradation by secretory ribonucleases from human skin (Figure 4.6).

4.5 Conclusions

Surfaces can be coated with PVS by a facile chemical synthesis. Such surfaces extract ribonucleases from solution quickly and completely, and can be used repeatedly. PVS-coated surfaces have many advantages over other known means to sequester ribonucleases and thereby preserve the integrity of RNA.

Figure 4.1   *A*, Structure of DNA (R = H) and RNA (R = OH) (top) and PVS (bottom).

B, Scheme for the synthesis of PVS-coated surfaces.

A

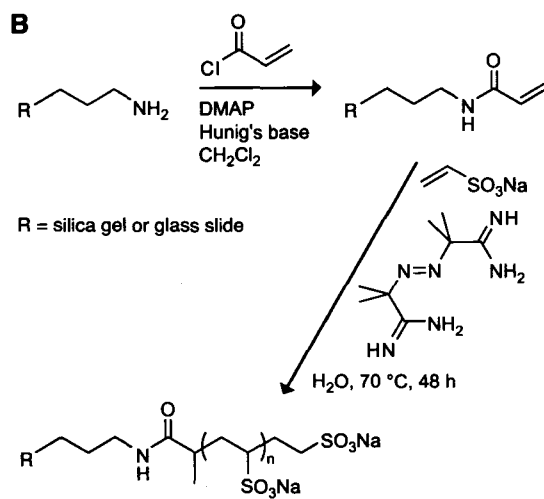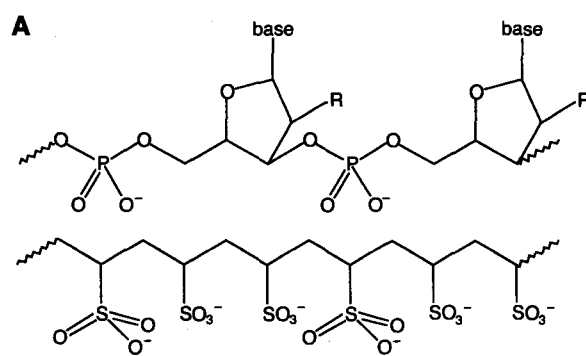B

R = silica gel or glass slide

Figure 4.2   PVS-coated surfaces sequester a ribonuclease. *A*, Bright-field image (60x)

of PVS-coated silica gel. *B*, Fluorescent image of panel A. *C*, Bright-field

image (60x) of PVS-coated silica gel in the presence of fluorescein–

RNase A. *D*, Fluorescent image of panel C. *E*, Fluorescent image of an

acrylamide-coated glass slide in the presence of fluorescein–RNase A. *F*,

Fluorescent image of a PVS-coated glass slide in the presence of
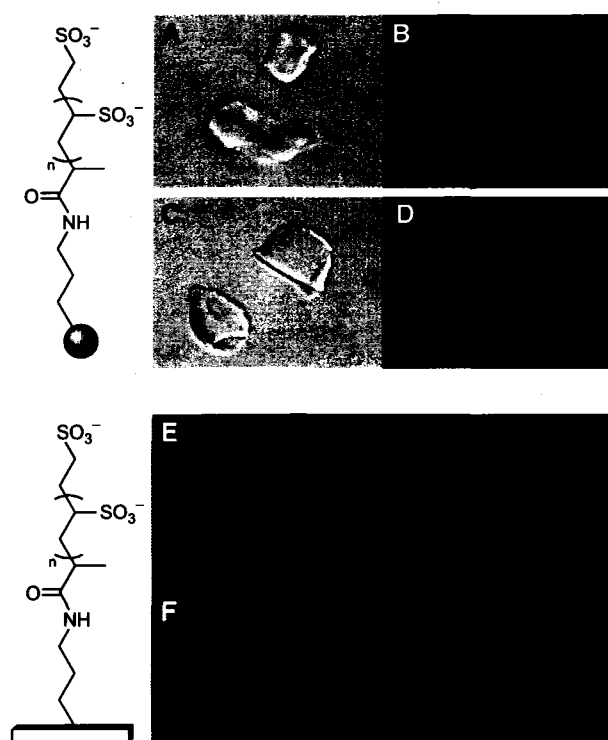
fluorescein–RNase A.

Figure 4.3 Quantitative analysis of the adsorption of a ribonuclease by PVS-coated

silica. *A*, Scatchard plot for the adsorption of RNase A by PVS-coated

silica in 50 mM MES–NaOH buffer, pH 6.0, containing NaCl (0.10 M).

Data are for tight-binding sites. *B*, Time-course for the adsorption of

RNase A by PVS-coated silica that has a twofold molar excess of tight-
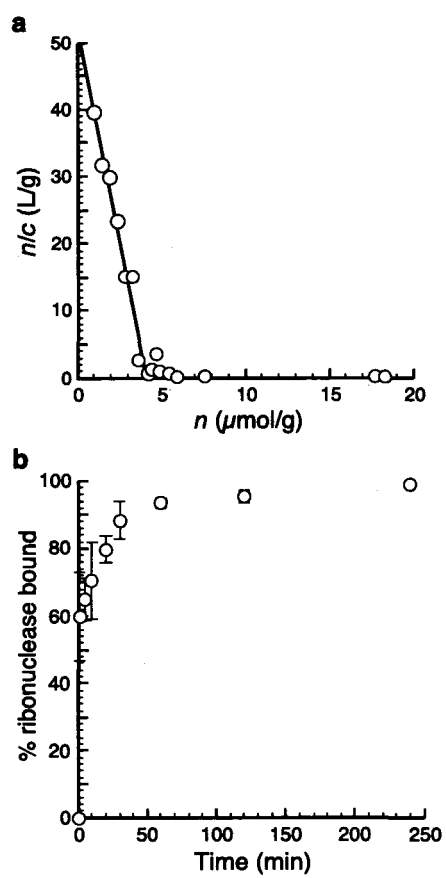
binding sites.

Figure 4.4 Non-adsorption of a ribonuclease by acrylamide-coated silica.

Acrylamide-coated silica (0.1 mg) was incubated at room temperature

with RNase A (2 μM) in 0.10 mL of 50 mM MES–NaOH buffer, pH 6.0,

containing NaCl (0.10 M). At known times, the resin was collected by

centrifugation, and an aliquot of supernatant was assayed for
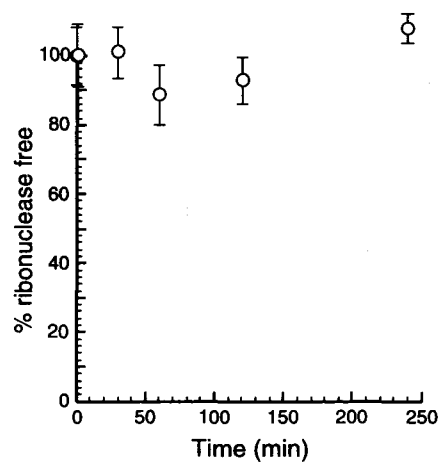
ribonucleolytic activity.

Figure 4.5   Adsorption of a ribonuclease during repeated use of a PVS-coated surface.

PVS-coated silica (10 mg) was mixed at room temperature for 2 h with

RNase A (1.0 μM) in 1.0 mL of 50 mM MES–NaOH buffer, pH 6.0,

containing NaCl (0.10 M). The resin was collected by centrifugation. The

supernatant was removed, and an aliquot was assayed for ribonucleolytic

activity. The resin was then washed with 1.0 M NaCl and collected by

centrifugation. The supernatant was again assayed for ribonucleolytic

activity. The resin was then washed thoroughly with H₂O. A new aliquot

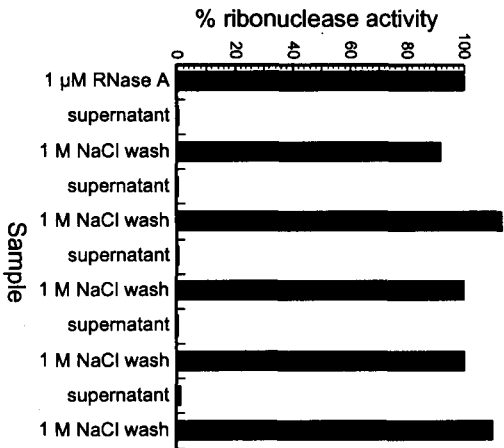of RNase A was added, and the process was repeated five times.

Figure 4.6 Adsorption of human secretory ribonucleases by a PVS-coated surface.

Buffer was intentionally contaminated with secretions from human skin.

The ability of PVS-coated silica to sequester secretory ribonucleases and

protect the integrity of rRNA was assessed qualitatively by agarose gel

electrophoresis.
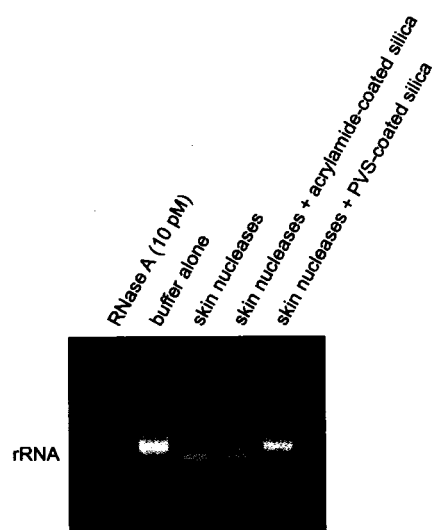
Chapter Five

Genetic Selection for Peptide Inhibitors of Angiogenin

Smith, B. D. and Raines, R. T. (2006) Genetic selection for peptide inhibitors of

angiogenin. *In Preparation.*

5.1 Abstract

Angiogenin, a homolog of bovine pancreatic ribonuclease (RNase A), uses its ribonucleolytic activity to promote the growth of new blood vessels. This process—angiogenesis—is critical for normal biological functions such as embryonic development and wound healing. Improperly regulated angiogenesis is implicit in a variety of diseases including arthritis and cancer. Inhibitors of angiogenin could therefore serve as potential therapeutics. Towards this goal, a genetic selection system was used to isolate inhibitors of angiogenin from a large library of random nine-residue peptides. This nonapeptide library was attached to the solvent exposed C-terminus of angiogenin via a glycine-rich linker to increase the effective molarity of the peptides. Angiogenin is toxic to the Origami™ strain of *Escherichia coli*, and colonies grow only if the ribonucleolytic activity of angiogenin is reduced significantly. Via this method, two peptides were identified, synthesized, and found to inhibit the ribonucleolytic activity of angiogenin *in vitro*. Both peptides also inhibit RNase A, though one peptide is selective for angiogenin. These peptides or their derivatives could have the potential to prevent tumor growth *in vivo*.

5.2 Introduction

Angiogenin was originally isolated as a human tumor-derived protein with the ability to promote angiogenesis, the growth of new blood vessels (Fett *et al.*, 1985). When the amino acid sequence of angiogenin was determined (Strydom *et al.*, 1985), surprisingly, it had 35% identity to that of the most studied enzyme of the 20th century, bovine

pancreatic ribonuclease (RNase A; 3.1.27.5) (Raines, 1998). Angiogenin contains the

active-site residues that are characteristic of this family of ribonucleases (Beintema *et al.*,

1988). Yet, initially there were doubts that angiogenin retained ribonucleolytic activity,

as it did not appear to degrade commonly used RNA substrates (Strydom *et al.*, 1985). It

was shown, however, that angiogenin was found to degrade rRNA to a limited extent

(Shapiro *et al.*, 1986; St Clair *et al.*, 1987). Using a more sensitive assay, angiogenin was

found to have ribonucleolytic activity ~10^5–10^6-fold lower than that of RNase A (Leland

et al., 2002). Nevertheless, the ribonucleolytic activity of angiogenin is required for

angiogenesis (Shapiro *et al.*, 1989; Shapiro and Vallee, 1989). The enzyme could act with

high activity on an as yet unidentified specific recognition sequence or RNA secondary

structural element (Shapiro *et al.*, 1986; Strydom, 1998; Leland *et al.*, 2002).

Improperly regulated angiogenesis is involved in many diseases, most notably tumor

growth (Gimbrone *et al.*, 1972). Angiogenin levels are elevated in a variety of cancers, as

angiogenesis is critical for the growth and metastasis of tumors (Katona *et al.*, 2005).

Inhibitors of angiogenic factors could lead to new cancer therapies (Folkman and Shing,

1992). The success of Avastin™ (a humanized monoclonal antibody targeting the potent

angiogenesis-promoter VEGF) at treating cancers provides ample evidence for the

success of this approach (Ferrara, 2005). Angiogenin is another promising anti-cancer

target. Indeed, monoclonal antibodies, an antisense oligonucleotide, and small molecule

inhibitors of angiogenin have been shown to possess antitumoral activity against

subcutaneous tumors in athymic mice (Olson *et al.*, 1995; Olson *et al.*, 2001; Kao *et al.*,

2002).

There are at least two possible approaches to prevent angiogenin function *in vivo*. Angiogenin-induced angiogenesis can be disrupted by inhibiting the enzymatic activity of angiogenin (Nobile *et al.*, 1998; Kao *et al.*, 2002; Jenkins and Shapiro, 2003) or by interfering with its internalization pathway (Choi *et al.*, 1997). Peptide libraries can be used to identify potent ligands of proteins, for both basic research and as potential drug leads (Cwirla *et al.*, 1990; Devlin *et al.*, 1990; Scott and Smith, 1990; Falciani *et al.*, 2005). Several phage-display libraries have been used to isolate peptides that disrupt the interaction between angiogenin and its receptor (Choi *et al.*, 1997; Gho *et al.*, 1997). However, these peptides do not inhibit the ribonucleolytic activity of angiogenin.

As an alternate strategy to disrupt angiogenin-induced angiogenesis, we reasoned that we could isolate peptide inhibitors that specifically block the ribonucleolytic activity of angiogenin by using a genetic selection system that requires the absence of enzymatic activity for cell growth. Angiogenin has three disulfide bonds and cannot fold in the reducing environment of the cytosol of a typical laboratory strain of *E. coli*. The Origami™ strain of *E. coli* has several mutations that generate a more oxidizing environment in the cytosol (Derman *et al.*, 1993; Bessette *et al.*, 1999). Consequently, plasmids encoding angiogenin are toxic to Origami™ cells. A relatively high level of reduction in the ribonucleolytic activity of angiogenin is needed to allow for cell growth. To increase the likelihood of identifying angiogenin inhibitors, the peptide library was attached in *cis* to the solvent-exposed C-terminus of angiogenin via a glycine-rich linker. This increases the effective molarity of the peptides, and potentially allows for the isolation of inhibitors that might not be identified if they were encoded in *trans*. A

degenerate oligonucleotide encoding the nonapeptide library was ligated in frame with the angiogenin cDNA via a sequence encoding for a glycine-rich linker. From this library of over 2×10^7 random peptides, we identified many sequences that were potential inhibitors of angiogenin. Two of these peptides were found to inhibit angiogenin *in vitro*, including one that is among the best inhibitors of angiogenin identified to date. Furthermore, there are few inhibitors that are selective for angiogenin over RNase A, which could be a precondition for a successful therapeutic. We find that one peptide is selectively inhibits angiogenin over RNase A. These peptides could serve as leads for new anti-cancer agents. In addition, the selection system described herein could be used to identify even more potent and more selective inhibitors from a variety of libraries, including cell-permeable small molecules.

5.3 Experimental Procedures

Materials. Escherichia coli Origami™ B(DE3) cells and DH5α cells were from Novagen (Madison, WI). Oligonucleotides were from Integrated DNA Technologies (Coralville, IA). The fluorogenic ribonuclease substrate, 6-FAM~dArUdAdA~6-TAMRA (where 6-FAM is a 5' 6-carboxyfluorescein group and 6-TAMRA is a 3' 6-carboxytetramethylrhodamine group), was from Integrated DNA Technologies (Coralville, IA). Peptides were obtained from the University of Wisconsin–Madison Peptide Synthesis Facility. MES buffer was purified prior to use to remove inhibitory contaminants as described previously (Smith *et al.*, 2003). All other commercial

chemicals and biochemicals were of reagent grade or better, and were used without further purification.

Instruments. UV absorbance measurements were made with a Cary Model 3 spectrophotometer (Varian, Palo Alto, CA). Fluorescence measurements were made with a QuantaMaster 1 Photon Counting Fluorometer equipped with sample stirring (Photon Technology International, South Brunswick, NJ).

Plasmids. The human angiogenin cDNA was inserted into pSH12 (Park and Raines, 2000), which is a pGEX-4T3 based plasmid, at its *Nde*I and *Sal*I restriction enzyme sites. This plasmid encodes for a methionine residue at the start of the gene, designated Met(-1). The stop codon was replaced by codons for three glycine residues, directly followed by the *Sal*I site. The *Sal*I site encodes for two consecutive serine residues that remain after ligation of the peptide library insert. This plasmid is designated pGEX-ANG-G3S2. Three additional glycine residues are encoded by the oligonucleotides for the peptide insert (*vide infra*), thus the full linker separating the final residue in angiogenin and the nonapeptide library is $Gly_3Ser_2Gly_3$. This linker is long enough and flexible enough to allow the peptides to fold back over the RNA binding cleft and active site of angiogenin.

Oligonucleotides for Peptide Library. The degenerate oligonucleotide, BS9, 5'-TCGAGC(GGT)$_3$(XNK)$_9$TAGTAGTCGC-3' encodes for a peptide of nine random amino acid residues. The base composition of the XNK codons, X = A(32%)/G(39%)/C(21%)/T(8%), N = A(25%)/G(25%)/C(25%)/T(25%), and K = G(50%)/T(50%) was similar to a library previously designed to reduce the number of

stop codons and closely mirror the natural abundance of amino acid residues in proteins

(LaBean and Kauffman, 1993; Park and Raines, 2000). Due to the complexity of nine

degenerate codons (4^{27}), special techniques are required for the preparation of duplex

DNA for ligation. We used the gapped-duplex method in which the degenerate

oligonucleotide is annealed to two shorter oligonucleotides that are complementary to its

nondegenerate termini (Figure 5.1A) (Cwirla *et al.*, 1990; Park and Raines, 2000). The

gap in the duplex DNA is filled after transformation of plasmid DNA into *E. coli*. The

gapped-duplex DNA was prepared by annealing the degenerate oligonucleotide with

oligonucleotides, BS11, 5'-ACCACCACCGC-3' and, BS10,

5'-GGCCGCGACTACTA-3'. All three oligonucleotides had been phosphorylated at

their 5' ends. The oligonucleotides (1.5×10^{-11} mol for BS9 and 2.86×10^{-10} mol for

BS10 and BS11) were annealed in 20 mM Tris-HCl pH 7.0, containing $MgCl_2$ (2 mM)

and NaCl (50 mM) in a total volume of 10 µL. The mixture was heated to 65 °C for 5

min and allowed to cool slowly to room temperature. The 5' and 3' ends of the annealed

duplex are compatible with *Sal*I and *Not*I cleavage sites, respectively.

Ligation Reactions. 10 µg of pGEX-ANG-G3S2 plasmid DNA was digested at 37°C

for 2 h with *Sal*I (15 U) and *Not*I (15 U) in 1X Promega Buffer D (6 mM Tris-HCl pH

7.9 containing $MgCl_2$ (6 mM), NaCl (150 mM) and DTT (1mM)) in a total volume of

100 µL. The restriction enzymes were inactivated by heating at 65 °C for 15 min. Sodium

acetate, pH 5.0 (0.3 M) and three volumes ice-cold ethanol were added to the reaction

mixture, and the tube was placed at -20 °C for 1 h to precipitate the DNA. The digested

DNA was subjected to centrifugation at 10,000*g* for 10 min at 4°C. The ethanol was

removed by aspiration, and 250 µL of an ice-cold aqueous solution of ethanol (70% v/v) was added. The sample was subjected to centrifugation again. The ethanol was removed by aspiration with a drawn pipette. The DNA pellet was dried for 1 min in a vacuum desiccator, and then dissolved in ddH$_2$O (20 µL). The sample was then desalted over an AutoSeq G50 column (GE Healthcare, Piscataway, NJ). The purified linear plasmid (20 µL) and annealed gapped-duplex oligonucleotides (10 µL) were added to a ligation reaction mixture (50 µL) containing 1 x ligase buffer, DNA ligase (8 U; Promega, Madison, WI), and additional ATP (1 mM). The ligation reactions were placed at 14 °C overnight. The ligation reactions were precipitated with ethanol as above. The dried DNA pellet containing purified ligated plasmid DNA was dissolved in ddH$_2$O (10 µL) and desalted over an AutoSeq G50 column.

Library Analysis. Ligated DNA was transformed by electroporation into competent *E. coli* DH5α cells to analyze the quality and randomness of the nonapeptide library (*nb*: plasmids encoding angiogenin are not toxic to this strain of *E. coli*). Cells were electroporated (1.80 kV, 200 Ω, 25 µF) with 1 µL of the desalted and purified ligated DNA. SOC (1.0 mL) was added immediately, and the cells were allowed to recover at 37 °C for 1 h before being plated on LB agar containing ampicillin (100 µg/mL). Electroporetic transformation of DH5α cells with ligated DNA yielded 2.4 x 10^7 transformants. Cultures (1 mL) were grown in LB medium containing ampicillin (100 µg/mL) and plasmid DNA was isolated with the Wizard SV Plus Miniprep kit (Promega, Madison, WI). DNA sequencing reactions (10 µL) contained Big Dye 3.1 (1.0 µL), Big Buffer (1.5 µL), ddH$_2$O (1.5 µL), primer (1 µL from a 10 µM stock), and

plasmid DNA (5.0 µL). Reaction mixtures were subjected to thermocycling (36 cycles; 96 °C for 20 s, 48 °C for 30 s, and 58 °C for 5 min). The sequencing reaction mixtures were purified with the CleanSEQ Dye-terminator Removal kit (Agencourt Bioscience, Beverly, MA). DNA sequences were obtained in the forward and reverse directions. Sequence analysis of a sample of this library indicated that >90% of clones carried inserts and that the nine XNK codons were indeed random. Of note, a fraction of the sequences (<5%) contained 1 bp inserts or deletions in the sequence encoding the nonapeptide library (though the BS9 oligonucleotide was PAGE purified, it is likely that sequences with 1 bp frameshifts would be present at a low level). These sequences were included for analysis, as stop codons are present downstream in all three reading frames.

Genetic Selection. Ligated DNA was transformed by electroporation into competent *E. coli* Origami™ cells as described above, with the following modifications. After transformation, SOC (1.0 mL) was added immediately, and the cells were allowed to recover at 37 °C for 1.5 h before being plated on LB agar containing ampicillin (100 µg/mL), kanamycin (15 µg/mL), and tetracycline (12.5 µg/mL). Origami™ cells grow more slowly than normal laboratory strains of *E. coli*, thus colonies were picked after 24–48 h growth. Plasmid DNA was isolated and sequenced as above.

Production of Ribonucleases. Plasmid pET-ANG (Leland *et al.*, 2002) directs the production of angiogenin in *E. coli*. Angiogenin was produced and purified as described previously with the following modifications. To avoid trace contamination by other ribonucleases, refolded and concentrated angiogenin was purified on a new HiTrap SPHP column (5 mL; GE Healthcare, Piscataway, NJ). All buffers were made with 0.1%

DEPC-treated, distilled and deionized H_2O. The column was equilibrated with 50 mM

sodium phosphate buffer (pH 7.2). Angiogenin (15 mg) was loaded onto the column. The

column was washed with 50 mM sodium phosphate buffer, pH 7.2 (20 mL) and then with

50 mM sodium phosphate buffer, pH 7.2 (50 mL) containing NaCl (0.25 M). Angiogenin

was eluted from the column with 50 mM sodium phosphate buffer, pH 7.2 (20 mL)

containing NaCl (0.35 M). Zymogram electrophoresis was performed to confirm that

purified angiogenin was free from contaminating ribonucleolytic activity, as described

previously (Leland et al., 2002). RNase A was produced and purified as described

previously (Kim and Raines, 1993; Smith et al., 2003).

Inhibition of Ribonucleolytic Activity. Inhibition of ribonucleolytic activity was

assessed at 25 °C in 2.0 mL of 50 mM MES-NaOH, pH 6.0, containing NaCl (0.1 M),

6-FAM~dArUdAdA~6-TAMRA (60 nM), and angiogenin (0.42 µM) or RNase A

(2 pM), as described previously (Kelemen et al., 1999; Park et al., 2001; Smith et al.,

2003). Peptide 1, *acetyl*-LDDAEEWGG, was dissolved in assay buffer. Peptide 2, *acetyl*-

AEDYDYSWW, was dissolved in assay buffer containing CH_3CN (20% v/v). Peptide 3,

acetyl-SYSALYEAG, was dissolved in assay buffer containing CH_3CN (40% v/v).

Fluorescence (F) was measured using 493 and 515 nm as the excitation and emission

wavelengths, respectively. The value of $\Delta F/\Delta t$ was measured for 3 min after the addition

of enzyme. Next, an aliquot of inhibitor (I) was added, and $\Delta F/\Delta t$ was measured in the

presence of the inhibitor for 2 min. The concentration of inhibitor in the assay was

doubled repeatedly in 2-min intervals. Excess RNase A was then added to the mixture to

ensure that less than 10% of the substrate had been cleaved prior to completion of the

inhibition assay. Apparent changes in ribonucleolytic activity due to dilution or other artifacts (such as protein binding to the sides of cuvettes during the course of the assay) were corrected by comparing values to an assay in which aliquots of buffer (or buffer containing CH_3CN (20% or 40% v/v)) were added to the assay. At the concentrations tested, CH_3CN had no effect on ribonucleolytic activity. Values of K_i were determined by non-linear least squares regression analysis of data fitted to Equation 1 (Kelemen *et al.*, 1999; Park *et al.*, 2001),

$$\Delta F/\Delta t = (\Delta F/\Delta t)_0(K_i/(K_i + [I])) \qquad \text{(Eq. 1)}$$

In Equation 1, $(\Delta F/\Delta t)_0$ was the ribonucleolytic activity prior to inhibitor addition.

5.4 Results and Discussion

Strategy. Useful drug leads can be obtained via scanning peptide libraries for protein ligands (Cwirla *et al.*, 1990; Landon *et al.*, 2004; Watt, 2006). Most peptide libraries are generated using phage display, a technique that can be used to identify tight binding ligands of a protein of interest. Here, we scan a peptide library *in vivo* to select for peptides that not only bind angiogenin, but also inhibit its ribonucleolytic activity.

Angiogenin production is not toxic to normal laboratory strains of *E. coli* such as DH5α cells (Figure 5.1B). Native angiogenin contains three essential disulfide bonds that cannot form in the reducing environment of the cytosol. The Origami™ strain of *E. coli* has mutations in the genes encoding glutathione reductase and thioredoxin reductase that

combine to allow for a more oxidizing environment in the cytosol and efficient disulfide bond formation in these cells (Figure 5.1C) (Derman *et al.*, 1993; Bessette *et al.*, 1999). Consequently, plasmids encoding angiogenin are highly toxic to Origami™ cells. The low level of angiogenin produced via leaky expression of the gene under control of a P_{tac} promoter is sufficiently lethal to these cells. The stringency of selection can be tuned by adding IPTG (Figure 5.2).

In the absence of IPTG, a ~50-fold reduction in the ribonucleolytic activity of angiogenin is needed to allow for cell growth (Figure 5.2). To increase the likelihood of isolating inhibitors that are capable of reducing the ribonucleolytic activity of angiogenin to this low level, a nonapeptide library was fused directly to the C-terminus of angiogenin via a $Gly_3Ser_2Gly_3$ linker (Figure 5.1A). The effective concentration of these peptides would be much higher than if the peptide library was fused to a secondary protein. This is, in principle, similar to the "tethering" strategy used to identify successful small-molecules inhibitors of enzymes (Erlanson *et al.*, 2000).

Peptide Library. The nonapeptide library was ligated to a linker encoded at the 3' end of the angiogenin gene using the gapped-duplex method (Figure 5.1A) (Cwirla *et al.*, 1990; Park and Raines, 2000). Transformation of the angiogenin/peptide library into *E. coli* DH5α cells yielded 2.4×10^7 transformants. Although the theoretical library size is 5×10^{11}, the actual library size is limited by the transformation efficiency of *E. coli*, among other factors. Nevertheless, the library contains much sequence diversity. DNA sequence analysis indicated that the nonapeptide library was random and had a low occurrence of stop codons (Tables 5.1 and 5.2).

Genetic Selection. Transformation of the angiogenin/peptide library into *E. coli* Origami™ cells yielded transformants at a frequency of ~10^{-4}. This frequency of selection includes false positives. Since we are selecting for the absence of ribonucleolytic activity, several artifacts can lead to cell growth. False positives can be caused by random mutations that occur in the angiogenin cDNA (including indels, stop codons, and substitution of essential residues), recombination of plasmid DNA to excise part or whole of the angiogenin gene, and star activity by restriction enzymes during preparation of the library. Originally, the restriction enzyme *Eag*I was used to prepare plasmid DNA for ligation. However, its rate of star activity led to many false positives (*i.e. Eag*I can cut at a site different than its consensus sequence in the plasmid causing a truncation or complete removal of the angiogenin gene in a portion of the library). Thus, the enzyme *Not*I was used, which yields few false positives via star activity in this selection system (data not shown).

Several hundred clones were sequenced that contained the intact angiogenin/peptide fusion. These potential positives were sorted into three classes (Table 5.3). First, the largest class of peptide sequences contained long stretches of hydrophobic amino acid residues. These peptides could prevent folding or cause aggregation of angiogenin in Origami™ cells. Alternatively, hydrophobic sequences at the C-terminus of proteins in *E. coli* are known to act as degradation signals (Parsell *et al.*, 1990). Perhaps cells could avoid angiogenin-induced death by degrading the protein prior to its attack on cellular RNA. A final possibility may be that some of these hydrophobic sequences are angiogenin inhibitors. It has been shown that certain largely hydrophobic peptides bind

angiogenin with high affinity (though these peptides do not inhibit angiogenin, perhaps similar peptides could) (Gho and Chae, 1997). However, it would be difficult to resolve whether the hydrophobic peptides selected herein function as angiogenin inhibitors, not only due to the other factors listed above, but also due to the difficulty of synthesis and solubility of these peptides.

The second class of peptide sequences occurred at a rate of ~2 x 10^{-6} and was characterized by having two C-terminal alanine residues (Table 5.3). Proteins containing an Ala-Ala dipeptide at their C-terminus are degraded by cellular proteases, including ClpXP (Parsell et al., 1990; Tu et al., 1995; Flynn et al., 2003; Levchenko et al., 2005). It seems likely that cell growth in these cases is due to degradation of angiogenin. Of note, this genetic selection system could be used to identify optimal substrates for various bacterial protein degradation pathways.

The third class of peptides, occurring at a rate of ~1 x 10^{-5} was comprised of sequences that did not fit into the two classes above and, therefore, could be potential inhibitors of angiogenin (Table 5.3). Further characterization of peptides containing cysteine residues was avoided, as they might interfere with the oxidative folding of angiogenin, thereby allowing for cell growth.

Peptide Inhibitors of Angiogenin. Studies involving the ribonucleolytic activity of angiogenin require special concern. The catalytic activity of angiogenin is 10^{5}–10^{6}-fold lower than that of RNase A. Thus, trace contamination of angiogenin by the common laboratory reagent RNase A in as little as 1 part in 10^{6} would affect results (Kao et al., 2002; Leland et al., 2002). In addition, solutions can be contaminated easily by

ribonucleases that are present in abundance on human skin (Holley *et al.*, 1961). Finally, grams of various ribonucleases are produced in our laboratory. Trace amounts of these ribonucleases can be transferred from laboratory glassware and equipment. Thus, angiogenin was purified in an extremely careful manner. Purified angiogenin was confirmed to be free of contaminating ribonucleases by zymogram electrophoresis (data not shown), a technique that can detect the ribonucleolytic activity of as little as 1 pg of RNase A. In addition, the different K_i values obtained for inhibition of RNase A and angiogenin by the peptides (*vide infra*) further substantiate that angiogenin is free from contaminating RNase A.

Three peptides were tested for inhibition of angiogenin. Peptides **1**, **2**, and **3** were *acetyl*-LDDAEEWGG, *acetyl*-AEDYDYSWW, and *acetyl*-SYSALYEAG, respectively (Table 5.4). Inhibition assays were performed in 0.05 M MES-NaOH, pH 6.0, containing NaCl (0.1 M). The K_i values for peptides **1** and **2** were (641 ± 53) μM and (56.4 ± 4.1) μM, respectively (Figure 5.3; Table 5.4). Peptide **3** exhibited only slight inhibition of angiogenin at concentrations >1.2 mM (data not shown).

Selectivity of Peptide Inhibitors. Humans have at least 12 homologs of angiogenin involved in various biological functions (Cho *et al.*, 2005). Accordingly, inhibitors used to prevent angiogenesis *in vivo* should be selective for angiogenin. The selectivity of the inhibitors was tested by determining K_i values for RNase A. Peptide **1** reduced the catalytic activity of RNase A by only ~30% at a concentration of 1.2 mM. Thus, this peptide exhibits ≥2-fold selectivity for angiogenin. Peptide **2**, surprisingly, inhibited RNase A with a K_i value of (17.5 ± 1.1) μM, or 3-fold lower than that for angiogenin

(Figure 5.3; Table 5.4). Peptide 3 had no inhibitory effect against RNase A at a concentration of 1.2 mM.

It has been notoriously difficult to generate inhibitors that are specific for angiogenin over RNase A (Jenkins and Shapiro, 2003). Nucleotide-based inhibitors bind angiogenin >100-fold worse than they do RNase A (Russo *et al.*, 1996; Russo *et al.*, 2001). Even small-molecule inhibitors identified from a large library of compounds screened solely against angiogenin had 2–3-fold greater selectivity for RNase A (Kao *et al.*, 2002; Jenkins and Shapiro, 2003). Rationally designed derivatives of these small molecules, however, were found to inhibit angiogenin ~2-fold better than RNase A (Jenkins and Shapiro, 2003), making them the most selective angiogenin inhibitors identified to date. Our findings further substantiate these results. Peptide inhibitors selected to inhibit the ribonucleolytic activity of angiogenin exhibited comparable inhibition of RNase A. Peptide 1 was ~2-fold more selective for angiogenin than RNase A, but peptide 2 had a 3-fold lower K_i value for RNase A than angiogenin. Thus, these peptides rank among the most selective inhibitors of angiogenin, though selectivity could be dramatically improved through future iterations. In addition, peptide 2 ranks as among the best small-molecule inhibitors of angiogenin. Its K_i value is within 12.5-fold of the tightest–binding inhibitor of angiogenin, benzopurpurin B (Jenkins and Shapiro, 2003), under similar buffer conditions. Notably, peptide 2 exhibits a K_i value that is equal to a small-molecule inhibitor that was found to exhibit antitumoral activity against subcutaneous tumors in athymic mice (Kao *et al.*, 2002; Jenkins and Shapiro, 2003).

Previous work with peptide-based inhibitors of ribonucleases revealed that peptides corresponding to the C-terminus of these enzymes could bind and/or inhibit angiogenin (Rybak *et al.*, 1989) or RNase A (Nakano and Sugimoto, 2003). A peptide based upon the C-terminal residues of angiogenin inhibits the enzyme with $K_i = 278$ µM, though at a different pH value and lower concentrations of NaCl from the assays used herein (Rybak *et al.*, 1989). Both salt and pH have large effects on inhibition assays of ribonucleases (Russo *et al.*, 2001; Smith *et al.*, 2003), thus direct comparison with these results is difficult.

Random copolymers of tyrosine and glutamate ~30 residues in length inhibit RNase A (Sela, 1962). Intriguingly, peptide 2 contains the sequence EDYDY and potently inhibits both angiogenin and RNase A (Table 5.4). The genetic selection system described herein could be used with a constrained peptide library to isolate the most potent peptides containing combinations of these amino acid residues.

5.5 Conclusions

Angiogenin is a potent inducer of angiogenesis and a potential target for anti-cancer drugs. Our genetic selection system has yielded peptide-based inhibitors of angiogenin that could serve as leads for therapeutic agents. By tethering a nonapeptide library to the C-terminus of angiogenin, we were able to isolate peptide inhibitors that exhibit comparable selectivity to the most selective angiogenin inhibitors. In addition, one peptide is among the best inhibitors of angiogenin identified to date. Finally, our genetic

selection system could, in principle, be used to isolate inhibitors from cell-permeable small-molecule libraries or from other biologically encoded molecules.

Table 5.1	Peptide library: Analysis of XNK codons					
	X	N	K	% X	% N	% K
A	190	122	1	39.1	25.1	0.2
C	114	69	0	23.5	14.2	0.0
T	49	146	262	10.1	30.0	53.9
G	133	149	223	27.4	30.7	45.9
Sum	486	486	486	100.0	100.0	100.0

Table 5.2   Peptide library:
Analysis of amino acid
distribution

Amino Acid	Occurrences	%
A	16	3.3
C	10	2.1
D	17	3.5
E	17	3.5
F	8	1.7
G	38	7.8
H	8	1.7
I	28	5.8
K	22	4.5
L	39	8.0
M	26	5.4
N	26	5.4
P	22	4.5
Q	17	3.5
R	63	13.0
S	40	8.2
T	25	5.1
V	45	9.3
W	4	0.8
Y	10	2.1
*	5	1.0
SUM	486	100.0

Table 5.3	Representative peptide sequences	
Class I	Class II	Class III
AGVVIVVVS	DHGDLVPAA	VDMLLAEEM
VLEVTVVVL	VFAMDDTAA	ALAQFENMV
VTMMVYIFN	VDRRAA*	TTIVEDAAD
VVIDVSMIM	QEDMSVLAA	YHECVSYAS
TVLIIDIRI	AERVVRRAA	AVETALMEA
VIVLILIAN	EDARHPRAA	SYSALYEAG
VIIIVIIGE	IAIHHMEAA	LDDAEEWGG
LLVVIMSWG	NQVLPKRAA	AEDYDYSWW
SSVVVTMII	NDRRAMKAA	NCEAAEDEE
IIPIFIVTV	NVIMPAHAA	SEYLAGYGV

Table 5.4   Peptide inhibition of angiogenin and RNase A

#	Sequence[a]	K_i Angiogenin[b]	K_i RNase A[b]
1	LDDAEEWGG	641 ± 53 μM	> 1200 μM
2	AEDYDYSWW	56.4 ± 4.1 μM	17.5 ± 1.1 μM
3	SYSALYEAG	> 1200 μM	> 1200 μM

[a]Peptides were acetylated at their N-terminus
[b]Values of K_i were obtained in 0.05 M MES-NaOH buffer (pH 6.0), containing 0.1 M NaCl.

Figure 5.1   Genetic selection for peptide inhibitors of angiogenin. *A*, The random

nonapeptide library was prepared via gapped-duplex ligation. The

degenerate oligonucleotide was ligated in frame with the 3' end of the

angiogenin cDNA after a linker encoding $Gly_3Ser_2Gly_3$. The gap is

ultimately filled in *E. coli*. *B*, Transformation of this library into *E. coli*

DH5α allows for analysis of the peptide library. Angiogenin cannot fold

in the reducing environment of the cytosol and is not toxic to these cells.

C, Peptides (red) that do not inhibit angiogenin and prevent degradation of

cellular RNA in Origami™ cells lead to cell death. Peptides that are

capable of inhibiting angiogenin allow for cell growth.

A $\quad$ ang $\quad$ (xnk)$_9$

B $\quad$ GSH $\quad$ angiogenin aggregation $\quad$ GSH

wild-type *E. coli* $\qquad$ live cells

C $\quad$ GSSG $\quad$ RNA cleavage $\quad$ **dead cells**

Origami™ *E. coli*

GSSG $\quad$ angiogenin inhibition $\quad$ GSSG

Origami™ *E. coli* $\qquad$ Origami™ *E. coli*
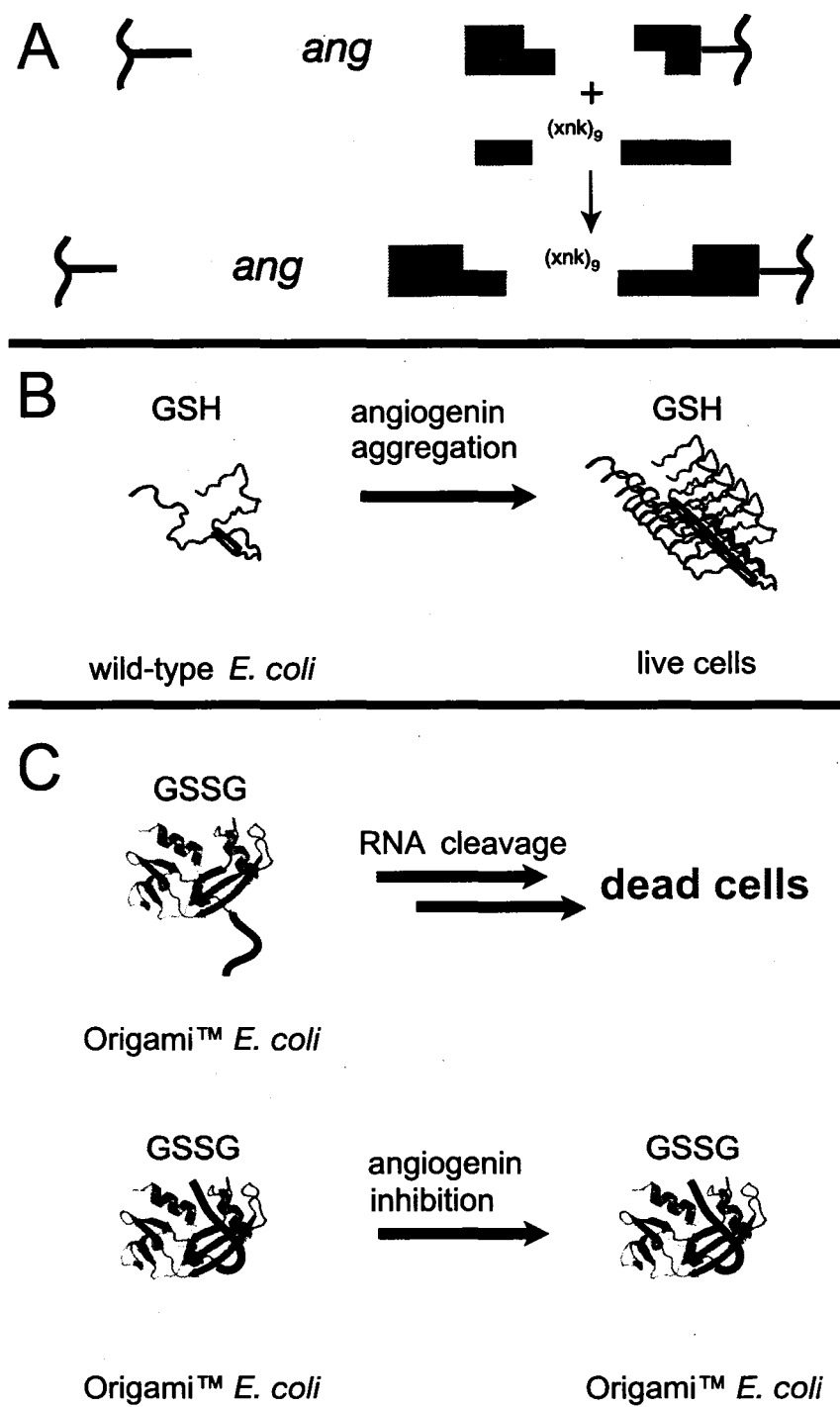
Figure 5.2   Activity threshold of genetic selection system. The activity threshold for

Origami™ cell growth was probed with active-site variants of angiogenin.

Clones were transformed into Origami™ cells and allowed to grow for 2 d

in the absence and presence of IPTG. 1) Angiogenin; 2) K40R angiogenin

(~2% of catalytic activity); 3) H13A angiogenin (~0.1% of catalytic

activity).
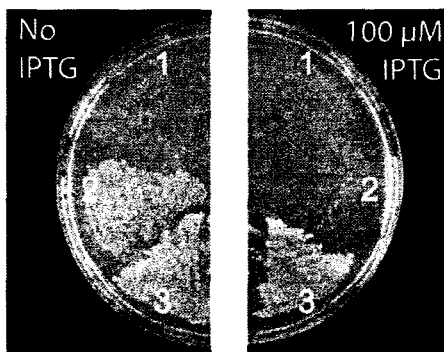
Figure 5.3   Peptide inhibition of angiogenin and RNase A. Assays were performed at

25 °C in 50 mM MES-NaOH buffer (pH 6.0) containing NaCl (0.1 M).

●, Inhibition of angiogenin by peptide **1**. ■, Inhibition of angiogenin by

peptide **2**. □, Inhibition of RNase A by peptide **2**. Rates were fitted to

Equation 1.
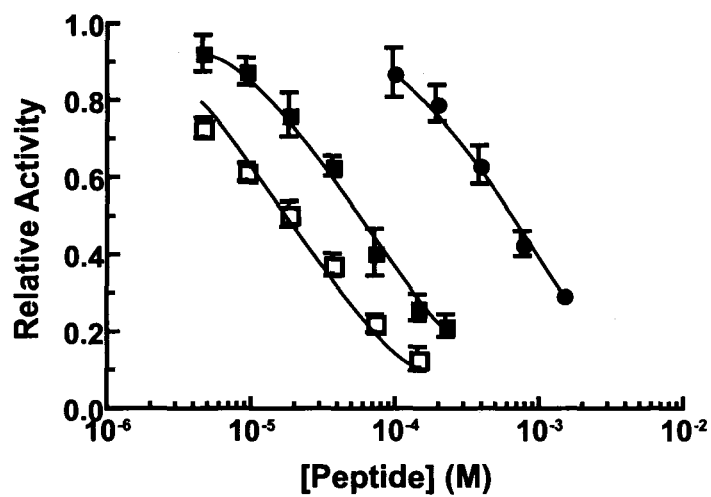
Appendix 1

Site-Specific Protein~Folate Conjugates

This unpublished work was done in collaboration with Joshua J. Higgin and Luke D. Lavis in the laboratory of Ronald T. Raines.

A1.1 Abstract

Certain cancer cells over-produce the folate receptor on their surface. Folate can be conjugated to small molecules, liposomes, and proteins to facilitate their entry into these cancer cells via folate receptor-mediated endocytosis. Thus, folate has emerged as an important drug-targeting agent. Current protein~folate coupling methods are nonspecific, producing heterogeneous products with compromised activity. We have synthesized a folate analog that can be attached to a cysteine residue installed in a protein sequence. In this folate analog, "bamfolate," an electrophilic bromoacetamido group replaces the nonessential γ-carboxyl group of folic acid. Bamfolate was coupled specifically to RNase A variants with free cysteine residues installed at appropriate positions. Whereas random folate conjugation to RNase A substantially decreased its catalytic activity, site-specific RNase~folate conjugates retained high catalytic activity. For further comparisons, random RNase~folate conjugates were also prepared by "protecting" the catalytically important residue Lys-41 by substituting the residue with arginine, thereby preventing folate conjugation at that position. These random RNase~folate conjugates retained the same catalytic activity as the unmodified enzyme. Yet, RNase~folate conjugates do not exhibit increased cytotoxic activity towards cell lines that over-produce the folate receptor, perhaps indicating that the normal ribonuclease internalization route remains the dominant pathway for cellular entry.

A1.2 Introduction

Ribonucleases are among the most toxic enzymes. Cells secrete ribonucleases into the

extracellular medium, yet contain an extremely high-affinity proteinaceous inhibitor

($K_d \sim 10^{-15}$ M) to prevent RNA degradation by secretory ribonucleases that inadvertently

enter the cytosol (Lee et al., 1989; Haigis et al., 2003; Dickson et al., 2005). Onconase™,

a secretory ribonuclease from the Northern leopard frog, was discovered based upon its

ability to kill cancer cells in vitro (Ardelt et al., 1991). Onconase™ is not inhibited by the

endogenous human ribonuclease inhibitor protein (RI) and can induce apoptosis by

digesting cellular RNA (Wu et al., 1993). Other homologs of Onconase™, including

bovine pancreatic ribonuclease (RNase A; EC 3.1.27.5), have an intrinsic ability to cross

cell membranes and kill cancer cells, as long as they are able to evade RI (Leland et al.,

1998). A single amino-acid substitution in RNase A is sufficient to weaken RI affinity

and to render it toxic to cancer cells (Leland et al., 1998).

The toxicity of ribonucleases is limited by the amount of enzyme that can cross the

cell membrane and reach the cytosol. Microinjection experiments show that RNase A is

$\sim 10^6$-fold more toxic when injected than when added to the extracellular medium (Saxena

et al., 1991). This intrinsic limitation could be overcome with strategies that enhance

binding and uptake of ribonucleases by cells.

Receptors for the B-vitamin folic acid are over-produced on the surface of some

cancer cells, such as those derived from ovarian, endometrial, and brain carcinomas

(Garin-Chesa et al., 1993; Ross et al., 1994). These receptors can be targeted with protein

toxins conjugated to folate (Leamon and Low, 1991; Leamon et al., 1993). Protein~folate

conjugates enter cells via folate receptor-mediated endocytosis (Figure A1.1), and exhibit both increased toxicity and specificity compared to corresponding non-targeted toxin (Leamon and Low, 1992; Leamon *et al.*, 1993). Conjugation of folate to toxic ribonucleases could enable more protein to enter the cytosol of cancer cells that over-produce the folate receptor, resulting in increased toxicity and specificity to these cells.

Methods for coupling folate to proteins have relied on nonspecific reactions that lead to a heterogeneous mixture of conjugates (Leamon and Low, 1992; Leamon *et al.*, 1993; Kranz *et al.*, 1995). Furthermore, random folate conjugation can affect adversely the structure or activity of a protein toxin (Atkinson *et al.*, 2001). The ability to couple folate to a specific position in a protein could alleviate these problems. Herein, we describe the chemical synthesis of a new folate analog that allows for the attachment of folate at a designated position in a protein of interest. We have attached this folate analog to cytotoxic variants of RNase A. These site-specific folate conjugates retain high enzymatic activity, but do not exhibit increased cytotoxicity. RNase A and its variants can already enter cells via endocytosis, thus the lack of enhanced cytotoxicity may indicate that the ribonuclease internalization pathway remains the main route of entry into cells. Nevertheless, the site-specific folate conjugation methodology developed herein may aid in the preparation of other homogenous protein~folate conjugates for drug delivery research.

A1.3 Experimental Procedures

Materials. K-562 cells, derived from a human chronic myelogenous leukemia line, and JAR cells, derived from a human choriocarcinoma line, were from the American Type Culture Collection (Manassas, VA). [*methyl*-^{3}H]Thymidine was from Perkin-Elmer Life Sciences (Boston, MA). The fluorogenic ribonuclease substrate, 6-FAM~dArUdAdA~6-TAMRA (where 6-FAM is a 5' 6-carboxyfluorescein group and 6-TAMRA is a 3' 6-carboxytetramethylrhodamine group), was from Integrated DNA Technologies (Coralville, IA). Folate-free RPMI (FFRPMI) medium and fetal bovine serum (FBS) were from Life Technologies (Carlsbad, CA). To remove inhibitory contaminants, MES buffer was purified by anion-exchange chromatography prior to use (Smith *et al.*, 2003). All other chemicals and reagents were of commercial grade or better, and were used without further purification.

Synthesis of Pteroic Azide. Pteroic Azide was synthesized as described previously (Luo *et al.*, 1997). Folic acid dihydrate (10.0 g, 20.9 mmol) was dissolved in THF (100 mL), and the resulting solution was stirred for 10 min and then cooled to 0 °C. Trifloroaceticanhydride (16 mL, 113 mmol) was added over 30 min. The reaction mixture was allowed to warm to 25 °C, and stirred overnight. The reaction mixture was concentrated by rotary evaporation to a thick dark viscous liquid, which was added dropwise into benzene (150 mL) to precipitate. The solid was removed by filtration, washed with ether, and allowed to dry under vacuum. THF (32 mL) was added to the solid along with ice (6.4 g), and the resulting slurry was stirred for 4 h. The mixture was then poured into ether to precipitate. The precipitate was removed by filtration, washed

with ether, and dried under vacuum. The dried solid was then dissolved in DMSO (165 mL) and the resulting solution was stirred at 25 °C in a water bath. Hydrazine (4.9 mL, 156 mmol) was added slowly, and the reaction was stirred for 8 h. MeOH (300 mL) was added to precipitate the hydrazide, which was filtered and washed with MeOH (3 x 50 mL), washed with ether (3 x 50 mL), and dried under vacuum. The hydrazide was dissolved in ice cold TFA at –10 °C with KSCN (63 mg, 0.648 mmol). tBuONO (1.72 mL, 14.8 mmol) was added slowly, and the reaction stirred for 4 h at –10 °C. The reaction mixture was then allowed to warm to 25 °C and NaN_3 (432 mg, 6.6 mmol) was added and the reaction was stirred for 10 min before isopropanol (150 mL) was slowly added to precipitate the product. The precipitate was collected by centrifugation. The product was washed in a similar manner with H_2O (3 x 50 mL), acetonitrile (3 x 50 mL), and ether (2 x 50 mL). The pteroic azide product was dried under vacuum. Yield 2.84 g; 8.4 mmol (40%).

Synthesis of N^δ-bromoacetyl-N^α-pteroyl-L-ornithine (Bamfolate). Bamfolate was synthesized on a solid support. Wang resin (600 mg, 100-200 mesh, 1.2 mmol/g) and Fmoc-ornithine-N^δ-methyltrityl (880 mg, 1.3 mmol) dissolved in DMF (10 mL) were added to a 25-mL solid-phase synthesis vessel. Pyridine (193 µL, 2.4 mmol) and 2,6-dichlorobenzoylchloride (209 µL, 1.5 mmol) were added to the resin, and the reaction mixture was put on an orbital shaker overnight. The resin was washed with DMF (3 x 20 mL) and CH_2Cl_2 (3 x 20 mL) and dried under vacuum. The resin was swelled in CH_2Cl_2 (8 mL) and benzoyl chloride (290 µL, 1.8 mmol) was added along with pyridine (290 µL, 3.6 mmol) to cap the resin. The reaction mixture was allowed to shake overnight. The

Fmoc group was removed with piperdine (20% v/v) in DMF (20 mL), and the resin was washed with DMF (3 x 20 mL) followed by CH_2Cl_2 (3 x 20 mL) and dried under vacuum. The resin was swelled in 50:50 DMSO (12 mL) and DMF (12 mL). Pteroyl azide (790 mg, 2.3 mmol) and tetramethylguanidine (400 μL, 3.2 mmol) were added. The mixture was allowed to shake overnight. The resin was washed with DMSO/DMF (50:50, 20 mL), followed by CH_2Cl_2 (20 mL), and then dried under vacuum. The methyltrityl group was removed with TFA (1% v/v) in CH_2Cl_2 (40 mL) until no more yellow color was apparent. The resin was washed with CH_2Cl_2 (40 mL), and then dried under vacuum. The resin was added to CH_2Cl_2 (5 mL) containing bromoacetylbromide (200 μL) and tetramethylguanidine (200 μL), and allowed to shake overnight. The resin was washed with CH_2Cl_2 (40 mL), and then dried under vacuum. The bamfolate product was cleaved from the resin with TFA (neat, 10 mL) and dripped into ice-cold ether. The precipitate was collected by centrifugation. The product was washed with ether (3 x 30 mL). The residue was taken up in H_2O and lyophilized. The fluffy solid was purified by reverse phase HPLC (20-35% v/v acetonitrile gradient with water) on a Varian C18 column (250 mm x 21 mm), and the solvent was removed by high-vacuum rotary evaporation and lyophilization. Yield: 30 mg, 0.05 mmol (7%). ESI MS m/z (M^+) 547, 549 (characteristic Br doublet); ^{1}H NMR (TFA-d, 300 MHz) δ 9.0 (s, 1H, Ar), 8.0 (m, 2H, Ar), 7.7 (m, 2H, Ar), 6.6 (m, 2H,), 5.3 (s, 2H, NH), 5.1 (s, 1H, OH), 4.1 (m, 1H, CH), 3.8 (m, 2H, CH_2), 3.4 (m, 4H), 3.1 (m, 3H, NH_3), 2.4 (m, 1H), 2.1 (m, 4H, CH_2CH_2), 1.4 (m, 2H, CH_2).

Instruments. UV absorbance measurements were made with a Cary Model 3 spectrophotometer (Varian, Palo Alto, CA). Fluorescence measurements were made with

a QuantaMaster 1 Photon Counting Fluorometer equipped with sample stirring (Photon Technology International, South Brunswick, NJ). Mass spectrometry was performed on a Voyager MALDI-TOF mass spectrometer (Perkin-Elmer, Boston, MA).

Production of RNase A. Plasmid pBXR (delCardayré *et al.*, 1995) directs the production of RNase A in *E. coli*. RNase A was produced and purified as described previously (Kim and Raines, 1993; Smith *et al.*, 2003). To prevent oxidative byproducts, RNase A variants with free cysteine residues were produced as described previously (Abel *et al.*, 2002). After protein refolding and purification, free cysteines residues were protected with Ellman's reagent as described previously (Abel *et al.*, 2002).

Site-specific Conjugation of Bamfolate to Ribonucleases. RNase A variants with free cysteine residues were stored protected as NTB disulfides. To remove the protecting group, the protein solution was adjusted to pH 8.0 and a 3-fold molar excess of DTT was added to the protein. A yellow color was observed, indicating that deprotection had occurred. Incubation for 5 min at room temperature led to complete deprotection. The protein solution was purified by size-exclusion chromatography on a HiTrap Desalting column (5 mL; Pharmacia, Piscataway, NJ). A 4-fold molar excess of bamfolate dissolved in DMF was then added to the deprotected protein. The reaction was stirred for 2 h at room temperature. To remove uncoupled bamfolate, the protein was again purified on a HiTrap Desalting column. The RNase~folate conjugate was dialyzed against PBS (10 L) at 4°C overnight. Protein concentration was determined using a Bicinchoninic Acid Protein Assay kit (Pierce, Rockford, IL), using RNase A as a standard. From these data, it was determined that the molar absorptivity constants for RNase A and bamfolate

were additive at 280 nm, therefore RNase~folate concentration was determined by UV

spectroscopy using ε = 35,745 $M^{-1}cm^{-1}$ at 280 nm.

Random Conjugation of Folate to Ribonucleases. RNase A and its K41R and

K41R/G88R variants were randomly conjugated to folic acid as described previously

(Leamon and Low, 1991). Briefly, folic acid was reacted with a 5-fold molar excess of 1-

ethyl-3-(3-dimethylaminopropyl)carbodiimide (EDC) in DMSO. A 4–10-fold molar

excess of the EDC-modified folate was added to a solution containing ribonuclease. The

reaction was allowed to proceed for 2 h at room temperature. The random RNase~folate

conjugate was purified by size-exclusion chromatography on a Hi-Trap Desalting

column. The conjugate was then dialyzed overnight against PBS (10 L) at 4 °C to remove

any remaining free folate. Protein concentration was determined using a Bicinchoninic

Acid Protein Assay kit (Pierce, Rockford, IL), using RNase A as a standard. The average

number of folates conjugated to the ribonuclease was determined by UV spectroscopy

using ε = 6,197 $M^{-1}cm^{-1}$ at 363 nm (Leamon and Low, 1991). Mass spectrometry was

used to confirm the average number of folates attached to the enzyme.

RNase Catalytic Activity Assays. Ribonucleolytic activity was assessed at 25 °C in

2.0 mL of 50 mM MES–NaOH buffer, pH 6.0, containing NaCl (0.10 M) and the

fluorescent substrate 6-FAM~dArUdAdA~6-TAMRA (20 nM), as described previously

(Kelemen *et al.*, 1999; Park *et al.*, 2001).

Ribonuclease Inhibitor Evasion Assays. An agarose gel-based assay was used to

obtain a qualitative measurement of RI affinity for RNase~folate conjugates as described

previously (Leland et al. 1998).

Cytotoxicity Assays. Cytotoxicity assays were performed as described previously (Leland *et al.*, 1998; Rutkoski *et al.*, 2005), with the following modifications. Folate-depleted JAR (FDJAR) cells were grown in FFRPMI medium supplemented with 10% FBS. Prior to experiments, cells were washed with FFRPMI and then resuspended in FFRPMI or FFRPMI supplemented with either 10% FBS or 10% dialyzed FBS.

A1.4 Results

Synthesis of an Electrophilic Folate Analog (Bamfolate). We have prepared a folate analog for site-specific conjugation to a free cysteine residue anywhere in a protein sequence. Synthesis of bamfolate uses solid-phase chemistry for facile purification (Figure A1.2). We first prepared pteroic azide in 40% yield, as described previously (Luo *et al.*, 1997). Pteroic azide was then coupled to ornithine on resin. The resulting resin-bound folate was reacted with bromoacetylbromide and then cleaved from the resin, releasing bamfolate. Finally, bamfolate was purified by HPLC. NMR spectroscopy and mass spectrometry were used to confirm the purity of bamfolate (data not shown).

Synthesis of RNase~folate Conjugates. RNase A~folate conjugates were prepared in two separate ways. First, for random folate conjugation (Leamon and Low, 1991), folate was activated with a 5-fold excess of EDC. A 4–10-fold excess of the activated folate was then added to RNase A variants to generate the random RNase A~folate conjugates. This method randomly attaches folate to primary amines in a protein. In addition, conjugates produced by this method are heterogeneous in the number of folates conjugated per protein. RNase A has many catalytically important lysine residues, most

notably Lys-41 (Messmore *et al.*, 1995). Random folate conjugation to RNase A

decreases its catalytic activity by greater than 99.5% (Table A1.1), presumably because

the most nucleophilic lysine residue (Lys-41) is modified (Cotham *et al.*, 2003).

Therefore, we attached folate to K41R/G88R RNase A. The K41R/G88R RNase variant

has 80-fold lower ribonucleolytic activity than wild-type RNase A, but is a potent

cytotoxin (Bretscher *et al.*, 2000). The arginine residue at position 41 acts essentially as a

protecting group to prevent folate from conjugating to that position. Mass spectrometry

of RNase~folate conjugates revealed that between zero and five folates were attached per

enzyme (Figure A1.4), though the average number of folates for each different

preparation of protein varied (data not shown). We randomly attached folate to the non-

cytotoxic K41R RNase A variant as a control.

Incorporating a free cysteine residue at any position in a protein by mutagenesis

allows for specific attachment of bamfolate to a protein in a 1:1 ratio. We have attached

folate specifically to the G88C RNase A variant, allowing this folate conjugate to evade

RI (Figures A1.3 and A1.5). Folate was attached to the A19C RNase A variant as a

control. Residue 19 of RNase A does not interact with RI, and modifications at position

do not affect RI binding (Figures A1.3 and A1.5). We used UV-visible

spectrophotometry and MALDI mass spectrometry to confirm that an RNase A variant

and bamfolate coupled in a 1:1 ratio (Figure A1.4).

Catalytic Activity of RNase A~folate Conjugates. Whereas random folate conjugation

to RNase A decreases its activity by more than 99.5%, random folate conjugation to a

K41R/G88R variant of RNase A allows the enzyme to retain similar catalytic activity to

the unmodified control (Table A1.1). The catalytic activity of the K41R RNase A~folate conjugate is similarly unaltered. Site-specific bamfolate conjugation to RNase A variants with free cysteine residues allows for the retention of high enzymatic activity (Table A1.1).

Evasion of Ribonuclease Inhibitor. An agarose gel based assay was used to determine whether a ribonuclease variant was able to evade RI (Leland *et al.*, 1998). The K41R/G88R~folate and G88C~bamfolate conjugates degrade rRNA in the presence of RI, showing that the inhibitor has lower affinity for these enzymes. K41R~folate and A19C~bamfolate are inhibited by RI (Figure A1.5), and can serve as controls for cytotoxicity experiments.

Cytotoxicity of RNase A~folate Conjugates. JAR cells from a placental choriocarcinoma line over-produce the folate receptor when maintained in folate-depleted media (Ross *et al.*, 1994). We tested the cytotoxicity of RNase~folate conjugates towards these cells. Surprisingly, RNase~folate conjugates exhibited lesser cytotoxicity than the corresponding unmodified enzymes (Figure A1.6). In addition, random folate conjugates were actually found to stimulate cell growth at certain protein concentrations.

We also tested the toxicity of RNase~folate conjugates towards K562 cells, a human erythroleukemia line that does not over-produce the folate receptor. RNase~folate conjugates have approximately the same cytotoxicity as the corresponding unmodified enzymes (data not shown).

A1.5 Discussion

The folate-binding protein is over-produced on a wide variety of human cancer cells (Ross *et al.*, 1994). Attachment of folate to proteins, small molecules, and liposomes has been shown previously to increase cellular internalization of that molecule (Leamon and Low, 1991; Reddy and Low, 1998). Thus, folate can be used as a drug-targeting agent to specifically target certain cancer cells with a toxin.

One inherent problem with drug-targeting moieties is that the conjugation often causes adverse effects to toxin activity or structure (Atkinson *et al.*, 2001). In the case of protein~folate conjugates, folate-coupling methodologies usually involve modifying lysine residues. These residues can be critical for toxin activity. Indeed, we found that RNase A was inactivated when reacted with folate (Table A1.1).

The folate receptor on cell surfaces has been found to bind a wide variety of folate analogs (Leamon *et al.*, 1999). Recently, a folate analog was synthesized to allow conjugation to carbohydrate residues of the glycoprotein gelonin. This allowed the protein to retain its cytotoxic activity, while allowing for increased internalization into cancer cells (Atkinson *et al.*, 2001). To allow for conjugation directly to a protein, we have created a new folate analog that can be attached specifically to any position in a protein sequence.

The folate analog, bamfolate, can be appended easily to any free cysteine residue in a protein sequence. Site-directed mutagenesis allows for the placement of a cysteine residue at any desired position in a protein. RNase~bamfolate coupling efficiencies are ~100%, as measured by HPLC (data not shown) and mass spectrometry (Figure A1.4).

Bamfolate could be attached readily to other proteins of interest. However, this modification strategy would not be useful for proteins with essential free cysteine residues. Yet, cysteine is the second least abundant amino acid residue in proteins (McCaldon and Argos, 1988). In addition, many cysteine residues form disulfide bonds, which are not susceptible to modification with this reagent. RNase A has eight cysteine residues, which form four disulfide bonds. Introduction of a ninth cysteine residue has no detectable effect on the enzyme, revealing the ease with which new cysteine residues can be introduced into proteins with disulfide bonds.

Site-specific conjugation of bamfolate to RNase A variants allows for the retention of the catalytic activity of the unmodified enzymes (Table A1.1). Ribonucleolytic activity is required for the cytotoxicity of RNase A variants (Bretscher *et al.*, 2000). Furthermore, only RNase A variants that retain activity in the presence of the endogenous ribonuclease inhibitor protein (RI) are cytotoxic (Bretscher *et al.*, 2000). Bamfolate can be attached to the G88C RNase A variant, resulting in a protein that has full enzymatic activity (Table A1.1) and lower affinity for RI (Figure A1.5).

RNase~bamfolate conjugates were less cytotoxic than the unmodified enzymes towards cancer cells that over-produce the folate receptor (Figure A1.6). These results indicate that RNase~bamfolate conjugates are not transported into the cytosol of cancer cells more efficiently than unmodified enzymes. Since RNase A and its variants can already internalize efficiently into cancer cells (Leland and Raines, 2001), the ribonuclease internalization pathway could be the dominant pathway for cellular entry. If the conjugates enter cells via ribonuclease-mediated endocytosis, then the folate moiety

would have little effect on cytotoxicity. It is possible that anionic variants of RNase A, which have impaired internalization (R. J. Johnson and R. T. Raines, unpublished results), could be used to test this hypothesis. Diverting more ribonuclease into the folate receptor-mediated endocytosis pathway may result in greater cytotoxicity. Alternatively, folate receptor-mediated endocytosis could be less efficient at delivering ribonucleases into the cytosol of cancer cells, in which case RNase A might actually be considered to be a better targeting agent.

RNase~bamfolate conjugates were tested for toxicity against the K-562 cancer cell line, which does not over-produce the folate receptor. Both the RNase~bamfolate conjugates and unmodified enzymes exhibited the same cytotoxicity (data not shown). Conjugates and unmodified enzymes that do not evade RI were not toxic to these cells.

For comparison, we prepared random RNase-folate conjugates. Randomly coupling folate to wild-type RNase A results in its inactivation (Table A1.1). Thus, we used an RNase A variant in which the essential residue Lys-41 is substituted with an arginine. This K41R RNase A variant has ~1% of the catalytic activity of wild-type RNase A (Bretscher *et al.*, 2000), but cannot be modified by folate at position 41. K41R/G88R RNase A was previously shown to be cytotoxic (Bretscher *et al.*, 2000), even though it has compromised catalytic activity. Its slightly better ability to evade RI offsets its loss in catalytic activity (Bretscher *et al.*, 2000). Both the K41R and K41R/G88R RNase~folate conjugates have similar enzymatic activities to the unmodified enzymes (Table A1.1).

K41R/G88R RNase~folate is less toxic than unmodified K41R/G88R RNase A towards cancer cells that over-produce the folate receptor. In addition, random

RNase~folate conjugates actually stimulate cell growth (Figure A1.6). It is possible that cells are able to degrade these conjugates and recycle the folate, leading to faster cell growth. When tested against cells that do not over-produce the folate receptor on their cell surface, the random folate conjugates exhibit the same toxicity as the unmodified enzymes, as expected (data not shown).

Herein, we have synthesized a new folate analog, bamfolate, which allows for site-specific attachment to any position in a protein sequence. We have shown that site-specific bamfolate conjugates are readily produced in ~100% yield. Site-specific bamfolate conjugation allows retention of full enzymatic activity, unlike random folate conjugation, which can adversely affect protein structure/function. Site-specific conjugation allows for preparation of a homogenous product, which is necessary for the optimization of the therapeutic value of a conjugate (Kochendoerfer et al., 2003). Bamfolate could be used to create site-specific conjugates of other cytotoxic proteins, or incorporated into other pharmaceutically important molecules such as liposomes, antisense oligonucleotides, and small-molecule drugs.

Table A1.1   Catalytic activity of RNase A variants and RNase~folate conjugates

Protein/Conjugate	k_{cat}/K_M (x 10^8 $M^{-1}s^{-1}$)[a]
RNase A	2.98 ± 0.23
RNase A~folate[b]	0.54 ± 0.05
RNase A~folate[c]	0.013 ± 0.006
K41R	0.054 ± 0.003
K41R~folate	0.029 ± 0.006
K41R/G88R	0.055 ± 0.003
K41R/G88R~folate	0.044 ± 0.005
G88R	1.86 ± 0.16
G88C~bamfolate	4.32 ± 0.69
A19C~bamfolate	3.90 ± 0.36

[a]Values of k_{cat}/K_m are for catalysis of 6-FAM~dArUdAdA~6-TAMRA cleavage in 0.05 M MES-NaOH buffer, pH 6.0, containing NaCl (0.1 M) at 25 °C.
[b]Average number of folate moieties per enzyme was 2.
[c]Average number of folate moieties per enzyme was 5.

Figure A1.1   Model for internalization and cytotoxicity of RNase~folate conjugates.

The conjugate binds to the folate receptor on the cell surface, then enters

the cell by folate receptor-mediated endocytosis. As the pH of the

endosome decreases, the conjugate transfers to the cytosol of the cell. If

the conjugate can evade the endogenous ribonuclease inhibitor protein,

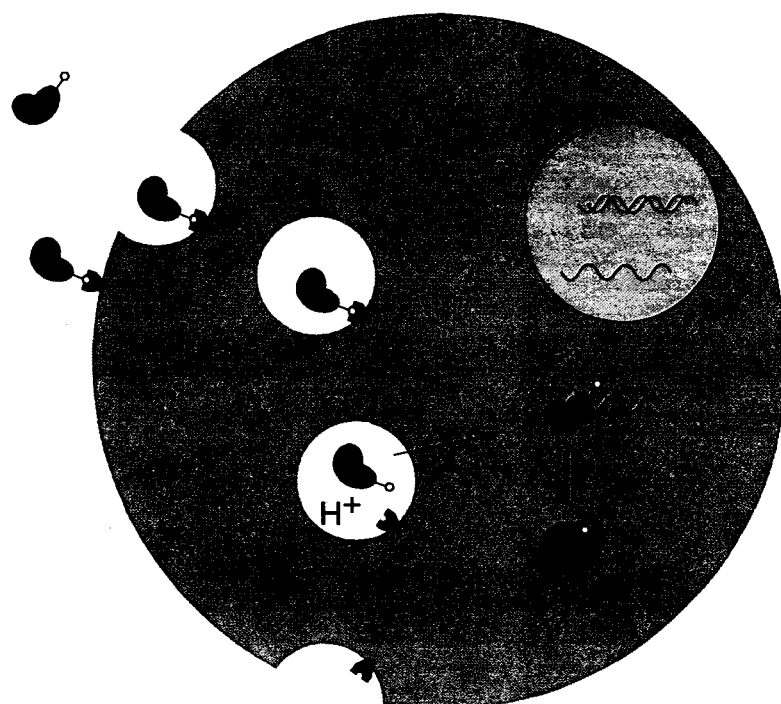then it can degrade RNA and cause cell death.
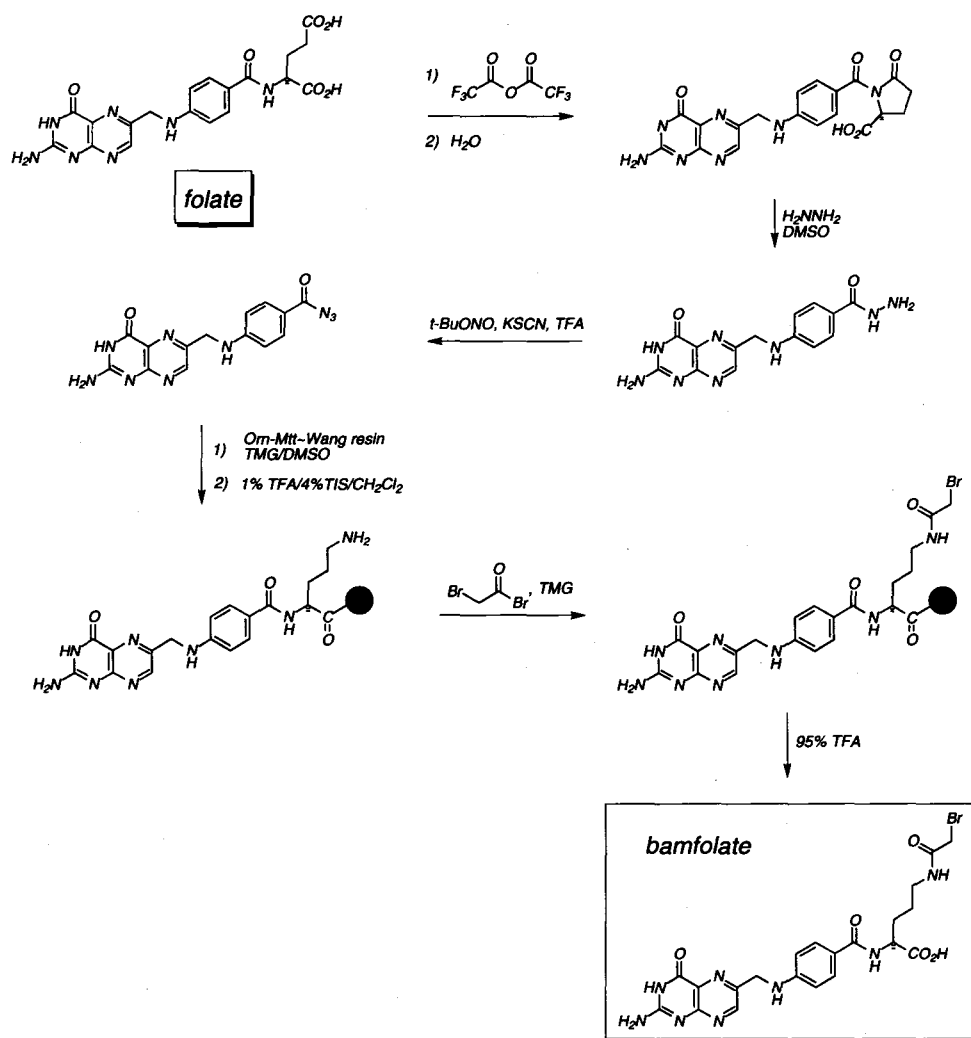
Figure A1.2 Synthesis of bamfolate.

folate

bamfolate

Figure A1.3 Structure of the crystalline ribonuclease A•ribonuclease inhibitor complex

(PDB entry 1DFJ (Kobe and Deisenhofer, 1995)). RNase A (blue) residue

Gly-88 interacts with three tryptophan residues in RI (red). Residue 88 can

be modified in order to create an RI-evasive ribonuclease. Residue 19 of

RNase A does not interact with any residues in RI. Modifications at this

position can be used for controls. The image of the structure was prepared

with Molscript (Avatar Software AB, Stockholm, Sweden).

Figure A1.4   Representative mass spectra of RNase~folate conjugates. *A*, The mass

spectrum of K41R/G88R~folate. This conjugate was prepared by random

folate conjugation. The number of folate moieties per enzyme is indicated

by n. *B*, The mass spectrum of G88C~bamfolate. This conjugate was

prepared by site-specific conjugation. The remaining small peaks on both

spectra are photochemically generated adducts of the matrix, 3,5-
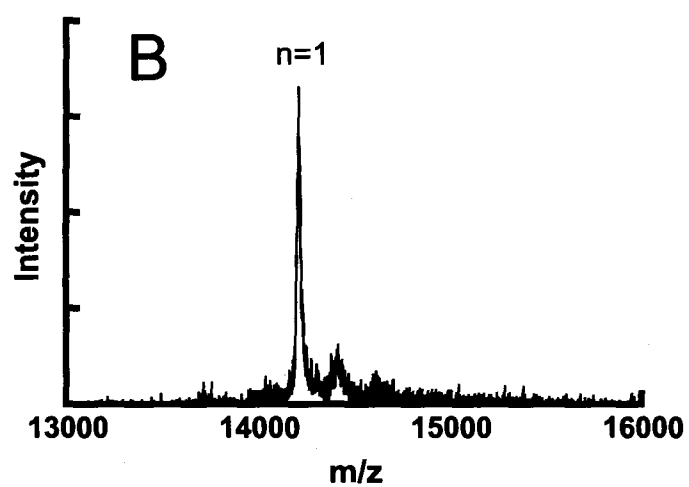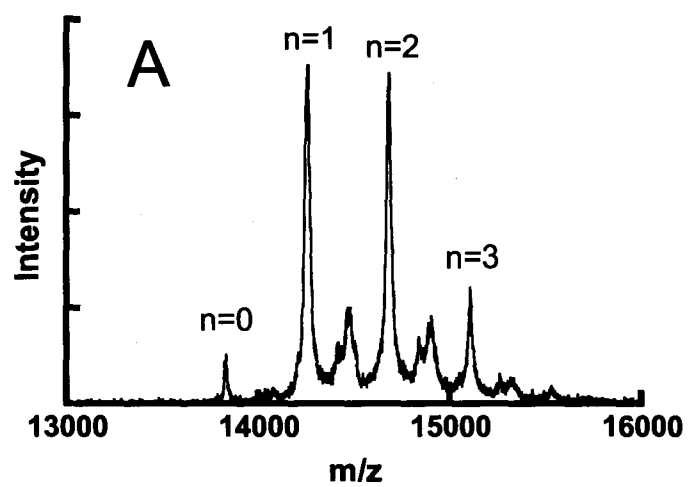
dimethoxy-4-hydroxycinnamic acid, with the proteins.

Figure A1.5 Ribonuclease inhibitor evasion assays. *A*, G88C~bamfolate degrades

rRNA in the presence of RI, similar to the G88R variant of RNase A.

A19C~bamfolate is inhibited by RI. *B*, K41R/G88R RNase~folate evades
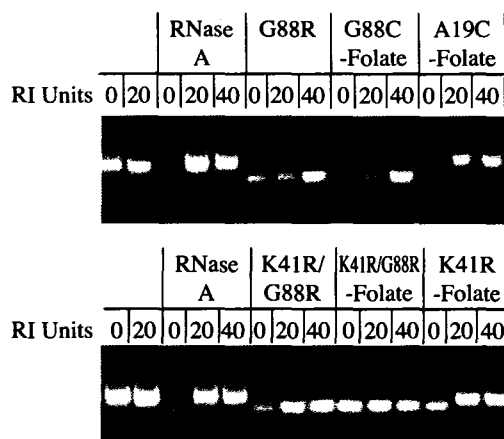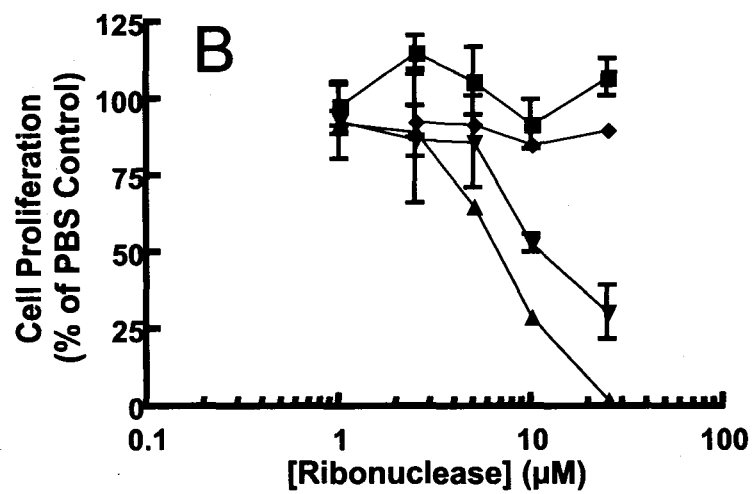
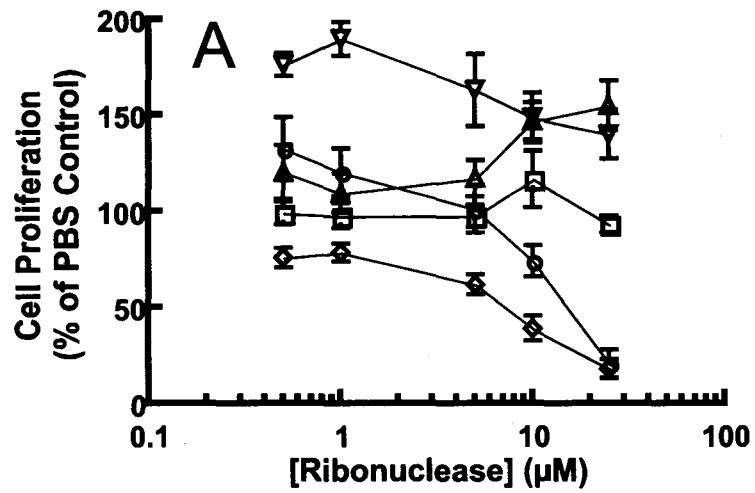RI, whereas K41R RNase~folate does not.

Figure A1.6 Cytotoxicity of RNase~folate conjugates. *A*. Cytotoxicity of random

RNase~folate conjugates. □, RNase A; △, K41R RNase A; ▽,

K41R~folate; ◇, K41R/G88R RNase A; ○, K41R/G88R~folate. *B*,

Cytotoxicity of site-specific RNase~bamfolate conjugates. ■, RNase A;

▲, G88R RNase A; ▼, G88C~bamfolate; ◆, A19C~bamfolate.

Appendix 2

Evaluating Charge–Protein Interactions

This unpublished work was done in collaboration with Burlingham, B. T., Johnson,

D. C., and Widlanski, T. S. from the Department of Chemistry at Indiana University.

Portions of this work were accepted for publication in 2004 as:

Burlingham, B. T., Smith, B. D., Raines, R. T., and Widlanski, T. S. (2006). In search of

the molecular glue: Evaluating charge–protein interactions. *J. Am. Chem. Soc.*, accepted

pending revisions.

A2.1 Abstract

Bovine pancreatic ribonuclease (RNase A) makes multiple contacts with an RNA substrate. RNase A is cationic at physiological pH (pI = 9.3) and has several positively-charged subsites that bind the sequential negatively-charged phosphoryl groups in the RNA backbone through Coulombic interactions. Many polyanions are known to inhibit catalysis by RNase A. Among the most potent inhibitors of RNase A are those that display groups with extra nonbridging oxygens as a substitute for phosphoryl groups in the RNA backbone. Such moieties can form strong hydrogen bonds in each phosphoryl-group binding subsite in RNase A. Here, we examine simple backbone mimics of RNA, and find that a backbone containing disulfonimide linkages, with their four nonbridging oxygens, are much more potent inhibitors than those containing phosphoryl groups. In addition, the incorporation of a sulfonamide group, with three nonbridging oxygens, into mono- and dinucleotide analogs allows for the creation of more effective inhibitors of RNase A. This appendix describes the inhibition of RNase A by these analogs.

A2.2 Introduction

Bovine pancreatic ribonuclease (RNase A; 3.1.27.5) is a cationic protein (pI = 9.3) under physiological conditions (Ui, 1971). Many of the excess cationic residues line the active-site cleft of the enzyme, where they can interact with the RNA phosphate backbone. Previous research has shown that single-stranded DNA forms 7 Coulombic interactions with RNase A (Record *et al.*, 1976). Unsurprisingly, many other polyanions are inhibitors of the enzyme (Richards and Wyckoff, 1971). Heparin, tyrosine–glutamate

copolymers, and various polysulfates and polyphosphates have been shown previously to inhibit catalysis by RNase A (Zöllner and Fellig, 1953; Heymann *et al.*, 1958; Sela, 1962).

The most potent small-molecule inhibitor of RNase A identified to date, oligo(vinylsulfonate) (OVS), inhibits RNase A with $K_i = 11$ pM under low-salt conditions (Smith *et al.*, 2003). One similarity of OVS and the RNA backbone is that the phosphorous atoms in a nucleic acid and alternating sulfur atoms in OVS are separated by 5 other atoms. With its 3 nonbridging oxygens per monomer unit, however, OVS provides many more opportunities to form strong hydrogen bonds than does a nucleic acid. Other potent small-molecule inhibitors of RNase A contain pyrophosphate-linkages. These moieties also display extra nonbridging oxygens, which likely enhance their affinity for RNase A (Russo and Shapiro, 1999).

To probe the contribution of nonbridging oxygens to the inhibition of RNase A, three simple backbone mimics of RNA were synthesized. Two of these mimics contained disulfonimide linkages, which have four nonbridging oxygens. These mimics were compared to an analog containing phosphoryl groups, which have only two nonbridging oxygens. The disulfonimide backbone analogs bind much more tightly to RNase A than the analog containing phosphoryl groups. In addition, when a sulfonamide group is placed in the context of mono- and dinucleotides, the resulting compounds are more effective inhibitors than those that have phosphoryl groups.

A2.3 Experimental Procedures

Materials. The fluorogenic ribonuclease substrate, 6-FAM~dArUdAdA~6-TAMRA

(where 6-FAM is a 5′ 6-carboxyfluorescein group and 6-TAMRA is a 3′ 6-

carboxytetramethylrhodamine group), was from Integrated DNA Technologies

(Coralville, IA). All other commercial chemicals and biochemicals were of reagent grade

or better, and were used without further purification.

Instruments. Fluorescence measurements were made with a QuantaMaster 1 Photon

Counting Fluorometer equipped with sample stirring (Photon Technology International,

South Brunswick, NJ).

Production of RNase A. Plasmid pBXR (delCardayré *et al.*, 1995) directs the

production of RNase A in *E. coli.* RNase A was produced and purified as described

previously (Kim and Raines, 1993; Smith *et al.*, 2003).

Inhibition of RNase A Catalysis. Inhibition of ribonucleolytic activity was assessed at

23 °C in 2.0 ml of 0.05 M Bistris-HCl buffer, pH 6.0 or 0.05 M MES-NaOH buffer, pH

6.0, containing NaCl (0.1 M), as described previously (Kelemen *et al.*, 1999; Smith *et al.*,

2003). Briefly, the buffered solutions contained 6-FAM~dArUdAdA~6-TAMRA (60

nM; Integrated DNA Technologies, Coralville, IA) and RNase A (1–5 pM). Fluorescence

(F) was measured using 493 and 515 nm as the excitation and emission wavelengths,

respectively. The value of $\Delta F/\Delta t$ was measured for 3 min after the addition of RNase A.

Next, an aliquot of inhibitor (I) dissolved in the assay buffer was added, and $\Delta F/\Delta t$ was

measured in the presence of the inhibitor for 3 min. The concentration of inhibitor in the

assay was doubled repeatedly in 3-min intervals. Excess RNase A was then added to the

mixture to ensure that less than 10% of the substrate had been cleaved prior to completion of the inhibition assay. Apparent changes in ribonucleolytic activity due to dilution were corrected by comparing values to an assay in which aliquots of buffer were added to the assay. Values of K_i were determined by non-linear least squares regression analysis of data fitted to equation 1, where $(\Delta F/\Delta t)_0$ was the activity prior to addition of inhibitor:

$$\Delta F/\Delta t = (\Delta F/\Delta t)_0(K_i/(K_i + [I])) \tag{1}$$

A2.4 Results and Discussion

Inhibition of RNase A by Backbone Analogs of RNA. The inhibition of RNase A was tested with three backbone analogs of RNA (Figure A2.1). To simplify study of the enzyme–inhibitor interaction, these analogs have only a simple polyanionic backbone with no nucleobase or ribose moieties. In the "tetraphosphate" analog, three carbons separate the phosphoryl groups, mimicking the backbone of RNA. To test the importance of nonbridging oxygens on enzyme inhibition, two "tetradisulfonimide" analogs were synthesized. The first, "tetradisulfonimide 1," has three carbons between disulfonimide linkages. The second, "tetradisulfonimide 2," has six carbons between disulfonimide moieties to aid in determining spatial effects on inhibition. Under low-salt conditions, tetradisulfonimide 1 inhibits RNase A with a K_i at least 100-fold lower that that of tetraphosphate (Table A2.1). The K_i for tetraphosphate under these conditions is >10 mM, and cannot be properly determined, as the increase in salt concentration upon

addition of millimolar amounts of the inhibitor significantly alters the low-salt conditions of the assay. Tetradisulfonimide 1 inhibits RNase A with $K_i = (109 \pm 17)$ μM (Figure A2.2). Tetradisulfonimide 2 inhibits RNase A with $K_i = (330 \pm 70)$ μM (Figure A2.2), showing that minor alterations in the structure of the backbone have little impact on the interaction with RNase A. In the presence of 0.1 M NaCl, tetradisulfonimides 1 and 2 inhibit RNase A with K_i values near 8 mM and 10 mM, respectively (data not shown). Thus, the tetradisulfonimides still bind more tightly to RNase A in the presence of 0.1 M NaCl than does tetraphosphate in the absence of added NaCl. These data indicate that the disulfonimide group, with its extra nonbridging oxygens, can be used to generate inhibitors of RNase A that are orders-of-magnitude better than those containing phosphoryl groups.

Inhibition of RNase A by Mono- and Dinucleotide Analogs. On the basis of the results above, four mono- or dinucleotide analogs were synthesized. In these analogs, a sulfonamide group, with three nonbridging oxygens, is substituted for the phosphoryl group of adenosine 5'-monophosphate (pA) and uridylyl-(3'→5')-adenosine (UpA) (Figure A2.3). The pA analogs inhibit RNase A with inhibition constants near 5 mM in the presence of 0.1 M NaCl (Table A2.2). The UpA analogs inhibit RNase A with K_i values near 400 μM in the presence of 0.1 M NaCl (Table A2.2; Figure A2.4). Replacing a ribose ring in the UpA analog with deoxyribose slightly increases the inhibition constant. Under similar conditions, thymidylyl-(3'→5')-2'-deoxyadenosine (TpdA) inhibits RNase A with $K_i = 1.2$ mM (Russo and Shapiro, 1999). Thus, the incorporation

of moieties with extra nonbridging oxygens into the backbone of RNA analogs allows for more potent inhibition of RNase A. This may represent a promising strategy for the future development of ribonuclease inhibitors.

Table A2.1   Inhibition of RNase A by RNA backbone analogs

Name	K_i at 0 M NaCl[a]	K_i at 0.1 M NaCl[b]
Tetraphosphate	> 10,000 μM	nd
Tetradisulfonimide 1	110 ± 20 μM	8.3 ± 1.7 mM
Tetradisulfonimide 2	330 ± 70 μM	~10 mM

[a]Values of K_i were obtained in 0.05 M Bistris-HCl buffer (pH 6.0).
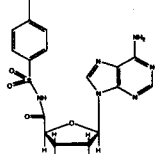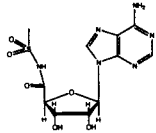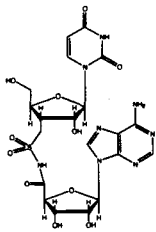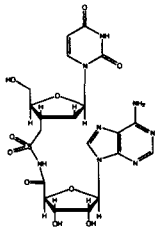[b]Values of K_i were obtained in 0.05 M MES-NaOH buffer (pH 6.0), containing 0.1 M NaCl.

Table A2.2 Inhibition of RNase A by pA and UpA analogs

Compound	Structure	K_i (M)[a]
A		$4.8 \pm 0.3 \times 10^{-3}$
B		$5.3 \pm 0.5 \times 10^{-3}$
C		$3.7 \pm 0.1 \times 10^{-4}$
D		$4.6 \pm 0.3 \times 10^{-4}$

[a]Values of K_i were obtained in 0.05 M MES-NaOH buffer (pH 6.0), containing 0.1 M NaCl.

Figure A2.1 RNA backbone analogs. These analogs have four anionic groups that can

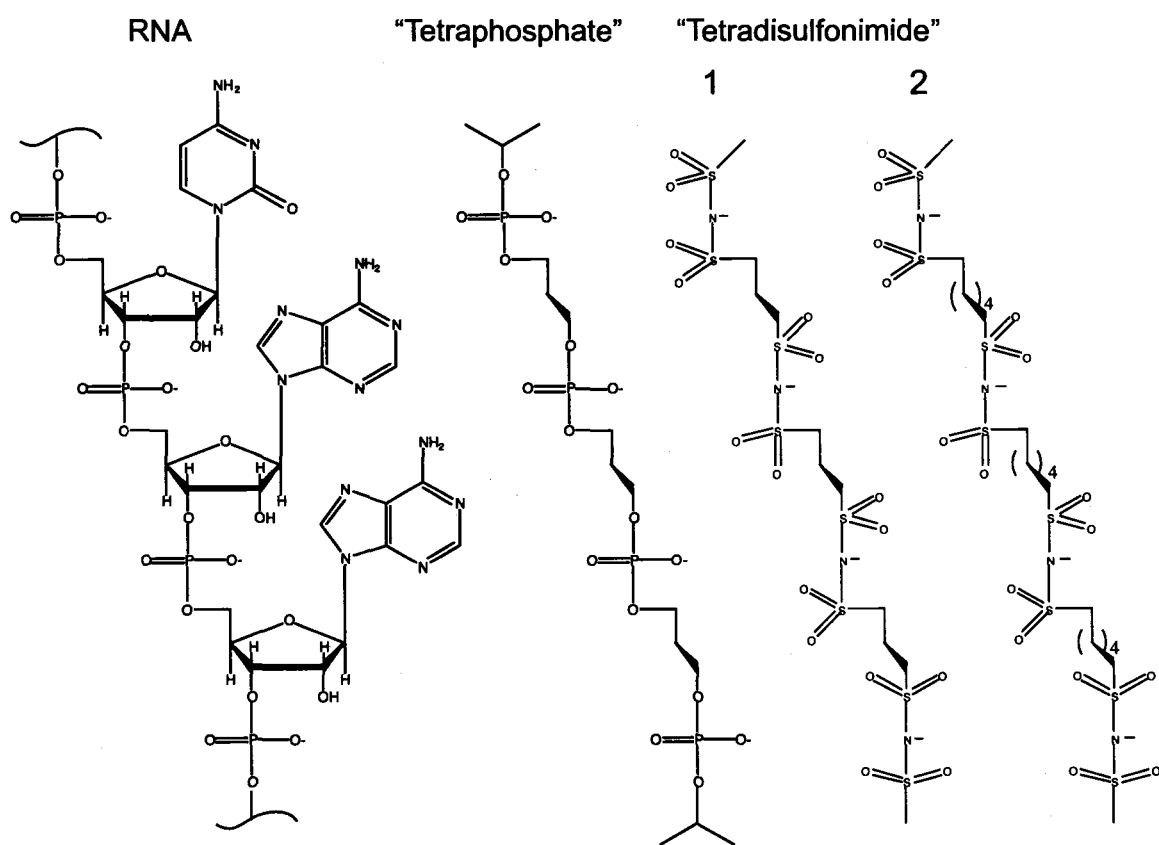interact with the sequential positively-charged phosphoryl group-binding

subsites on RNase A.

RNA   "Tetraphosphate"   "Tetradisulfonimide"

1   2

Figure A2.2   Inhibition of RNase A by tetradisulfonimides. Assays were performed in

0.05 M Bistris-HCl, pH 6.0, with no added salt. Data were fitted using

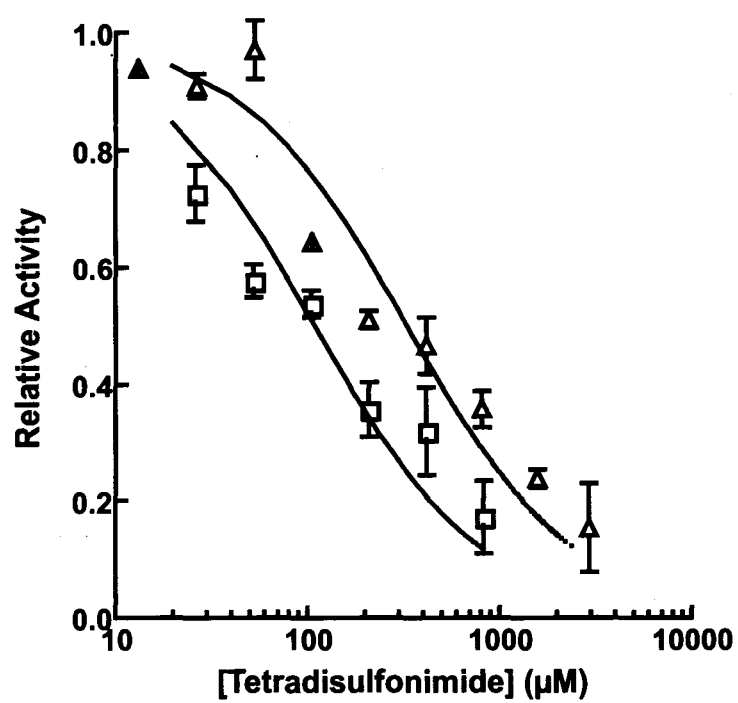equation 1. □, Tetradisulfonimide 1; △, Tetradisulfonimide 2.

Figure A2.3 pA and UpA analogs. *A*, Adenosine 5'-phosphate (pA); *B*, 5'-*N*-

acylsulfonamide pA analogs; *C*, Uridylyl-(3'→5')-adenosine (UpA); *D*,

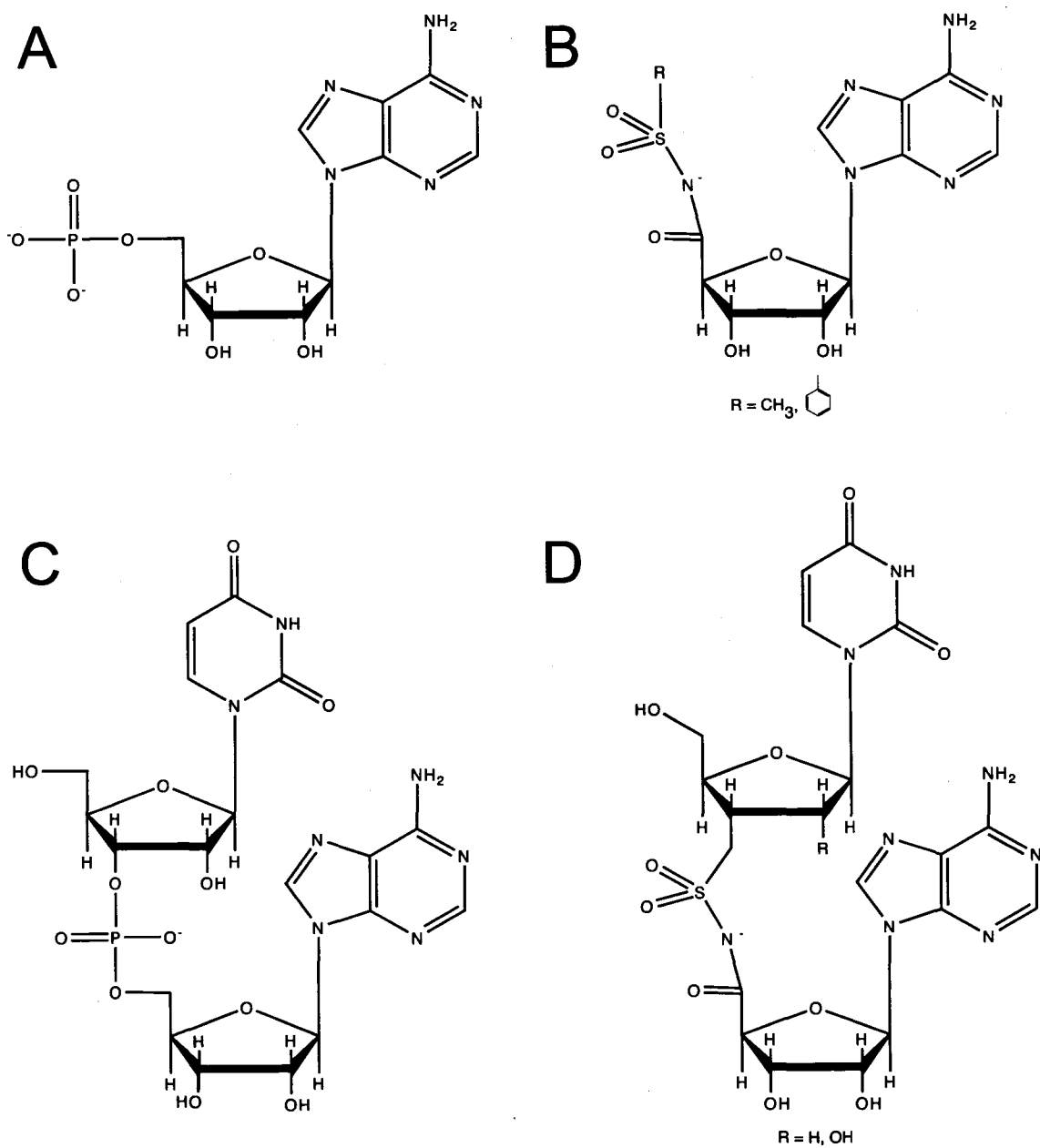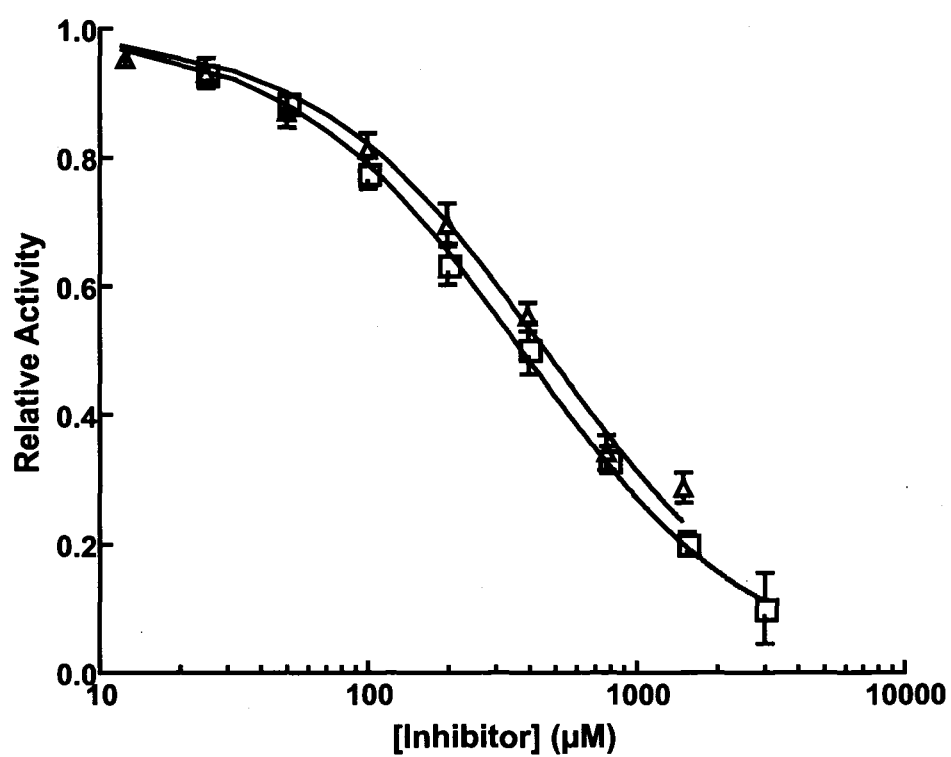Sulfonamide UpA analogs.

Figure A2.4 Inhibition of RNase A by UpA analogs. Assays were performed in 0.05 M

MES-NaOH, pH 6.0, containing NaCl (0.1 M). Data were fitted using

equation 1. □, Sulfonamide UpA analog; △, Sulfonamide deoxy-UpA

analog.

Appendix 3

Production and Purification of Human Ribonuclease Inhibitor

This work was done in collaboration with T. J. Rutkoski in the Raines laboratory.

Portions of this work were published as:

Rutkoski, T. J., Kurten, E. L., Mitchell, J. C., and Raines, R. T. (2005). Disruption of shape-complementarity markers to create cytotoxic variants of ribonuclease A. *J. Mol. Biol.* **354**, 41-54.

A3.1 Abstract

Human ribonuclease inhibitor (hRI) is a cytosolic protein that inhibits secretory pancreatic-type ribonucleases. The 50-kDa inhibitor binds tightly ($K_d \leq 10^{-12}$ M) to many divergent ribonuclease homologs. In addition, hRI moderates the cytotoxicity of antitumoral ribonucleases, and likely modulates angiogenin-induced angiogenesis. These factors make this protein–protein interaction of great interest for numerous researchers. Biochemical and biophysical studies of hRI are dependent upon the availability of large quantities of purified protein. Yet, a previous production system for hRI only yielded ~0.3 mg of purified protein per liter of culture. Here, we reexamine and optimize hRI production using the pET system in *Escherichia coli* and find that we can obtain >25 mg of purified hRI per liter of culture. This work has enabled the determination of the x-ray crystal structure of the hRI•human ribonuclease 1 complex, as well as allowed for the detailed analysis of the interaction between hRI and cytotoxic ribonuclease variants.

A3.2 Introduction

Human ribonuclease inhibitor (hRI) is emerging as an important regulator of the biological functions of a myriad of pancreatic-type ribonucleases (Dickson *et al.*, 2005). For example, hRI appears to modulate angiogenin-induced angiogenesis (Dickson, K. A. and Raines, R. T., unpublished results). hRI competitively inhibits angiogenin with $K_i \sim 10^{-16}$ M, making this interaction one of the tightest known protein–protein interactions (Lee *et al.*, 1989). In addition, hRI tightly binds and inhibits many divergent human pancreatic-type ribonucleases (Dickson *et al.*, 2005). Given its incredible affinity for

these ribonucleases, it is not surprising that the cytotoxicity of exogenously added antitumoral ribonucleases is limited by hRI in the cytosol of cancer cells (Haigis *et al.*, 2003). Indeed, disrupting the ribonuclease–hRI interaction has been of great interest for cancer research (Leland and Raines, 2001). Further basic and applied research studies using hRI depend upon obtaining the purified protein in large quantities.

A previous pET production system for hRI yielded only 0.3 mg of purified protein per liter of culture (Leland *et al.*, 1998). Slight improvements in yield were accomplished by switching to a plasmid that uses a relatively weak *trp* promoter for expression of the hRI cDNA (Klink, T. A., and Raines, R. T., unpublished results). Although purified porcine RI could be produced with this system in quantities of ~15 mg per liter of culture (Klink *et al.*, 2001), hRI was produced in quantities of <2 mg per liter of culture. In addition, this production system was undesirable for future research, since the DNA sequence for this 10-kb plasmid was only partially known. Among other concerns, the lack of sequence information hampered recombinant DNA techniques (*e.g.*, restriction enzyme digests could produce any number of DNA fragments).

Due to the availability of large quantities of porcine RI, much work on studying the interaction of pancreatic-type ribonucleases with RI was done with the porcine inhibitor (Abel *et al.*, 2002; Haigis *et al.*, 2002; Dickson *et al.*, 2003). Although porcine RI and hRI are 77% identical, studies on the effect of cytotoxic ribonucleases on human cancer cells would ideally use purified hRI for *in vitro* experiments. Indeed, porcine RI and hRI do interact differently with ribonuclease variants (Rutkoski *et al.*, 2005).

Previous results indicated that hRI was not produced in large quantities from a T7 promoter (Leland *et al.*, 1998). DNA sequencing of the previously used pET-hRI plasmid revealed that the cDNA for hRI was cloned with its poly(A) tail still attached. When expression of the hRI cDNA is induced from this plasmid, the resulting mRNA would contain a poly(A) tail on its 3' end. Polyadenylated mRNAs are degraded quickly in *E. coli* (Dreyfus and Regnier, 2002). Thus, mRNA degradation may account for the poor yield of hRI determined previously (Leland *et al.*, 1998). Here, we generate a new construct for producing hRI with the pET system. In addition, we optimize conditions for protein production and make minor modifications to previous purification protocols. We are able to produce >25 mg of purified hRI per liter of culture.

A3.3 Experimental Procedures

Materials. Plasmid pET-22b(+) was from Novagen (Madison, WI). *Escherichia coli* BL21(DE3) cells were from Novagen (Madison, WI). RNase A was coupled to a HiTrap NHS HP column (5 mL; Pharmacia, Piscataway, NJ) following the manufacturer's instructions. All other commercial chemicals and biochemicals were of reagent grade or better, and were used without further purification.

Plasmids. The hRI gene was amplified from pET-hRI-poly(A). The reverse primer for this PCR introduced a *Sal*I restriction enzyme consensus sequence directly downstream of the stop codon for hRI. This PCR fragment was double-digested with *Nde*I and *Sal*I, and the corresponding fragment was cloned into pET-22b(+) that had been digested with the same restriction enzymes. The product of this ligation was named pET-

hRI. The hRI gene is this plasmid was sequenced in both directions to ensure that the sequence was correct.

Optimization of hRI Production. Plasmid pET-hRI was transformed into *E. coli* BL21(DE3) cells. A single colony was grown overnight in LB broth (25 mL) containing ampicillin (100 μg/mL). The next day, this culture was inoculated at an $OD_{600} = 0.005$ into LB broth (200 mL) containing ampicillin (200 μg/mL), and grown at 37 °C at 250 rpm. The expression of the hRI cDNA was induced by the addition of IPTG (0.5 mM) at an $OD_{600} = 1.0$, and the culture was divided equally into four flasks that were placed at 18 °C, 25 °C, 30 °C, and 37 °C. Cultures were grown for an additional 24 h, with samples (1.5 mL) removed at the following timepoints (0 h, 1 h, 2 h, 4 h, 8 h, 16 h, and 24 h). The cells were isolated by centrifugation (6,000g for 5 min), the supernatant was aspirated, and the pellets were stored at -20 °C. For analysis by SDS-PAGE, samples were resuspended in ddH$_2$O (20 μL). Cells (2 μL) were diluted 10-fold into 20 mM Tris-HCl, pH 7.6, containing EDTA (10 mM). SDS-PAGE loading dye (20 μL) was added and the samples were boiled for 5 min. The crude lysate (5 μL) was loaded onto an SDS-PAGE gel for analysis.

Production of hRI. Two induction temperatures and times were chosen for further analysis. Cells were inoculated at an $OD_{600} = 0.005$ into TB (2 x 1 L) containing ampicillin (200 μg/mL), and grown at 37 °C at 250 rpm. The expression of the hRI cDNA was induced by the addition of IPTG (0.5 mM) at an $OD_{600} = 1.8$. One culture was induced for 8 h at 25 °C. A second culture was induced for 16 h at 18 °C. Cells were collected by centrifugation at 6,000g for 15 min. hRI contains 32 cysteine residues and is

readily inactivated by oxidation (Kim *et al.*, 1999), thus DTT was added to all buffers during purification. The pellets were resuspended in 20 mM Tris-HCl, pH 7.6, containing EDTA (10 mM), NaCl (0.1 M), DTT (10 mM), and phenylmethanesulfonyl fluoride (40 μM). Cells were passed twice through a French pressure cell (16,000 psi). Crude lysate was spun at 10,000g for 30 min. The supernatant was passed through a 0.2 μm filter and loaded onto a HiTrap~RNase A affinity column that had been equilibrated with 50 mM potassium phosphate, pH 6.4, containing EDTA (1 mM) and DTT (10 mM). The column was washed with equilibration buffer (300 mL). Next, the column was washed with equilibration buffer containing NaCl (1 M) (300 mL). hRI was eluted with 0.1 M sodium acetate, pH 5.0, containing NaCl (3 M), DTT (10 mM), and EDTA (1 mM). Fractions containing hRI were pooled and dialyzed overnight against 20 mM Tris-HCl, pH 7.5 (4 L), containing DTT (10 mM) and EDTA (1 mM). hRI was then purified over a HiTrap Q anion-exchange column, as described previously (Klink *et al.*, 2001).

A3.4 Results and Discussion

The hRI cDNA was cloned into pET-22b(+) at its *Nde*I and *Sal*I restriction enzyme sites, generating pET-hRI. Test productions of hRI were performed in *E. coli* BL21(DE3) cells. After induction, cells were grown at four temperatures for an additional 24 h. The amount of hRI produced was assessed at several time points (Figure A3.1).

Two conditions were chosen for further analysis. One liter cultures of *E. coli* harboring the pET-hRI plasmid were grown at 37 °C to an $OD_{600} = 1.8$. Expression of the hRI cDNA was induced with IPTG, and cultures were grown for an additional 8 h at

25 °C or for 16 h at 18 °C. Cells were collected by centrifugation and lysed using a

French pressure cell. hRI was purified by affinity chromatography on a HiTrap~RNase A

column and then by anion-exchange chromatography on a HiTrap Q column. Significant

amounts of hRI were found in the insoluble fraction of crude lysate from cells that had

been induced at 25 °C (Figure A3.2). Nevertheless, ~ 3 mg of purified hRI was produced

per liter of culture. The insoluble fraction of crude lysate from cells that had been induced

at 18 °C contained less hRI (data not shown), presumably because the slower production

of hRI at this temperature allowed a larger fraction of hRI to fold and remain soluble.

Several purification trials of hRI from cells induced at 18 °C revealed that 10–28 mg of

purified hRI (Figure A3.3) could be produced per liter of culture. This yield represents

nearly a 100-fold improvement over previous results (Leland *et al.*, 1998).

The ability to generate large quantities of purified hRI has already aided immensely

in studies of the interaction of hRI with ribonucleases. The x-ray crystal structure for the

hRI•human ribonuclease 1 complex (PDB entry 1Z7X) has been solved (Johnson, R. J.,

McCoy, J. G., Bingman, C. A., Phillips Jr., G. N., and Raines, R. T., unpublished results).

In addition, the interaction of cytotoxic ribonucleases with hRI has been studied in detail

(Lee and Raines, 2005; Rutkoski *et al.*, 2005). These experiments revealed that hRI binds

differently to these cytotoxic ribonucleases than does porcine RI (Rutkoski *et al.*, 2005).

Accordingly, purified hRI produced via the methods herein allows for the more accurate

determination of the important interactions of ribonucleases with RI in human cells.

Figure A3.1 Test productions of hRI in *Escherichia coli*. A culture was grown at 37 °C

to an $OD_{600} = 1.0$ and induced with IPTG. This culture was then separated

into flasks at four different temperatures, and the amount of hRI produced

at the indicated time points was determined by SDS-PAGE analysis. *A*,

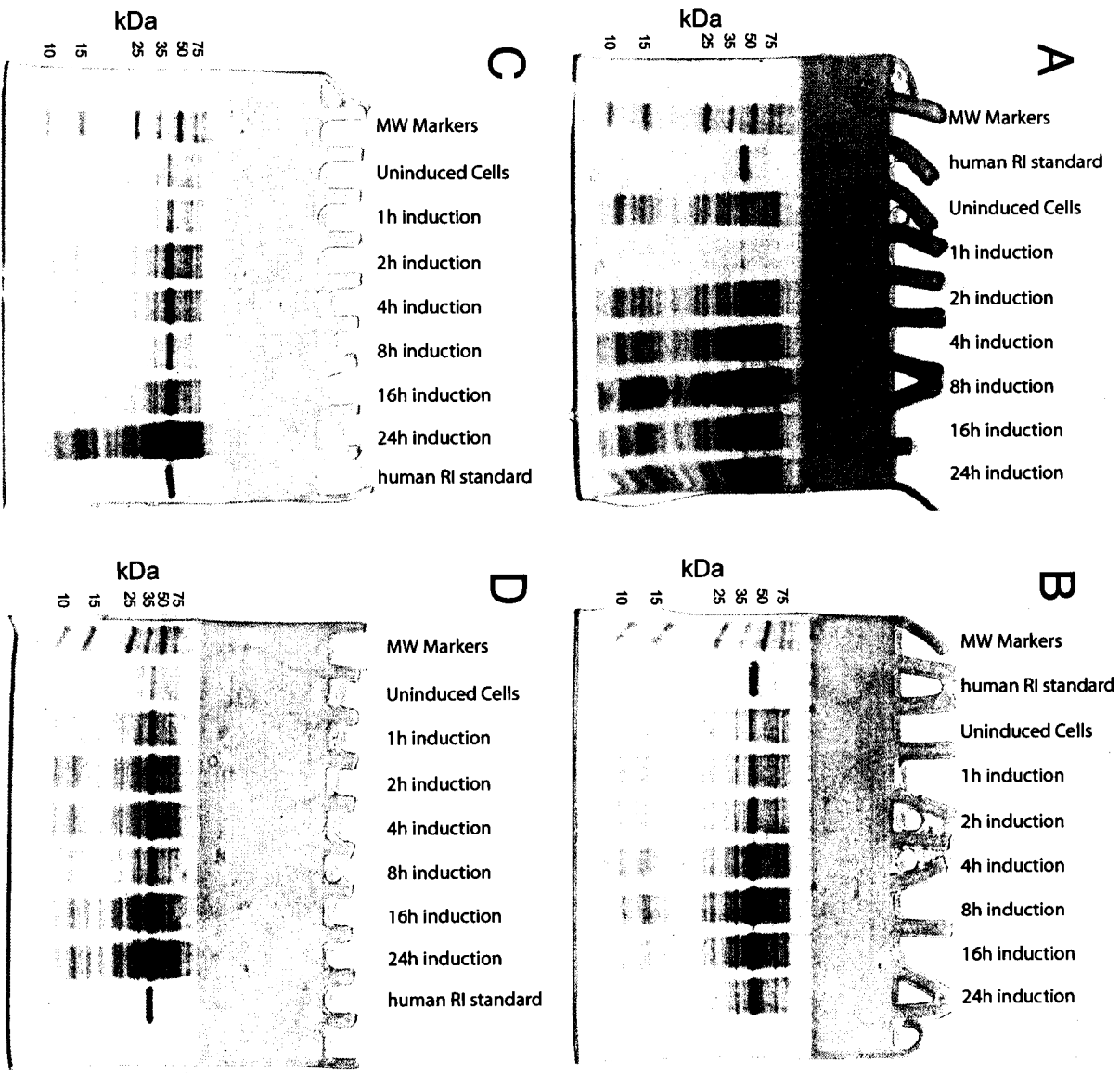18 °C; *B*, 25 °C; *C*, 30 °C; *D*, 37 °C.

Figure A3.2 Purification of hRI. A culture was grown at 37 °C to an $OD_{600} = 1.8$ and

induced with IPTG for 8 h at 25 °C. At various stages of the purification

process, samples were taken for SDS-PAGE analysis. A significant

fraction of hRI is in the insoluble fraction of the crude lysate.

kDa

75
50
35
25
15

MW Markers

human RI standard

French Press pellet

French Press supernatant

Affinity column flow-through
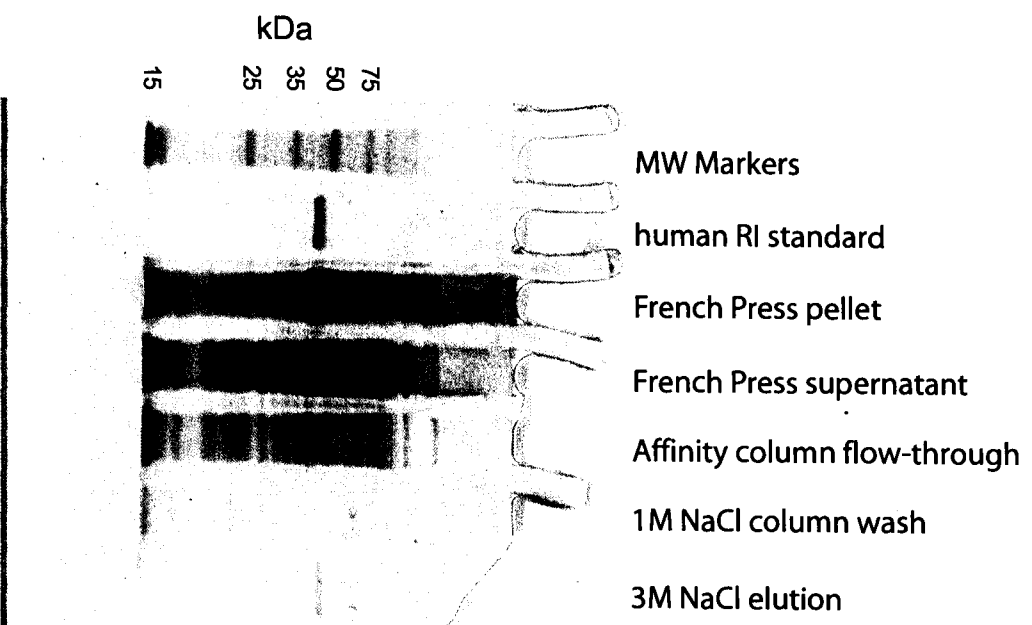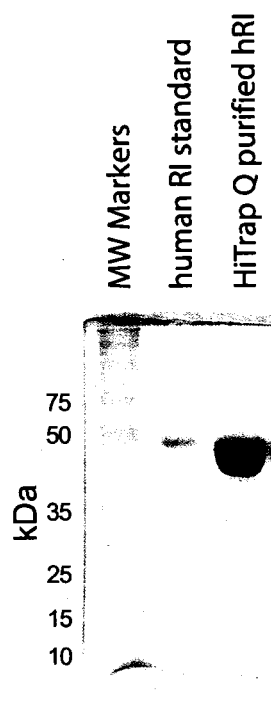
1M NaCl column wash

3M NaCl elution

Figure A3.3 Purified hRI. Affinity-purified, anion-exchange purified hRI was

intentionally over-loaded onto an SDS–PAGE gel to check for impurities.

References

Abel, R. L., Haigis, M. C., Park, C. & Raines, R. T. (2002). Fluorescence assay for the binding of ribonuclease A to the ribonuclease inhibitor protein. *Anal. Biochem.* **306**, 100-107.

Acharya, K. R., Shapiro, R., Allen, S. C., Riordan, J. F. & Vallee, B. L. (1994). Crystal structure of human angiogenin reveals the structural basis for its functional divergence from ribonuclease. *Proc. Natl. Acad. Sci. U.S.A.* **91**, 2915-2919.

Althaus, I. W., LeMay, R. J., Gonzales, A. J., Deibel, M. R., Sharma, S. K., Kezdy, F. J., Resnick, L., Busso, M. E., Aristoff, P. A. & Reusser, F. (1992). Enzymatic kinetic studies with the non-nucleoside HIV reverse transcriptase inhibitor U-9843. *Experientia* **48**, 1127-1132.

Anfinsen, C. B. (1973). Principles that govern the folding of protein chains. *Science* **181**, 223-230.

Anslyn, E. & Breslow, R. (1989). On the mechanism of catalysis by ribonuclease: Cleavage and isomerization of the dinucleotide UpU catalyzed by imidazole buffers. *J. Am. Chem. Soc.* **111**, 4473-4482.

Ardelt, W., Mikulski, S. M. & Shogen, K. (1991). Amino acid sequence of an anti-tumor protein from *Rana pipiens* oocytes and early embryos. *J. Biol. Chem.* **266**, 245-251.

Atkinson, S. F., Bettinger, T., Seymour, L. W., Behr, J. P. & Ward, C. M. (2001). Conjugation of folate via gelonin carbohydrate residues retains ribosomal-inactivating properties of the toxin and permits targeting to folate receptor positive cells. *J. Biol. Chem.* **276**, 27930-27935.

Axe, D. D., Foster, N. W. & Fersht, A. R. (1996). Active barnase variants with completely random hydrophobic cores. *Proc. Natl. Acad. Sci. U.S.A.* **93**, 5590-5594.

Axe, D. D., Foster, N. W. & Fersht, A. R. (1998). A search for single substitutions that eliminate enzymatic function in a bacterial ribonuclease. *Biochemistry* **37**, 7157-7166.

Axe, D. D., Foster, N. W. & Fersht, A. R. (1999). An irregular beta-bulge common to a group of bacterial RNases is an important determinant of stability and function in barnase. *J. Mol. Biol.* **286**, 1471-1485.

Bach, M. K. (1964). The inhibition of deoxyribonucleotidyl transferase, DNAase and RNAase by sodium poly ethylenesulfonic acid. Effect of the molecular weight of the inhibitor. *Biochim. Biophys. Acta* **91**, 619-626.

Balaji, S., Aruna, S. & Srinivasan, N. (2003). Tolerance to the substitution of buried apolar residues by charged residues in the homologous protein structures. *Proteins* **53**, 783-791.

Barnard, E. A. (1969). Biological function of pancreatic ribonuclease. *Nature* **221**, 340-344.

Beintema, J. J. (1987). Structure, properties and molecular evolution of pancreatic-type ribonucleases. *Life Chem. Rep.* **4**, 333-389.

Beintema, J. J. & Kleineidam, R. G. (1998). The ribonuclease A superfamily: General discussion. *Cell. Mol. Life Sci.* **54**, 825-832.

Beintema, J. J., Schüller, C., Irie, M. & Carsana, A. (1988). Molecular evolution of the ribonuclease superfamily. *Prog. Biophys. Molec. Biol.* **51**, 165-192.

Bessette, P. H., Aslund, F., Beckwith, J. & Georgiou, G. (1999). Efficient folding of proteins with multiple disulfide bonds in the *Escherichia coli* cytoplasm. *Proc. Natl. Acad. Sci. U.S.A.* **96**, 13703-13708.

Blackburn, P. & Moore, S. (1982). Pancreatic ribonuclease. *The Enzymes* **XV**, 317-433.

Bowie, J. U., Reidhaar-Olson, J. F., Lim, W. A. & Sauer, R. T. (1990). Deciphering the message in protein sequences: Tolerance to amino acid substitutions. *Science* **247**, 1306-1310.

Bowie, J. U. & Sauer, R. T. (1989). Identifying determinants of folding and activity for a protein of unknown structure. *Proc. Natl. Acad. Sci. U.S.A.* **86**, 2152-2156.

Breslow, D. S. & Hulse, G. E. (1954). The synthesis and polymerization of ethylenesulfonic acid. *J. Am. Chem. Soc.* **76**, 6399-6401.

Breslow, R. & Xu, R. (1993). Quantitative evidence for the mechanism of RNA cleavage by enzyme mimics. Cleavage and isomerization of UpU by morpholine buffers. *J. Am. Chem. Soc.* **115**, 10705-10713.

Bretscher, L. E., Abel, R. L. & Raines, R. T. (2000). A ribonuclease A variant with low catalytic activity but potent cytotoxicity. *J. Biol. Chem.* **275**, 9893-9896.

Cadwell, R. C. & Joyce, G. F. (1992). Randomization of genes by PCR mutagenesis. *PCR Methods Appl.* **2**, 28-33.

Campbell-Valois, F. X., Tarassov, K. & Michnick, S. W. (2005). Massive sequence perturbation of a small protein. *Proc. Natl. Acad. Sci. U.S.A.* **102**, 14988-14993.

Chambon, P., Ramuz, M., Mandel, P. & Doly, J. (1967). Inhibition of RNA polymerase by sodium polyethylene sulphonate. *Biochim. Biophys. Acta* **149**, 584-586.

Chatani, E. & Hayashi, R. (2001). Functional and structural roles of constituent amino acid residues of bovine pancreatic ribonuclease A. *J. Biosci. Bioeng.* **92**, 98-107.

Chatani, E., Nonomura, K., Hayashi, R., Balny, C. & Lange, R. (2002). Comparison of heat- and pressure-induced unfolding of ribonuclease A: The critical role of Phe46 which appears to belong to a new hydrophobic chain-folding initiation site. *Biochemistry* **41**, 4567-4574.

Cheng, T., Polmar, S. K. & Kazazian, H. H., Jr. (1974). Isolation and characterization of modified globin messenger ribonucleic acid from erythropoietic mouse spleen. *J. Biol. Chem.* **249**, 1781-1786.

Chimpanzee Sequencing and Analysis Consortium (2005). Initial sequence of the chimpanzee genome and comparison with the human genome. *Nature* **437**, 69-87.

Cho, S., Beintema, J. J. & Zhang, J. (2005). The ribonuclease A superfamily of mammals and birds: Identifying new members and tracing evolutionary histories. *Genomics* **85**, 208-220.

Cho, S. & Zhang, J. (2006). Ancient expansion of the ribonuclease A superfamily revealed by genomic analysis of placental and marsupial mammals. *Gene In Press*.

Choi, S. J., Ahn, M., Lee, J. S. & Jung, W. J. (1997). Selection of a high affinity angiogenin-binding peptide from a peptide library displayed on phage coat protein. *Mol. Cells* **7**, 575-581.

Chothia, C. & Lesk, A. M. (1986). The relation between the divergence of sequence and structure in proteins. *EMBO J.* **5**, 823-826.

Ciglic, M. I., Jackson, P. J., Raillard, S. A., Haugg, M., Jermann, T. M., Opitz, J. G., Trabesinger-Ruf, N. & Benner, S. A. (1998). Origin of dimeric structure in the ribonuclease superfamily. *Biochemistry* **37**, 4008-4022.

Cleland, W. W. (1977). Determining the chemical mechanisms of enzyme-catalyzed reactions by kinetic studies. *Adv. Enzymol. Relat. Areas Mol. Biol.* **45**, 273-387.

Cline, J. & Hogrefe, H. (2000). Randomize gene sequences with new PCR mutagenesis kit. *Strategies Newsletter* **13**, 157-162.

Coll, M. G., Protasevich, II, Torrent, J., Ribo, M., Lobachov, V. M., Makarov, A. A. & Vilanova, M. (1999). Valine 108, a chain-folding initiation site-belonging residue, crucial for the ribonuclease A stability. *Biochem. Biophys. Res. Commun.* **265**, 356-360.

Collaborative Computational Project Number 4 (1994). The CCP4 suite: Programs for protein crystallography. *Acta Crystallogr. D Biol. Crystallogr.* **50**, 760-763.

Cotham, W. E., Hinton, D. J., Metz, T. O., Brock, J. W., Thorpe, S. R., Baynes, J. W. & Ames, J. M. (2003). Mass spectrometric analysis of glucose-modified ribonuclease. *Biochem. Soc. Trans.* **31**, 1426-1427.

Crestfield, A. M., Stein, W. H. & Moore, S. (1963). Alkylation and identification of the histidine residues at the active site of ribonuclease. *J. Biol. Chem.* **238**, 2413-2419.

Cuchillo, C. M., Vilanova, M. & Nogués, M. V. (1997). Pancreatic ribonucleases. Ribonucleases: Structures and Functions. D'Alessio, G and Riordan, J F. New York, Academic Press: 271-304.

Curran, T. P., Shapiro, R. & Riordan, J. F. (1993). Alteration of the enzymatic specificity of human angiogenin by site-directed mutagenesis. *Biochemistry* **32**, 2307-2313.

Cwirla, S. E., Peters, E. A., Barrett, R. W. & Dower, W. J. (1990). Peptides on phage: A vast library of peptides for identifying ligands. *Proc. Natl. Acad. Sci. U.S.A.* **87**, 6378-6382.

Dawson, P. E., Muir, T. W., Clark-Lewis, I. & Kent, S. B. (1994). Synthesis of proteins by native chemical ligation. *Science* **4**, 776-779.

del Rosario, E. J. & Hammes, G. G. (1969). Kinetic and equilibrium studies of the ribonuclease-catalyzed hydrolysis of uridine 2',3'-cyclic phosphate. *Biochemistry* **8**, 1884-1889.

delCardayré, S. B. & Raines, R. T. (1994). Structural determinants of enzymatic processivity. *Biochemistry* **33**, 6031-6037.

delCardayré, S. B. & Raines, R. T. (1995). A residue to residue hydrogen bond mediates the nucleotide specificity of ribonuclease A. *J. Mol. Biol.* **252**, 328-336.

delCardayré, S. B., Ribó, M., Yokel, E. M., Quirk, D. J., Rutter, W. J. & Raines, R. T. (1995). Engineering ribonuclease A: Production, purification, and characterization of wild-type enzyme and mutants at Gln11. *Protein Eng.* **8**, 261-273.

Derman, A. I., Prinz, W. A., Belin, D. & Beckwith, J. (1993). Mutations that allow disulfide bond formation in the cytoplasm of *Escherichia coli*. *Science* **262**, 1744-1747.

Devlin, J. J., Panganiban, L. C. & Devlin, P. E. (1990). Random peptide libraries: A source of specific protein binding molecules. *Science* **249**, 404-406.

Dickson, K. A., Dahlberg, C. L. & Raines, R. T. (2003). Compensating effects on the cytotoxicity of ribonuclease A variants. *Arch. Biochem. Biophys.* **415**, 172-177.

Dickson, K. A., Haigis, M. C. & Raines, R. T. (2005). Ribonuclease inhibitor: Structure and function. *Prog. Nucleic Acid Res. Mol. Biol.* **80**, 349-374.

DiLella, A. G., Marvit, J., Brayton, K. & Woo, S. L. (1987). An amino-acid substitution involved in phenylketonuria is in linkage disequilibrium with DNA haplotype 2. *Nature* **327**, 333-336.

Domachowske, J. B., Dyer, K. D., Adams, A. G., Leto, T. L. & Rosenberg, H. F. (1998). Eosinophil cationic protein/RNase 3 is another RNase A-family ribonuclease with direct antiviral activity. *Nucleic Acids Res.* **26**, 3358-3363.

Dower, W. J., Miller, J. F. & Ragsdale, C. W. (1988). High efficiency transformation of *E. coli* by high voltage electroporation. *Nucleic Acids Res.* **16**, 6127-6145.

Dreyfus, M. & Regnier, P. (2002). The poly(A) tail of mRNAs: Bodyguard in eukaryotes, scavenger in bacteria. *Cell* **111**, 611-613.

Duret, L., Mouchiroud, D. & Gouy, M. (1994). HOVERGEN: A database of homologous vertebrate genes. *Nucleic Acids Res.* **22**, 2360-2365.

D'Alessio, G. & Riordan, J. F., Eds. (1997). Ribonucleases: Structures and functions. New York, Academic Press.

Eberhardt, E. S., Wittmayer, P. K., Templer, B. M. & Raines, R. T. (1996). Contribution of a tyrosine side chain to ribonuclease A catalysis and stability. *Protein Sci.* **5**, 1697-1703.

Edelhoch, H. & Coleman, J. (1956). The kinetics of the enzymatic hydrolysis of ribonucleic acid. *J. Biol. Chem.* **219**, 351-363.

Erlanson, D. A., Braisted, A. C., Raphael, D. R., Randal, M., Stroud, R. M., Gordon, E. M. & Wells, J. A. (2000). Site-directed ligand discovery. *Proc. Natl. Acad. Sci. U.S.A.* **97**, 9367-9372.

Falciani, C., Lozzi, L., Pini, A. & Bracci, L. (2005). Bioactive peptides from libraries. *Chem. Biol.* **12**, 417-426.

Fellig, J. & Wiley, C. E. (1959). The inhibition of pancreatic ribonuclease by anionic polymers. *Arch. Biochem. Biophys.* **85**, 313-316.

Ferrara, N. (2005). VEGF as a therapeutic target in cancer. *Oncology* **69**, 11-16.

Fett, J. W., Strydom, D. J., Lobb, R. R., Alderman, E. M., Bethune, J. L., Riordan, J. F. & Vallee, B. L. (1985). Isolation and characterization of angiogenin, an angiogenic protein from human carcinoma cells. *Biochemistry* **24**, 5480-5486.

Findlay, D., Herries, D. G., Mathias, A. P., Rabin, B. R. & Ross, C. A. (1961). The active site and mechanism of action of bovine pancreatic ribonuclease. *Nature* **190**, 781-784.

Findlay, D., Mathias, A. P. & Rabin, B. R. (1962). The active site and mechanism of action of bovine pancreatic ribonuclease. 7. The catalytic mechanism. *Biochem. J.* **85**, 139-144.

Fisher, B. M., Grilley, J. E. & Raines, R. T. (1998). A new remote subsite in ribonuclease A. *J. Biol. Chem.* **273**, 34134-34138.

Flynn, J. M., Neher, S. B., Kim, Y. I., Sauer, R. T. & Baker, T. A. (2003). Proteomic discovery of cellular substrates of the ClpXP protease reveals five classes of ClpX-recognition signals. *Mol. Cell* **11**, 671-683.

Folkman, J. & Shing, Y. (1992). Angiogenesis. *J. Biol. Chem.* **267**, 10931-10934.

Fontecilla-Camps, J. C., de Llorens, R., le Du, M. H. & Cuchillo, C. M. (1994). Crystal structure of ribonuclease A•d(ApTpApApG) complex. *J. Biol. Chem.* **269**, 21526-21531.

Fujii, S., Akiyama, M., Aoki, K., Sugaya, Y., Higuchi, K., Hiraoka, M., Miki, Y., Saitoh, N., Yoshiyama, K., Ihara, K., Seki, M., Ohtsubo, E. & Maki, H. (1999). DNA replication errors produced by the replicative apparatus of *Escherichia coli*. *J. Mol. Biol.* **289**, 835-850.

Furman, P. A., Fyfe, J. A., St Clair, M. H., Weinhold, K., Rideout, J. L., Freeman, G. A., Lehrman, S. N., Bolognesi, D. P., Broder, S., Mitsuya, H. & et al. (1986). Phosphorylation of 3'-azido-3'-deoxythymidine and selective interaction of the 5'-triphosphate with human immunodeficiency virus reverse transcriptase. *Proc. Natl. Acad. Sci. U.S.A.* **83**, 8333-8337.

Futami, J., Tada, H., Seno, M., Ishikami, S. & Yamada, H. (2000). Stabilization of human RNase 1 by introduction of a disulfide bond between residues 4 and 118. *J. Biochem. (Tokyo)* **128**, 245-250.

Ganguly, T., Chen, P., Teetsel, R., Zhang, L. P., Papaioannou, E. & Cianciarulo, J. (2005). High-throughput sequencing of high copy number plasmids from bacterial cultures by heat lysis. *Biotechniques* **39**, 304-308.

Garin-Chesa, P., Campbell, I., Saigo, P. E., Lewis, J. L., Jr., Old, L. J. & Rettig, W. J. (1993). Trophoblast and ovarian cancer antigen LK26. Sensitivity and specificity in immunopathology and molecular identification as a folate-binding protein. *Am. J. Pathol.* **142**, 557-567.

Gho, Y. S. & Chae, C. B. (1997). Anti-angiogenin activity of the peptides complementary to the receptor-binding site of angiogenin. *J. Biol. Chem.* **272**, 24294-24299.

Gho, Y. S., Lee, J. E., Oh, K. S., Bae, D. G. & Chae, C. B. (1997). Development of antiangiogenin peptide using a phage-displayed peptide library. *Cancer Res.* **57**, 3733-3740.

Gimbrone, M. A., Jr., Leapman, S. B., Cotran, R. S. & Folkman, J. (1972). Tumor dormancy *in vivo* by prevention of neovascularization. *J. Exp. Med.* **136**, 261-276.

Good, N. E., Winget, G. D., Winter, W., Connolly, T. N., Izawa, S. & Singh, R. M. (1966). Hydrogen ion buffers for biological research. *Biochemistry* **5**, 467-477.

Greenway, M. J., Andersen, P. M., Russ, C., Ennis, S., Cashman, S., Donaghy, C., Patterson, V., Swingler, R., Kieran, D., Prehn, J., Morrison, K. E., Green, A., Acharya, K. R., Brown, R. H. & Hardiman, O. (2006). ANG mutations segregate with familial and 'sporadic' amyotrophic lateral sclerosis. *Nature Genet.* **In Press**.

Guo, H. H., Choe, J. & Loeb, L. A. (2004). Protein tolerance to random amino acid change. *Proc. Natl. Acad. Sci. U.S.A.* **101**, 9205-9210.

Gutte, B. (1978). Synthetic 63-residue RNase A analogs. Simultaneous exchange of asparagine 44 by leucine and of threonine 45 by valine. *J. Biol. Chem.* **253**, 3837-3842.

Haigis, M. C., Kurten, E. L., Abel, R. L. & Raines, R. T. (2002). KFERQ sequence in ribonuclease A-mediated cytotoxicity. *J. Biol. Chem.* **277**, 11576-11581.

Haigis, M. C., Kurten, E. L. & Raines, R. T. (2003). Ribonuclease inhibitor as an intracellular sentry. *Nucleic Acids Res.* **31**, 1024-1032.

Hammes, G. G. (2002). Multiple conformational changes in enzyme catalysis. *Biochemistry* **41**, 8221-8228.

Harper, J. W. & Vallee, B. L. (1989). A covalent angiogenin/ribonuclease hybrid with a fourth disulfide bond generated by regional mutagenesis. *Biochemistry* **28**, 1875-1884.

Henderson, P. J. F. (1972). A linear equation that describes the steady-state kinetics of enzymes and subcellular particles interacting with tightly bound inhibitors. *Biochem. J.* **127**, 321-333.

Hengen, P. N. (1996). Is RNase-free really RNase for free? *Trends Biochem. Sci.* **21**, 112-113.

Herschlag, D. (1994). Ribonuclease revisited: Catalysis via the classical general acid – base mechanism or a triester-like mechanism. *J. Am. Chem. Soc.* **116**, 11631-11635.

Heymann, H., Gulick, Z. R., Boer, C. J. D., Stevens, G. d. & Mayer, R. L. (1958). The inhibition of ribonuclease by acidic polymers and their use as possible antiviral agents. *Arch. Biochem. Biophys.* **73**, 366-383.

Hofsteenge, J. (1997). Ribonuclease inhibitor. Ribonucleases: Structures and Functions. D'Alessio, G and Riordan, J F. New York, Academic Press: 621-658.

Holley, R. W., Apgar, J. & Merrill, S. H. (1961). Evidence for the liberation of a nuclease from human fingers. *J. Biol. Chem.* **236**, PC42-43.

Holloway, D. E., Chavali, G. B., Hares, M. C., Subramanian, V. & Acharya, K. R. (2005). Structure of murine angiogenin: Features of the substrate- and cell-binding regions and prospects for inhibitor-binding studies. *Acta Crystallogr. D Biol. Crystallogr.* **61**, 1568-1578.

Hooper, L. V., Stappenbeck, T. S., Hong, C. V. & Gordon, J. I. (2003). Angiogenins: A new class of microbicidal proteins involved in innate immunity. *Nature Immunol.* **4**, 269-273.

Hu, G. F., Riordan, J. F. & Vallee, B. L. (1997). A putative angiogenin receptor in angiogenin-responsive human endothelial cells. *Proc. Natl. Acad. Sci. U.S.A.* **94**, 2204-2209.

Hutchison, C. A., Phillips, S. A., Edgell, M. H., Gillam, S., Jahnke, P. & Smith, M. (1978). Mutagenesis at a specific position in a DNA sequence. *J. Biol. Chem.* **253**, 6551-6560.

Irie, M. (1965). Effects of salts on the reaction of bovine pancreatic ribonuclease. *J. Biochem. (Tokyo)* **57**, 355-362.

Jenkins, J. L. & Shapiro, R. (2003). Identification of small-molecule inhibitors of human angiogenin and characterization of their binding interactions guided by computational docking. *Biochemistry* **42**, 6674-6687.

Juminaga, D., Wedemeyer, W. J. & Scheraga, H. A. (1998). Proline isomerization in bovine pancreatic ribonuclease A. 1. Unfolding conditions. *Biochemistry* **37**, 11614-11620.

Kadonosono, T., Chatani, E., Hayashi, R., Moriyama, H. & Ueki, T. (2003). Minimization of cavity size ensures protein stability and folding: Structures of Phe46-replaced bovine pancreatic RNase A. *Biochemistry* **42**, 10651-10658.

Kao, R. Y., Jenkins, J. L., Olson, K. A., Key, M. E., Fett, J. W. & Shapiro, R. (2002). A small-molecule inhibitor of the ribonucleolytic activity of human angiogenin that possesses antitumor activity. *Proc. Natl. Acad. Sci. U.S.A.* **99**, 10066-10071.

Kartha, G., Bello, J. & Harker, D. (1967). Tertiary structure of ribonuclease. *Nature* **213**, 862-865.

Katona, T. M., Neubauer, B. L., Iversen, P. W., Zhang, S., Baldridge, L. A. & Cheng, L. (2005). Elevated expression of angiogenin in prostate cancer and its precursors. *Clin. Cancer. Res.* **11**, 8358-8363.

Kelemen, B. R., Klink, T. A., Behlke, M. A., Eubanks, S. R., Leland, P. A. & Raines, R. T. (1999). Hypersensitive substrate for ribonucleases. *Nucleic Acids Res.* **27**, 3696-3701.

Kelemen, B. R., Schultz, L. W., Sweeney, R. Y. & Raines, R. T. (2000). Excavating an active site: The nucleobase specificity of ribonuclease A. *Biochemistry* **39**, 14487-14494.

Kim, B.-M., Schultz, L. W. & Raines, R. T. (1999). Variants of ribonuclease inhibitor that resist oxidation. *Protein Sci.* **8**, 430-434.

Kim, J.-S. & Raines, R. T. (1993). Bovine seminal ribonuclease produced from a synthetic gene. *J. Biol. Chem.* **268**, 17392-17396.

Klink, T. A. & Raines, R. T. (2000). Conformational stability is a determinant of ribonuclease A cytotoxicity. *J. Biol. Chem.* **275**, 17463-17467.

Klink, T. A., Vicentini, A. M., Hofsteenge, J. & Raines, R. T. (2001). High-level soluble production and characterization of porcine ribonuclease inhibitor. *Protein Expr. Purif.* **22**, 174-179.

Klink, T. A., Woycechowsky, K. J., Taylor, K. M. & Raines, R. T. (2000). Contribution of disulfide bonds to the conformational stability and catalytic activity of ribonuclease A. *Eur. J. Biochem.* **267**, 566-572.

Knowles, J. R. (1987). Tinkering with enzymes: What are we learning? *Science* **236**, 1252-1258.

Kobe, B. & Deisenhofer, J. (1995). A structural basis of the interactions between leucine-rich repeats and protein ligands. *Nature* **374**, 183-186.

Kobe, B. & Deisenhofer, J. (1996). Mechanism of ribonuclease inhibition by ribonuclease inhibitor protein based on the crystal structure of its complex with ribonuclease A. *J. Mol. Biol.* **264**, 1028-1043.

Kochendoerfer, G. G., Chen, S. Y., Mao, F., Cressman, S., Traviglia, S., Shao, H., Hunter, C. L., Low, D. W., Cagle, E. N., Carnevali, M., Gueriguian, V., Keogh, P. J., Porter, H., Stratton, S. M., Wiedeke, M. C., Wilken, J., Tang, J., Levy, J. J., Miranda, L. P., Crnogorac, M. M., Kalbag, S., Botti, P., Schindler-Horvat, J., Savatski, L., Adamson, J. W., Kung, A., Kent, S. B. & Bradburne, J. A. (2003). Design and chemical synthesis of a homogeneous polymer-modified erythropoiesis protein. *Science* **299**, 884-887.

Kolbanovskaya, E. Y., Morozov, N. Y., Gavryushov, S. A., Ilin, V. A., Beintema, J. J., Wlodawer, A. & Karpeisky, M. Y. (1993). Structural-functional analysis of ribonuclease A and related proteins. *Mol. Biol.* **27**, 821-836.

Kolbanovskaya, E. Y., Sathyanarayana, B. K., Wlodawer, A. & Karpeisky, M. Y. (1992). Intramolecular interactions in pancreatic ribonucleases. *Protein Sci.* **1**, 1050-1060.

Koshland, D. (1958). Application of a theory of enzyme specificity to protein synthesis. *Proc. Natl. Acad. Sci. U.S.A.* **44**, 98-104.

Koshland, D. E., Jr., Ray, W. J., Jr. & Erwin, M. J. (1958). Protein structure and enzyme action. *Fed. Proc.* **17**, 1145-1150.

Kranz, D. M., Patrick, T. A., Brigle, K. E., Spinella, M. J. & Roy, E. J. (1995). Conjugates of folate and anti-T-cell-receptor antibodies specifically target folate-

receptor-positive tumor cells for lysis. *Proc. Natl. Acad. Sci. U.S.A.* **92**, 9057-9061.

Kunkel, T. A. (1985). Rapid and efficient site-specific mutagenesis without phenotypic selection. *Proc. Natl. Acad. Sci. U.S.A.* **82**, 488-492.

LaBean, T. H. & Kauffman, S. A. (1993). Design of synthetic gene libraries encoding random sequence proteins with desired ensemble characteristics. *Protein Sci.* **2**, 1249-1254.

Laity, J. H., Shimotakahara, S. & Scheraga, H. A. (1993). Expression of wild-type and mutant bovine pancreatic ribonuclease A in *Escherichia coli. Proc. Natl. Acad. Sci. U.S.A.* **90**, 615-619.

Landon, L. A., Zou, J. & Deutscher, S. L. (2004). Is phage display technology on target for developing peptide-based cancer drugs? *Curr. Drug. Discov. Technol.* **1**, 113-132.

Leamon, C. P., DePrince, R. B. & Hendren, R. W. (1999). Folate-mediated drug delivery: Effect of alternative conjugation chemistry. *J. Drug Target.* **7**, 157-169.

Leamon, C. P. & Low, P. S. (1991). Delivery of macromolecules into living cells: A method that exploits folate receptor endocytosis. *Proc. Natl. Acad. Sci. U.S.A.* **88**, 5572-5576.

Leamon, C. P. & Low, P. S. (1992). Cytotoxicity of momordin-folate conjugates in cultured human cells. *J. Biol. Chem.* **267**, 24966-24971.

Leamon, C. P., Pastan, I. & Low, P. S. (1993). Cytotoxicity of folate–*Pseudomonas* exotoxin conjugates toward tumor cells. Contribution of translocation domain. *J. Biol. Chem.* **268**, 24847-24854.

Lee, F. S., Shapiro, R. & Vallee, B. L. (1989). Tight-binding inhibition of angiogenin and ribonuclease A by placental ribonuclease inhibitor. *Biochemistry* **28**, 225-230.

Lee, J. E. & Raines, R. T. (2005). Cytotoxicity of bovine seminal ribonuclease: Monomer versus dimer. *Biochemistry* **44**, 15760-15767.

Leland, P. A. & Raines, R. T. (2001). Cancer chemotherapy—ribonucleases to the rescue. *Chem. Biol.* **8**, 405-425.

Leland, P. A., Schultz, L. W., Kim, B.-M. & Raines, R. T. (1998). Ribonuclease A variants with potent cytotoxic activity. *Proc. Natl. Acad. Sci. U.S.A.* **98**, 10407-10412.

Leland, P. A., Staniszewski, K. E., Kim, B. & Raines, R. T. (2000). A synapomorphic disulfide bond is critical for the conformational stability and cytotoxicity of an amphibian ribonuclease. *FEBS Lett.* **477**, 203-207.

Leland, P. A., Staniszewski, K. E., Park, C., Kelemen, B. R. & Raines, R. T. (2002). The ribonucleolytic activity of angiogenin. *Biochemistry* **41**, 1343-1350.

Lenstra, J. A., Hofsteenge, J. & Beintema, J. J. (1977). Invariant features of the structure of pancreatic ribonuclease. A test of different predictive models. *J. Mol. Biol.* **109**, 185-193.

Leonidas, D. D., Shapiro, R., Allen, S. C., Subbarao, G. V., Veluraja, K. & Acharya, K. R. (1999). Refined crystal structures of native human angiogenin and two active site variants: Implications for the unique functional properties of an enzyme involved in neovascularisation during tumour growth. *J. Mol. Biol.* **285**, 1209-1233.

Lesaicherre, M. L., Uttamchandani, M., Chen, G. Y. & Yao, S. Q. (2002). Developing site-specific immobilization strategies of peptides in a microarray. *Bioorg. Med. Chem. Lett.* **12**, 2079-2083.

Leu, Y. J., Chern, S. S., Wang, S. C., Hsiao, Y. Y., Amiraslanov, I., Liaw, Y. C. & Liao, Y. D. (2003). Residues involved in the catalysis, base specificity, and cytotoxicity of ribonuclease from *Rana catesbeiana* based upon mutagenesis and x-ray crystallography. *J. Biol. Chem.* **278**, 7300-7309.

Levchenko, I., Grant, R. A., Flynn, J. M., Sauer, R. T. & Baker, T. A. (2005). Versatile modes of peptide recognition by the AAA+ adaptor protein SspB. *Nature Struct. Mol. Biol.* **12**, 520-525.

Libonati, M. & Sorrentino, S. (1992). Revisiting the action of bovine ribonuclease A and pancreatic-type ribonucleases on double-stranded RNA. *Mol. Cell. Biochem.* **117**, 139-151.

Littauer, U. Z. & Sela, M. (1962). An ultracentrifugal study of the efficiency of some macromolecular inhibitors of ribonuclease. *Biochim. Biophys. Acta* **61**, 609-611.

Loeb, D. D., Swanstrom, R., Everitt, L., Manchester, M., Stamper, S. E. & Hutchison, C. A., 3rd (1989). Complete mutagenesis of the HIV-1 protease. *Nature* **340**, 397-400.

Luo, J., Smith, M. D., Lantrip, D. A., Wang, S. & Fuchs, P. L. (1997). Efficient syntheses of pyrofolic acid and pteroyl azide, reagents for the production of carboxyl-differentiated derivatives of folic acid. *J. Am. Chem. Soc.* **119**, 10004-10013.

Mach, B., Koblet, H. & Gros, D. (1968). Chemical identification of specific immunoglobulins as the product of a cell-free system from plasmocytoma tumors. *Proc. Natl. Acad. Sci. U.S.A.* **59**, 445-452.

Markert, Y., Köditz, J., Vriend, G., Mansfeld, J., Arnold, U. & Ulbrich-Hofmann, R. (2001). Increased proteolytic resistance of ribonuclease A by protein engineering. *Protein Eng.* **14**, 791-796.

Markiewicz, P., Kleina, L. G., Cruz, C., Ehret, S. & Miller, J. H. (1994). Genetic studies of the lac repressor. XIV. Analysis of 4000 altered *Escherichia coli* lac repressors reveals essential and non-essential residues, as well as "spacers" which do not require a specific sequence. *J. Mol. Biol.* **240**, 421-433.

Matheson, R. R. & Scheraga, H. A. (1978). Method for predicting nucleation sites for protein folding based on hydrophobic contacts. *Macromolecules* **11**, 819-829.

Matheson, R. R. & Scheraga, H. A. (1979). Steps in the pathway of the thermal unfolding of ribonuclease A. A nonspecific photo-chemical surface-labeling study. *Biochemistry* **18**, 2437-2445.

Matousek, J. & D'Alessio, G. (1991). Bull seminal ribonuclease (BS RNase), its immunosuppressive and other biological effects—a review. *Anim. Sci. Papers Rep.* **7**, 5-14.

Matsumura, I. & Ellington, A. D. (2002). Mutagenic polymerase chain reaction of protein-coding genes for *in vitro* evolution. *Methods Mol. Biol.* **182**, 259-267.

McCaldon, P. & Argos, P. (1988). Oligopeptide biases in protein sequences and their use in predicting protein coding regions in nucleotide sequences. *Proteins* **4**, 99-122.

McGhee, J. D. & von Hippel, P. H. (1974). Theoretical aspects of DNA-protein interactions: Co-operative and non-co-operative binding of large ligands to a one-dimensional homogeneous lattice. *J. Mol. Biol.* **86**, 469-489.

Messmore, J. M., Fuchs, D. N. & Raines, R. T. (1995). Ribonuclease A: Revealing structure – function relationships with semisynthesis. *J. Am. Chem. Soc.* **117**, 8057-8060.

Mikulski, S. M., Costanzi, J. J., Vogelzang, N. J., McCachren, S., Taub, R. N., Chun, H., Mittelman, A., Panella, T., Puccio, C., Fine, R. & Shogen, K. (2002). Phase II trial of a single weekly intravenous dose of ranpirnase in patients with unresectable malignant mesothelioma. *J. Clin. Oncol.* **20**, 274-281.

Miles, E. W. (1977). Modification of histidyl residues in proteins by diethylpyrocarbonate. *Methods Enzymol.* **47**, 431-442.

Miller, B. G. & Wolfenden, R. (2002). Catalytic proficiency: The unusual case of OMP decarboxylase. *Annu. Rev. Biochem.* **71**, 847-885.

Montelione, G. T. & Scheraga, H. A. (1989). Formation of local structures in protein folding. *Acc. Chem. Res.* **22**, 70-76.

Muir, T. W., Sondhi, D. & Cole, P. A. (1998). Expressed protein ligation: A general method for protein engineering. *Proc. Natl. Acad. Sci. U.S.A.* **95**, 6705-6710.

Nakano, S. & Sugimoto, N. (2003). An oligopeptide containing the C-terminal sequence of RNase A has a potent RNase A binding property. *J. Am. Chem. Soc.* **125**, 8728-8729.

Narang, U., Rahman, M. H., Wang, J. H., Prasad, P. N. & Bright, F. V. (1995). Removal of ribonucleases from solution using and inhibitor-based sol–gel-derived biogel. *Anal. Chem.* **67**, 1935-1939.

Navon, A., Ittah, V., Laity, J. H., Scheraga, H. A., Haas, E. & Gussakovsky, E. E. (2001). Local and long-range interactions in the thermal unfolding transition of bovine pancreatic ribonuclease A. *Biochemistry* **40**, 93-104.

Nelson, C. A. & Hummel, J. P. (1961). The inhibition of pancreatic ribonuclease by 2'-cytidylic acid. *J. Biol. Chem.* **236**, 3173-3176.

Neylon, C. (2004). Chemical and biochemical strategies for the randomization of protein encoding DNA sequences: Library construction methods for directed evolution. *Nucleic Acids Res.* **32**, 1448-1459.

Niehaus, W. G. & Flynn, T. (1993). A potent specific inhibitor of 6-phosphogluconate dehydrogenase of *Cryptococcus neoformans* and of certain other fungal enzymes. *Mycopathologia* **123**, 155-158.

Niehaus, W. G., White, R. H., Richardson, S. B., Bourne, A. & Ray, W. K. (1995). Polyethylene sulfonate: A tight-binding inhibitor of 6-phosphogluconate dehydrogenase of *Cryptococcus neoformans*. *Arch. Biochem. Biophys.* **324**, 325-330.

Nobile, V., Russo, N., Hu, G. & Riordan, J. F. (1998). Inhibition of human angiogenin by DNA aptamers: Nuclear colocalization of an angiogenin-inhibitor complex. *Biochemistry* **37**, 6857-6863.

Notomista, E., Catanzano, F., Graziano, G., Dal Piaz, F., Barone, G., D'Alessio, G. & Di Donato, A. (2000). Onconase: An unusually stable protein. *Biochemistry* **39**, 8711-8718.

Olson, K. A., Byers, H. R., Key, M. E. & Fett, J. W. (2001). Prevention of human prostate tumor metastasis in athymic mice by antisense targeting of human angiogenin. *Clin. Cancer. Res.* **7**, 3598-3605.

Olson, K. A., Fett, J. W., French, T. C., Key, M. E. & Vallee, B. L. (1995). Angiogenin antagonists prevent tumor growth *in vivo*. *Proc. Natl. Acad. Sci. U.S.A.* **92**, 442-446.

Park, C., Kelemen, B. R., Klink, T. A., Sweeney, R. Y., Behlke, M. A., Eubanks, S. R. & Raines, R. T. (2001). Fast, facile, hypersensitive assays for ribonucleolytic activity. *Methods Enzymol.* **341**, 81-94.

Park, C. & Raines, R. T. (2000). Origin of the 'inactivation' of ribonuclease A at low salt concentration. *FEBS Lett.* **468**, 199-202.

Park, C. & Raines, R. T. (2001). Quantitative analysis of the effect of salt concentration on enzymatic catalysis. *J. Am. Chem. Soc.* **123**, 11472-11479.

Park, C. & Raines, R. T. (2003). Catalysis by ribonuclease A is limited by the rate of substrate association. *Biochemistry* **42**, 3509-3518.

Park, C., Schultz, L. W. & Raines, R. T. (2001). Contribution of the active site histidine residues of ribonuclease A to nucleic acid binding. *Biochemistry* **40**, 4949-4956.

Park, S. H. & Raines, R. T. (2000). Genetic selection for dissociative inhibitors of designated protein-protein interactions. *Nature Biotechnol.* **18**, 847-851.

Parsell, D. A., Silber, K. R. & Sauer, R. T. (1990). Carboxy-terminal determinants of intracellular protein degradation. *Genes Dev.* **4**, 277-286.

Pasloske, B. L. (2001). Ribonuclease inhibitors. *Methods Mol. Biol.* **160**, 105-111.

Pearson, M. A., Karplus, P. A., Dodge, R. W., Laity, J. H. & Scheraga, H. A. (1998). Crystal structures of two mutants that have implications for the folding of bovine pancreatic ribonuclease A. *Protein Sci.* **7**, 1255-1258.

Peracchi, A. (2001). Enzyme catalysis: Removing chemically 'essential' residues by site-directed mutagenesis. *Trends Biochem. Sci.* **26**, 497-503.

Perutz, M. F., Kendrew, J. C. & Watson, H. C. (1965). Structure and function of haemoglobin II. Some relations between polypeptide chain configuration and amino acid sequence. *J. Mol. Biol.* **13**, 669-678.

Poteete, A. R., Rennell, D. & Bouvier, S. E. (1992). Functional significance of conserved amino acid residues. *Proteins* **13**, 38-40.

Prinz, W. A., Aslund, F., Holmgren, A. & Beckwith, J. (1997). The role of the thioredoxin and glutaredoxin pathways in reducing protein disulfide bonds in the *Escherichia coli* cytoplasm. *J. Biol. Chem.* **272**, 15661-15667.

Rahman, M. H., Kang, I., Waterbury, R. G., Narang, U., Bright, F. V. & Wang, J. H. (1996). Selective removal of ribonucleases from solution with covalently anchored macromolecular inhibitor. *Anal. Chem.* **68**, 134-138.

Raines, R. T. (1998). Ribonuclease A. *Chem. Rev.* **98**, 1045-1065.

Raines, R. T., Toscano, M. P., Nierengarten, D. M., Ha, J. H. & Auerbach, R. (1995). Replacing a surface loop endows ribonuclease A with angiogenic activity. *J. Biol. Chem.* **270**, 17180-17184.

Ratnaparkhi, G. S. & Varadarajan, R. (2000). Thermodynamic and structural studies of cavity formation in proteins suggest that loss of packing interactions rather than the hydrophobic effect dominates the observed energetics. *Biochemistry* **39**, 12365-12374.

Record, M. T., Jr., Lohman, T. M. & de Haseth, P. (1976). Ion effects on ligand – nucleic acid interactions. *J. Mol. Biol.* **107**, 145-158.

Reddy, J. A. & Low, P. S. (1998). Folate-mediated targeting of therapeutic and imaging agents to cancers. *Crit. Rev. Ther. Drug Carrier Syst.* **15**, 587-627.

Rennell, D., Bouvier, S. E., Hardy, L. W. & Poteete, A. R. (1991). Systematic mutation of bacteriophage T4 lysozyme. *J. Mol. Biol.* **222**, 67-88.

Richards, F. M. & Wyckoff, H. W. (1971). Bovine pancreatic ribonuclease. *The Enzymes* **IV**, 647-806.

Ross, J. (1996). Control of messenger RNA stability in higher eukaryotes. *Trends Genet.* **12**, 171-175.

Ross, J. F., Chaudhuri, P. K. & Ratnam, M. (1994). Differential regulation of folate receptor isoforms in normal and malignant tissues *in vivo* and in established cell lines. Physiologic and clinical implications. *Cancer* **73**, 2432-2443.

Rowe, L. A., Geddie, M. L., Alexander, O. B. & Matsumura, I. (2003). A comparison of directed evolution approaches using the beta-glucuronidase model system. *J. Mol. Biol.* **332**, 851-860.

Russo, A., Acharya, K. R. & Shapiro, R. (2001). Small molecule inhibitors of RNase A and related enzymes. *Methods Enzymol.* **341**, 629-648.

Russo, N., Acharya, K. R., Vallee, B. L. & Shapiro, R. (1996). A combined kinetic and modeling study of the catalytic center subsites of human angiogenin. *Proc. Natl. Acad. Sci. U.S.A.* **93**, 804-808.

Russo, N. & Shapiro, R. (1999). Potent inhibition of mammalian ribonucleases by 3',5'-pyrophosphate-linked nucleotides. *J. Biol. Chem.* **274**, 14902-14908.

Rutkoski, T. J., Kurten, E. L., Mitchell, J. C. & Raines, R. T. (2005). Disruption of shape-complementarity markers to create cytotoxic variants of ribonuclease A. *J. Mol. Biol.* **354**, 41-54.

Rybak, S. M., Auld, D. S., St Clair, D. K., Yao, Q. Z. & Fett, J. W. (1989). C-terminal angiogenin peptides inhibit the biological and enzymatic activities of angiogenin. *Biochem. Biophys. Res. Commun.* **162**, 535-543.

Saxena, S. K., Rybak, S. M., Winkler, G., Meade, H. M., McGray, P., Youle, R. J. & Ackerman, E. J. (1991). Comparison of RNases and toxins upon injection into *Xenopus* oocytes. *J. Biol. Chem.* **266**, 21208-21214.

Schein, C. H. (1997). From housekeeper to microsurgeon: The diagnostic and therapeutic potential of ribonucleases. *Nature Biotechnol.* **15**, 529-536.

Schultz, L. W., Quirk, D. J. & Raines, R. T. (1998). His···Asp catalytic dyad of ribonuclease A: Structure and function of the wild-type, D121N, and D121A enzymes. *Biochemistry* **37**, 8886-8898.

Scott, J. K. & Smith, G. P. (1990). Searching for peptide ligands with an epitope library. *Science* **249**, 386-390.

Sela, M. (1962). Inhibition of ribonuclease by copolymers of glutamic acid and aromatic amino acids. *J. Biol. Chem.* **237**, 418-421.

Sela, M., Anfinsen, C. B. & Harrington, W. F. (1957). The correlation of ribonuclease activity with specific aspects of tertiary structure. *Biochim. Biophys. Acta* **26**, 502-512.

Sela, M., White, F. H., Jr. & Anfinsen, C. B. (1957). Reductive cleavage of disulfide bridges in ribonuclease. *Science* **125**, 691-692.

Shapiro, R. (1998). Structural features that determine the enzymatic potency and specificity of human angiogenin: Threonine-80 and residues 58-70 and 116-123. *Biochemistry* **37**, 6847-6856.

Shapiro, R. (2001). Cytoplasmic ribonuclease inhibitor. *Methods Enzymol.* **341**, 611-628.

Shapiro, R., Fox, E. A. & Riordan, J. F. (1989). Role of lysines in human angiogenin: Chemical modification and site-directed mutagenesis. *Biochemistry* **28**, 1726-1732.

Shapiro, R., Harper, J. W., Fox, E. A., Jansen, H. W., Hein, F. & Uhlmann, E. (1988). Expression of Met-(-1) angiogenin in *Escherichia coli*: Conversion to the authentic <Glu-1 protein. *Anal. Biochem.* **175**, 450-461.

Shapiro, R., Riordan, J. F. & Vallee, B. L. (1986). Characteristic ribonucleolytic activity of human angiogenin. *Biochemistry* **25**, 3527-3532.

Shapiro, R. & Vallee, B. L. (1989). Site-directed mutagenesis of histidine-13 and histidine-114 of human angiogenin. Alanine derivatives inhibit angiogenin-induced angiogenesis. *Biochemistry* **28**, 7401-7408.

Shapiro, R. & Vallee, B. L. (1992). Identification of functional arginines in human angiogenin by site-directed mutagenesis. *Biochemistry* **31**, 12477-12485.

Shimotakahara, S., Ríos, C. B., Laity, J. H., Zimmerman, D. E., Scheraga, H. A. & Montelione, G. T. (1997). NMR structural analysis of an analog of an intermediate formed in the rate-determining step of one pathway in the oxidative folding of bovine pancreatic ribonuclease A: Automated analysis of 1H, 13C, and 15N resonance assignments for wild-type and [C65S, C72S] mutant forms. *Biochemistry* **36**, 6915-6929.

Shin, H. C., Narayan, M., Song, M. C. & Scheraga, H. A. (2003). Role of the [65-72] disulfide bond in oxidative folding of bovine pancreatic ribonuclease A. *Biochemistry* **42**, 11514-11519.

Shoemaker, K. R., Fairman, R., Schultz, D. A., Robertson, A. D., York, E. J., Stewart, J. M. & Baldwin, R. L. (1990). Side-chain interactions in the C-peptide helix: Phe 8. His 12+. *Biopolymers* **29**, 1-11.

Smith, B. D., Soellner, M. B. & Raines, R. T. (2003). Potent inhibition of ribonuclease A by oligo(vinylsulfonic acid). *J. Biol. Chem.* **278**, 20934-20938.

Smith, B. D., Soellner, M. B. & Raines, R. T. (2003). Potent inhibition of ribonuclease A by oligo(vinylsulfonic acid). *J. Biol. Chem.* **278**, 20934-20938.

Sowa, G. A., Hengge, A. C. & Cleland, W. W. (1997). ^{18}O isotope effects support a concerted mechanism for ribonuclease A. *J. Am. Chem. Soc.* **119**, 2319-2320.

Spreitzer, R. J. & Salvucci, M. E. (2002). Rubisco: Structure, regulatory interactions, and possibilities for a better enzyme. *Annu. Rev. Plant. Biol.* **53**, 449-475.

Spring, D. R. (2005). Chemical genetics to chemical genomics: Small molecules offer big insights. *Chem. Soc. Rev.* **34**, 472-482.

St Clair, D. K., Rybak, S. M., Riordan, J. F. & Vallee, B. L. (1987). Angiogenin abolishes cell-free protein synthesis by specific ribonucleolytic inactivation of ribosomes. *Proc. Natl. Acad. Sci. U.S.A.* **84**, 8330-8334.

St Clair, D. K., Rybak, S. M., Riordan, J. F. & Vallee, B. L. (1988). Angiogenin abolishes cell-free protein synthesis by specific ribonucleolytic inactivation of 40S ribosomes. *Biochemistry* **27**, 7263-7268.

Staden, R., Beal, K. F. & Bonfield, J. K. (2000). The Staden package, 1998. *Methods Mol. Biol.* **132**, 115-130.

Stemmer, W. P. (1994). Rapid evolution of a protein in vitro by DNA shuffling. *Nature* **370**, 389-391.

Stowell, J. K., Widlanski, T. S., Kutateladze, T. G. & Raines, R. T. (1995). Mechanism-based inactivation of ribonuclease A. *J. Org. Chem.* **60**, 6930-6936.

Strydom, D. J. (1998). The angiogenins. *Cell. Mol. Life Sci.* **54**, 811-824.

Strydom, D. J., Fett, J. W., Lobb, R. R., Alderman, E. M., Bethune, J. L., Riordan, J. F. & Vallee, B. L. (1985). Amino acid sequence of human tumor derived angiogenin. *Biochemistry* **24**, 5486-5494.

Studier, F. W., Rosenberg, A. H., Dunn, J. J. & Dubendorff, J. W. (1990). Use of T7 RNA polymerase to direct expression of cloned genes. *Methods Enzymol.* **185**, 60-89.

Suckow, J., Markiewicz, P., Kleina, L. G., Miller, J., Kisters-Woike, B. & Muller-Hill, B. (1996). Genetic studies of the lac repressor. XV. 4000 single amino acid substitutions and analysis of the resulting phenotypes on the basis of the protein structure. *J. Mol. Biol.* **261**, 509-523.

Sweeney, R. Y., Kelemen, B. R., Woycechowsky, K. J. & Raines, R. T. (2000). A highly active immobilized ribonuclease. *Anal. Biochem.* **286**, 312-314.

Tanimizu, N., Ueno, H. & Hayashi, R. (1998). Role of Phe120 in the activity and structure of bovine pancreatic ribonuclease A. *J. Biochem. (Tokyo)* **124**, 410-416.

Tarragona-Fiol, A., Eggelte, H. J., Harbron, S., Sanchez, E., Taylorson, C. J., Ward, J. M. & Rabin, B. R. (1993). Identification by site-directed mutagenesis of amino acids in the B2 subsite of bovine pancreatic ribonuclease A. *Protein Eng.* **6**, 901-906.

Tenson, T. & Mankin, A. (2006). Antibiotics and the ribosome. *Mol. Microbiol.* **59**, 1664-1677.

Thompson, J. E., Kutateladze, T. G., Schuster, M. C., Venegas, F. D., Messmore, J. M. & Raines, R. T. (1995). Limits to catalysis by ribonuclease A. *Bioorg. Chem.* **23**, 471-481.

Thompson, J. E. & Raines, R. T. (1994). Value of general acid-base catalysis to ribonuclease A. *J. Am. Chem. Soc.* **116**, 5467-5468.

Thompson, J. E., Venegas, F. D. & Raines, R. T. (1994). Energetics of catalysis by ribonucleases: Fate of the 2',3'-cyclic intermediate. *Biochemistry* **33**, 7408-7414.

Torrent, J., Connelly, J. P., Coll, M. G., Ribo, M., Lange, R. & Vilanova, M. (1999). Pressure versus heat-induced unfolding of ribonuclease A: The case of hydrophobic interactions within a chain-folding initiation site. *Biochemistry* **38**, 15952-15961.

Torrent, J., Rubens, P., Ribo, M., Heremans, K. & Vilanova, M. (2001). Pressure versus temperature unfolding of ribonuclease A: An FTIR spectroscopic characterization of 10 variants at the carboxy-terminal site. *Protein Sci.* **10**, 725-734.

Tu, G. F., Reid, G. E., Zhang, J. G., Moritz, R. L. & Simpson, R. J. (1995). C-terminal extension of truncated recombinant proteins in *Escherichia coli* with a 10Sa RNA decapeptide. *J. Biol. Chem.* **270**, 9322-9326.

Tunis, M. & Regelson, W. (1963). A comparative study of the inhibiting effects of anionic polyelectrolytes on deoxyribonucleases. *Arch. Biochem. Biophys.* **101**, 448-455.

Ui, N. (1971). Isoelectric points and conformation of proteins. I. Effect of urea on the behavior of some proteins in isoelectric focusing. *Biochim. Biophys. Acta* **229**, 567-581.

Vanhercke, T., Ampe, C., Tirry, L. & Denolf, P. (2005). Reducing mutational bias in random protein libraries. *Anal. Biochem.* **339**, 9-14.

Walsh, C. (2001). Enabling the chemistry of life. *Nature* **409**, 226-231.

Walz, C. & Sattler, M. (2006). Novel targeted therapies to overcome imatinib mesylate resistance in chronic myeloid leukemia (CML). *Crit. Rev. Oncol. Hematol.* **57**, 145-164.

Watt, P. M. (2006). Screening for peptide drugs from the natural repertoire of biodiverse protein folds. *Nature Biotechnol.* **24**, 177-183.

Wedemeyer, W. J., Welker, E., Narayan, M. & Scheraga, H. A. (2000). Disulfide bonds and protein folding. *Biochemistry* **39**, 4207-4216.

Wlodawer, A., Anders, L. A., Sjölin, L. & Gilliland, G. L. (1988). Structure of phosphate-free ribonuclease A refined at 1.26 Å. *Biochemistry* **27**, 2705-2717.

Wolfenden, R. & Snider, M. J. (2001). The depth of chemical time and the power of enzymes as catalysts. *Acc. Chem. Res.* **34**, 938-945.

Woycechowsky, K. J. & Hilvert, D. (2004). Deciphering enzymes. Genetic selection as a probe of structure and mechanism. *Eur. J. Biochem.* **271**, 1630-1637.

Wu, Y., Mikulski, S. M., Ardelt, W., Rybak, S. M. & Youle, R. J. (1993). A cytotoxic ribonuclease. Study of the mechanism of onconase cytotoxicity. *J. Biol. Chem.* **268**, 10686-10693.

Xu, Z. P., Tsuji, T., Riordan, J. F. & Hu, G. F. (2003). Identification and characterization of an angiogenin-binding DNA sequence that stimulates luciferase reporter gene expression. *Biochemistry* **42**, 121-128.

Yakovlev, G. I., Moiseyev, G. P., Bezborodova, S. I., Both, V. & Sevcik, J. (1992). A comparative study on the catalytic properties of guanyl-specific ribonucleases. *Eur. J. Biochem.* **204**, 187-190.

Zöllner, N. & Fellig, J. (1953). Nature of inhibition of ribonuclease by heparin. *Am. J. Physiol.* **173**, 223-228.